R-01-11

PROJECT SAFE

Gas related processes in SFR

Luis Moreno
Department of Chemical Engineering
Royal Institute of Technology

Kristina Skagius, Sara Södergren, Marie Wiborgh
Kemakta Konsult AB

June 2001

Svensk Kärnbränslehantering AB
Swedish Nuclear Fuel
and Waste Management Co
Box 5864
SE-102 40 Stockholm Sweden
Tel 08-459 84 00
+46 8 459 84 00
Fax 08-661 57 19
+46 8 661 57 19

ISSN 1402-3091
SKB Rapport R-01-11

PROJECT SAFE

Gas related processes in SFR

Luis Moreno
Department of Chemical Engineering
Royal Institute of Technology

Kristina Skagius, Sara Södergren, Marie Wiborgh
Kemakta Konsult AB

June 2001

Keywords: Gas generation, repository, anaerobic corrosion

Abstract

The radionuclide release from the SFR repository caused by gas generation was calculated for different scenarios for three repository parts (Silo, BMA and 1BTF). The calculation cases are based on the way the gas escapes from the concrete structures. In the basic cases the gas escapes through the evacuation pipes in the concrete lid of the Silo, through existing gaps between the concrete walls and the lid in BMA, and through the concrete backfill surrounding the waste packages in 1BTF. These cases correspond to the situation that we expect to occur. Another category of cases corresponds to the situation where an initial fracture exists in the concrete structures. The fracture is assumed to exist at the bottom of the respective concrete structure in the Silo and BMA. For 1BTF the initial defect is represented by a fracture transversely crossing the section containing the steel drums with ashes. Other cases were also calculated with the purpose of studying some special situations. For example, the consequences of a silo repository without evacuation pipes and backfill in the interior of BMA.

The radionuclide release, for some radionuclides, may be increased by several orders of magnitude when contaminated water is expelled by gas from the interior of the concrete structures. However, the impact on the total doses during the first thousands years after closure of the repository is limited. The total dose is dominated by the release of organic ^{14}C. Since the radionuclides are released to the coastal area during the first thousand years the dilution is considerable, which results in a very low dose.

Sammanfattning

Radionuklidutsläppet från tre delar av SFR (silon, BMA och 1BTF) till följd av gasbildning har beräknats för olika scenarier. Beräkningsfallen utgår från hur gasen strömmar ut från betongkonstruktionerna. I basfallen strömmar gasen ut genom gasavledningsrören i silons betonglock, genom befintliga springor mellan betongväggarna och locket i BMA och genom återfyllnadsbetongen som omger avfallskollina i 1BTF. Dessa fall motsvarar det förväntade händelseförloppet. Andra beräkningsfall bygger på att en spricka finns i betongkonstruktionerna initialt. För silon och BMA antas sprickan vara belägen i botten av respektive betongkonstruktion. För 1BTF antas den initiala defekten utgöras av en spricka rakt igenom den del av förvaret där stålfaten med askor förvaras. Ytterligare beräkningsfall genomfördes med avsikt att studera speciella situationer, till exempel konsekvenserna av ett siloförvar utan gasavledningsrör eller kringgjutning av avfallet i BMA. Radionuklidutsläppet kan, för vissa nuklider, öka med flera tiopotenser när kontaminerat vatten pressas ut av gas inifrån betongkonstruktionerna. Trots det påverkas inte totaldoserna nämnvärt under de första tusen åren efter förslutning av förvaret. För samtliga studerade förvarsdelar domineras totaldosen av utsläppet av organiskt ^{14}C. Eftersom utsläppet av radionuklider under de första tusen åren sker till kustområdet erhålls en betydande utspädning, vilket medför att dosen blir mycket låg.

Executive summary

The radionuclide release from the SFR repository caused by gas generation was calculated for different scenarios for three repository parts (Silo, BMA and 1BTF). The calculation cases are based on the way the gas escapes from the concrete structures. In the basic cases the gas escapes through the evacuation pipes in the concrete lid of the Silo, through existing gaps between the concrete walls and the lid in BMA, and through the concrete backfill surrounding the waste packages in 1BTF. These cases correspond to the situation that we expect to occur. Another category of cases corresponds to the situation where an initial fracture exists in the concrete structures. The fracture is assumed to exist at the bottom of the respective encapsulation in the Silo and BMA. For 1BTF the initial defect is represented by a fracture transversely crossing the section containing the steel drums with ashes. Other cases were also calculated with the purpose of studying some special situations. For example, the consequences of a silo repository without evacuation pipes and backfilling the interior of BMA.

The amount of gas generated, by corrosion of metals, microbial degradation and radiolytic decomposition, in all repository parts in SFR is estimated. The estimated amounts are based on a revised waste inventory and present plans for waste allocation in SFR. The gas generation rates are initially dominated by the corrosion of aluminium and iron and the contribution from radiolysis is negligible in all repository parts. Heat generation from corrosion of aluminium and radiolysis is also estimated and the expected temperature elevation in the repository and the adjacent rock is not more than a few degrees.

In the models, it is assumed that all the structures and waste containers are totally water saturated directly after the repository is sealed. If air is present in the concrete structure when the gas generation starts, the volume of potential contaminated water to be expelled in the initial period from the respective concrete structure will be smaller. It is also assumed that the gas generation starts very early in the repository and that the gas generation rate is large enough to expel the water in one year. The former implies that the oxygen entrapped in the repository is consumed very soon. The second assumption is based on the high corrosion rate of aluminium, therefore the gas production in the first year will be enough to expel the water required to open paths for the gas flow.

It is also considered in the calculations that water is not a limiting factor for the gas generation, once that water has penetrated the waste containers. This is due to that the volume of water needed to generate gas is quite small. About one litre of water is used for generating one Nm^3 of gas. Moreover, since the waste packages are not hermetic, it is expected that water flows into the waste when the repository is sealed and that the gas generated in the interior may escape through openings in the top of the packages.

From the calculations, it may be pointed out that:

- For the base scenario, the situation that is expected to occur, the impact of the gas generation on the radionuclide release is small.

- For the cases where initial fractures exist in the concrete structures, the impact of the gas generation on the radionuclide release may be important for short-lived radionuclides with little or no sorption in the barrier materials.

- The impact of the gas generation on the release of the long-lived radionuclides is, in general, small. For these radionuclides the maximum release is determined mainly by the diffusive transport.

- For the silo, the evacuation pipes are essential for adequate function. If evacuation pipes are not mounted in the lid the pressure in the silo may be increased and a large volume of potentially contaminated water may be expelled.

- For BMA, the existence of gaps between the concrete lid and the walls, where the lid is supported, is decisive for the amount of contaminated water expelled. The use of concrete backfill in the interior of BMA is very important if a fracture originates in the lower part of the concrete structure and gas can not escape through the gaps on the top. Backfill reduces the volume of water that is possible to expel from the encapsulation.

The radionuclide release, for some radionuclides, may be increased by several orders of magnitude when contaminated water is expelled by gas from the interior of the concrete structures. However, the impact on the total doses during the first thousand years after closure of the repository is limited. The total dose is dominated by the release of organic ^{14}C. Since the radionuclides are released to the coastal area during the first thousand years the dilution is considerable, which results in a very low dose.

Contents

Page

List of Figures

List of Tables

1 Introduction

1.1 Aim and background

In the SFR repository, gas will be generated due to various processes: anaerobic corrosion of metals, degradation of organic material and radiolysis. The gas generation may push out a certain volume of potentially contaminated water from the repository into the gravel/sand surrounding the encapsulation. A certain volume of water may be expelled when channels are opened through the porous materials to allow the gas flow. Water may be also expelled from the concrete constructions to equilibrate the higher pressure in the interior of the encapsulation.

This volume of potentially contaminated water expelled from the repository may strongly increase the release of radioactivity into the geosphere. The consequences may, however, be different for different radionuclides. Therefore calculations were performed for a set of radionuclides.

The aim of this report is to study the consequences of the gas generation on the release of radionuclides from the repository. No nuclide-specific calculations were performed, but the release was determined for a set of radionuclides. Radionuclides with different properties (half-lives, sorption properties) were selected. Nuclides with a large impact on the total release were also included in these calculations. No doses are calculated.

1.2 Structure of report

In the next chapter, a short description of the Silo and the storage tunnels (BMA, 1BTF, 2BTF and BLA) is presented. The waste packages located in the different parts of the repository are also described. Chapter 3 shows the gas generation due to metal corrosion, microbial degradation of organic materials and by radiolysis. The conceptual model of gas escape and effects on the radionuclide release are shown in Chapter 4. The data used in the calculations are presented in Chapter 5. The data include hydraulic conductivity and capillary properties of the materials, free and capillary bound water and diffusion and sorption properties. Chapter 6 presents the calculated cases and the results for the Silo, BMA and 1BTF are presented in the Chapters 7, 8 and 9 respectively. Discussion and conclusions are found in Chapter 10 and references in Chapter 11.

2 Repository description and waste inventory

In this chapter an overview is given of the design of the Silo, the repository vaults and the waste inventory. The estimated material volumes, voids and amounts of gas generating materials in both the repository barriers and in the different waste types that have been used in this report are given in Appendix A. The information in this chapter is based on information given in the background material to the SAFE study /SKB, 2001; Riggare and Johansson, 2001/.

2.1 Silo

2.1.1 Design

The design of the Silo is schematically shown in Figure 2-1. It consists of a concrete cylinder with a height of about 53 m and an outer diameter of about 28 m. The thickness of the concrete walls is 0.8 m and the concrete bottom plate is 1 m thick. The interior of the concrete cylinder is divided into vertical shafts with intervening concrete walls, 0.2 m thick. The waste packages are placed in the shafts and the voids between the waste packages are gradually backfilled with concrete grout.

The slot between the cylindrical concrete walls and the surrounding rock is filled with bentonite, on average 1.2 m thick. The concrete cylinder is resting on a 1.5 m thick mixture of 10 weight % bentonite and 90 weight % sand.

According to present plans, the sealing of the Silo will be carried out by placing a 1 m thick concrete lid on top of the concrete cylinder. The lid can be equipped with evacuation pipes in order to allow escape of gas that is generated inside the concrete cylinder. The top of the lid will be covered by a thin layer of sand (about 100 mm) and a 1.5 m thick mixture of 10 weight % bentonite and 90 weight % sand. The remaining void (about 6 000 m^3) above the mixture of bentonite and sand will be filled with sand or gravel or with sand stabilised in cement /SKB, 1998/.

All concrete walls as well as the concrete bottom and lid are reinforced. The type of reinforcement bars and the amount of iron used are given in Appendix A.

2.1.2 Waste inventory

The Silo is designed for approximately 18 500 m^3 of conditioned waste /SKB, 1998/. Most of the waste, about 98%, is ion-exchange resins and the remaining 2% are scrap and trash. All of the waste is conditioned, about 80% in cement and 20% in bitumen.

The waste allocated to the Silo is packed in concrete moulds, steel moulds and in steel drums. The dimensions of the moulds are 1.2×1.2×1.2 m and the drums have a diameter of about 0.6 m and a height of about 0.9 m. Steel drums are placed on a steel plate or in a steel box with the same dimensions as the moulds loaded into the shaft in the Silo.

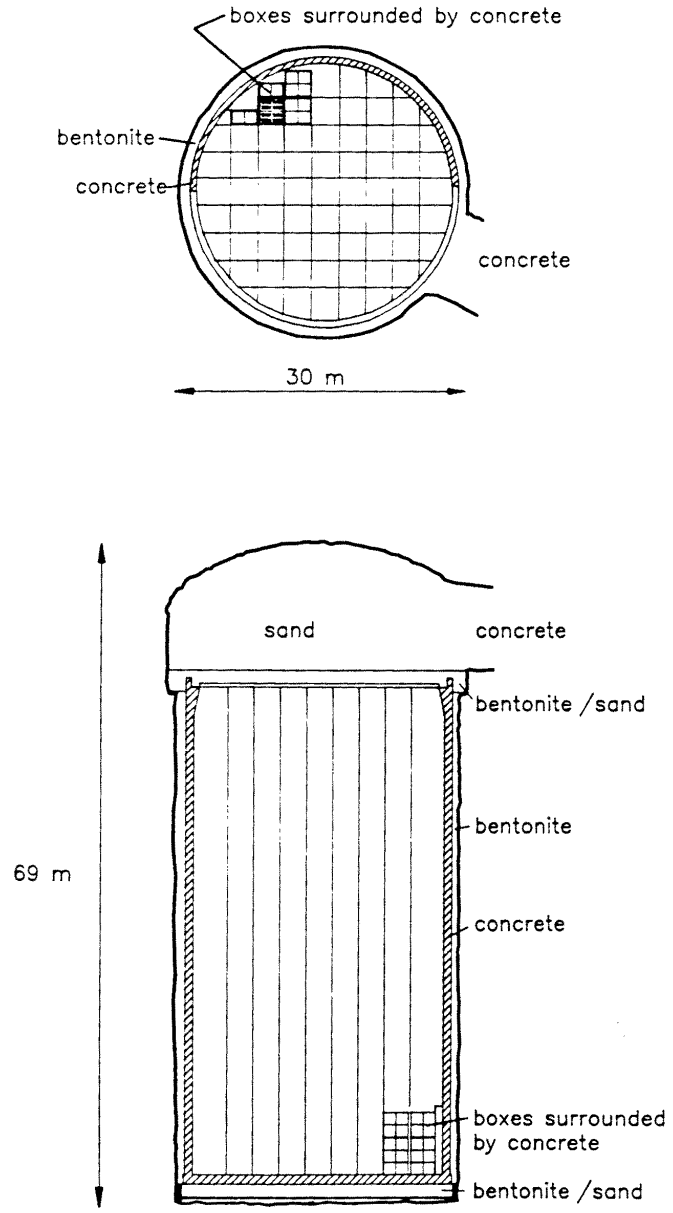

Figure 2-1. *Schematic illustration of the Silo.*

The waste allocated to the Silo can be divided into the following categories:

- Concrete moulds with waste stabilised in cement.
- Steel moulds with waste stabilised in cement.
- Steel drums with waste stabilised in cement.
- Steel moulds with waste stabilised in bitumen.
- Steel drums with waste stabilised in bitumen.

About 43% of the waste volume consists of concrete moulds, 47% of steel moulds and 10% of steel drums.

Detailed information on quantity of materials and geometrical data for barriers, waste packages and gas generating materials are found in Appendix A.

2.2 BMA

2.2.1 Design

The rock vault for intermediate level waste, BMA, is 160 m long with a wall height of 11.5 m and a maximum height of 16.5 m and a width of 19.6 m, see Figure 2-2. The waste packages are placed into a concrete structure, 140 m long and 8.4 m high and 15.6 m wide. The concrete structure is divided into 13 large compartments and two small compartments by inner concrete walls. The inner length of the large compartments in the length-direction of the vault is 9.9 m and the cross sectional inner length is 15.6 m. The two small compartments have an inner length of about 5 m in the length direction of the vault and the inner length in the cross-sectional direction of the vault is 7.2 . Both the outer and inner concrete walls are 0.4 m thick except for the cross-sectional wall facing the reloading zone, which is 0.6 m thick. The bottom of the compartments consists of a concrete floor, 0.25 m thick, that rests on a layer of gravel.

The waste packages are piled on the concrete floor in the compartments in such a way that each compartment will have at least two rows of concrete moulds that act as a support for pre-fabricated reinforced concrete lids. The lids are put in position as soon as a compartment is filled and after that a 5 cm thick concrete layer is cast on top of the lid in order to prevent water intrusion during the operational phase.

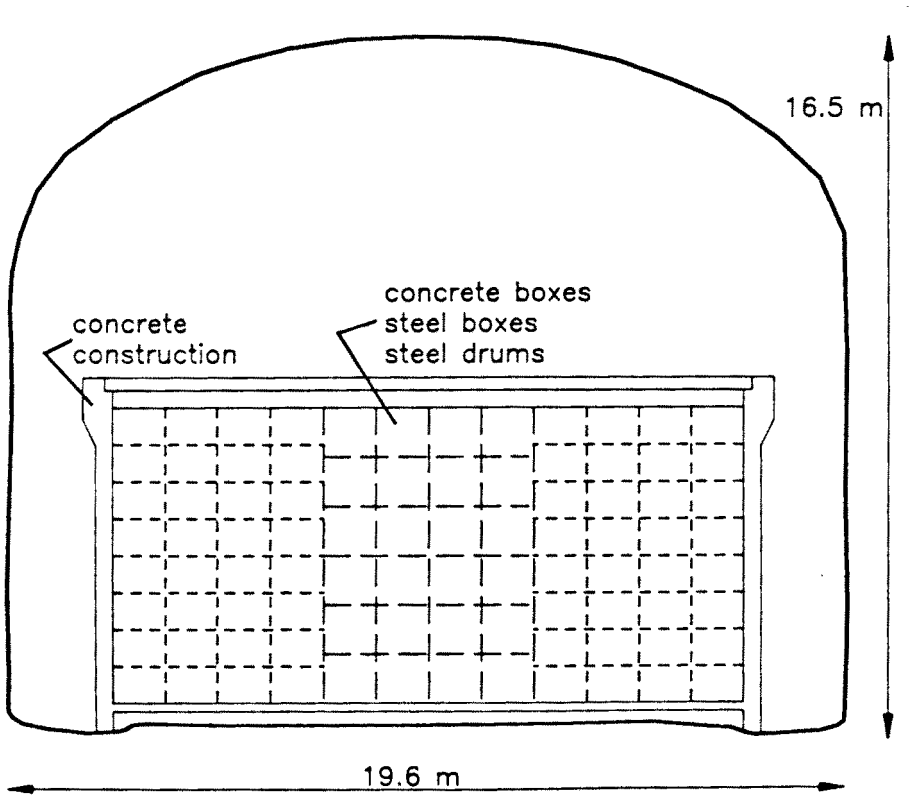

Figure 2-2. *Schematic view of a cross-section through a large concrete compartment in BMA.*

At repository closure, an additional 0.5 m thick reinforced concrete lid will be cast on top of the compartments. The space between the waste packages inside the compartments will either be left empty or filled with the same type of concrete grout that is used as backfill material inside the Silo. The space between the concrete structure and the rock walls, about 2 m wide on each side, as well as the re-loading zone will be filled with sand. The space above the concrete lid will either be left unfilled or will be filled with sand. In the SAFE-project it is assumed that the space is filled with sand.

All concrete walls as well as the concrete bottom and lid are reinforced. The quantity of reinforcement bars per m^3 of concrete is about 100 kg /Forsgren et al., 1996/. This gives in total about 400 tonnes of reinforcement bars in the concrete structures.

2.2.2 Waste inventory

The BMA vault is designed for 13 400 m^3 of conditioned waste. The waste types are similar to those allocated to the Silo, e.g. ion-exchange resins and scrap and trash conditioned in cement or bitumen. About 55% of the waste volume is ion-exchange resins and the remaining 45% scrap and trash. All of the waste is conditioned, about 76% in cement and 24% in bitumen.

The waste allocated to BMA is packed in concrete moulds, steel moulds and in steel drums with the same design and dimensions as those used for the Silo waste. Steel drums are placed on a steel plate or in a steel box with the same dimensions as the moulds before being loaded into the compartments in BMA.

The waste allocated to BMA can be divided into the following categories:

- Concrete moulds with waste stabilised in cement.
- Steel moulds with waste stabilised in cement.
- Steel drums with waste stabilised in cement.
- Steel moulds with waste stabilised in bitumen.
- Steel drums with waste stabilised in bitumen.

In addition to the waste types specified above some ‘Odd waste’ will be allocated to BMA. Presently this waste is only defined in terms of metal content and quantity of cement used to stabilise the waste.

About 54% of the waste volume consists of concrete moulds, 27% of steel moulds and 16% of steel drums. The ‘Odd waste’ amounts to about 3% of the waste volume.

Detailed information on quantity of materials and geometrical data for barriers, waste packages and gas generating materials are found in Appendix A.

2.3 1BTF and 2BTF

2.3.1 Design

The rock vaults for concrete tanks, 1BTF and 2BTF, consists of two identical rock vaults, 160 m long with a wall height of 6.5 m, a maximum height of 9.5 m and a width of 14.7 m. The bottom of the vaults is covered by a 0.3 m thick layer of gravel and a 0.4 m thick concrete floor on top of the gravel.

In the vault 1BTF, concrete tanks are stacked two high around the walls of the vault, see Figure 2-3. Concrete moulds are used to make "compartments" where drums with ashes can be stacked. To make a separating "wall" the moulds are stacked four moulds high and nine moulds wide. A total of six compartments are needed to make room for 6 479 steel drums. Five of the compartments will be completely filled, containing 1 110 drums each, and the last compartment will hold 929 drums. When a compartment is filled with drums, it is sealed using concrete grout. The rest of the vault is used for concrete tanks, steel boxes and odd waste.

At repository closure of 1BTF, 0.4 m thick prefabricated concrete lids will be placed on top of the concrete tanks. Concrete is then used to fill the space between the rock walls and the waste packages in the whole vault up to a height of 5.4 m. The space between the concrete tanks in the part of the vault used for concrete tanks is also filled with concrete to the same height. On top of the cement a 0.4 m thick reinforced slate of concrete will be casted and the remaining volume is backfilled using sand. In 2BTF, the concrete tanks are stacked in rows of four tanks side by side and two tanks high.

At repository closure, prefabricated concrete lids will be placed on top of the concrete tanks in 2BTF in the same way as in 1BTF. The vault will be sealed with concrete and sand in the same way as 1BTF.

The concrete structures in 1BTF as well as in 2BTF are reinforced. The quantity of reinforcement bars per m^3 of concrete is about 100 kg /Forsgren et al., 1996/. This gives in total about 190 tonnes of reinforcement bars in 1BTF and 250 tonnes in 2BTF.

2.3.2 Waste inventory

The two vaults, 1BTF and 2BTF, are designed for about 10 000 m^3 of waste each. The effective volume of the vaults is about 20 000 m^3. In 1BTF the waste is comprised of ion exchange resins (27%), ashes (20%), graphite (1%), sludge (0.5%), trash (less than 0.2%) and steel waste (52%), and in 2BTF the waste consists of ion exchange resins. Most of the resins in 1BTF are unsolidified, 85%, but there are also conditioned resins. The ashes, the sludge and the trash are conditioned with cement, while the graphite and the steel waste are unconditioned. In 2BTF all the waste is unsolidified.

The waste allocated to 1BTF is packed in concrete tanks, steel drums in steel drums, steel boxes and concrete moulds. In 2BTF only concrete tanks are used. The dimensions of the concrete moulds are the same as the concrete moulds used in the Silo and BMA. The concrete tanks are 3.3 m long, 1.3 m wide and 2.3 m high and the steel drums are a 100 l drum placed in a 200 l drum with concrete between. The outer drum has a diameter of about 0.6 m and a height of about 0.9 m. The steel boxes are 1.2 m long and 0.8 m wide and high.

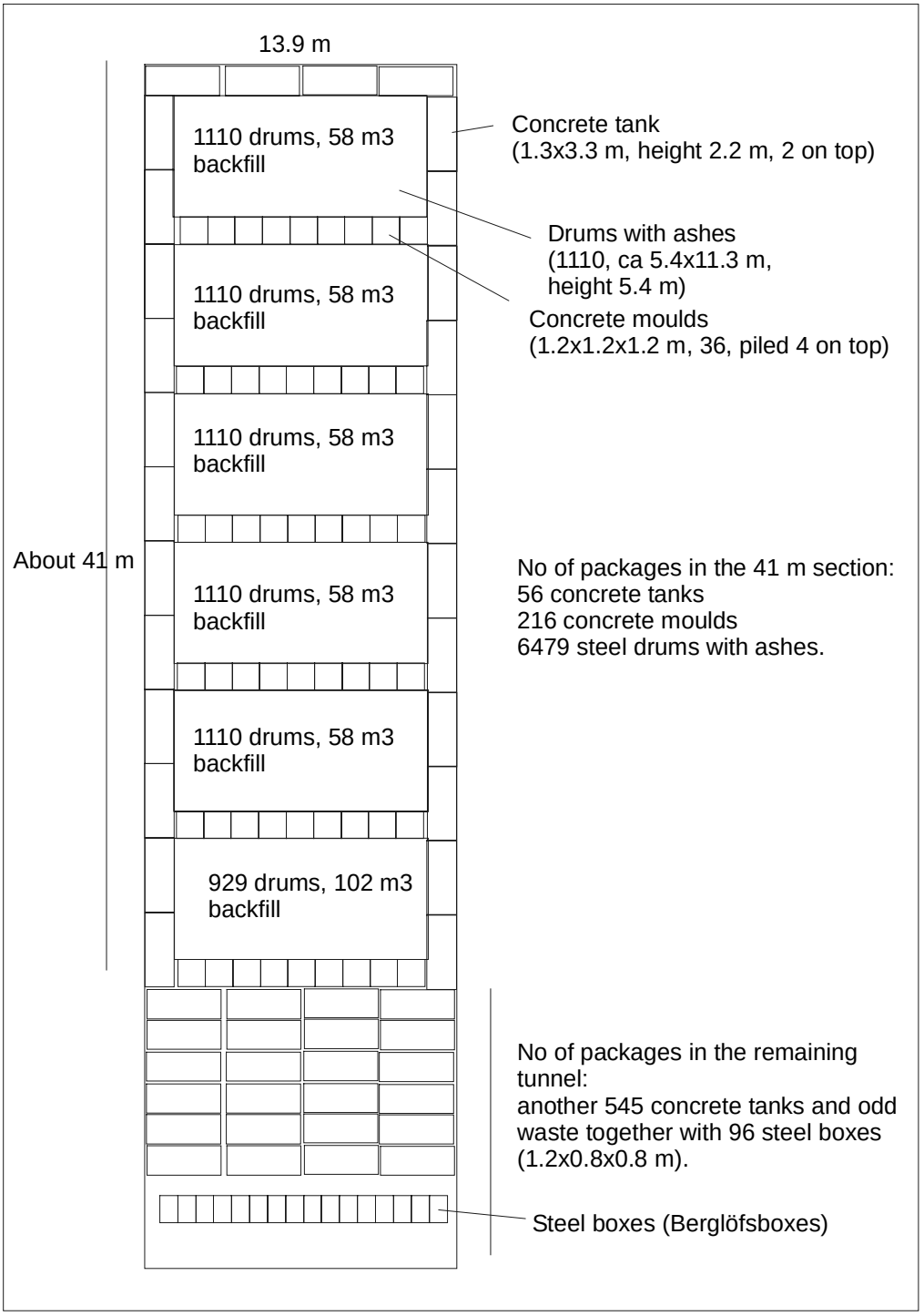

Figure 2-3. *Schematic view of the allocation of waste in 1BTF.*

The waste allocated to 1BTF can be divided into the following categories:

- Concrete tanks with unsolidified resins.
- Steel drum in steel drum with cement between, containing ashes.
- “Berglöfsbox”, a steel box 1.2x0.8x0.8 m, containing unconditioned graphite.
- Concrete mould with waste stabilised in cement.

In addition to the waste types specified above ‘Odd waste’ will be allocated to 1BTF. This waste is only defined in terms of metal content.

About 22% of the waste volume in 1BTF consist of concrete tanks, 25% of steel drums, less than 0.1% of steel boxes and 4% of concrete moulds. The ‘Odd waste’ amounts to about 49% of the waste volume.

The waste allocated to 2BTF is of one category: concrete tanks with unsolidified resins.

Detailed information on quantity of materials and geometrical data for barriers, waste packages and gas generating materials are found in Appendix A.

2.4 BLA

2.4.1 Design

The rock vault for low level waste, BLA, is 160 m long, 14.7 m wide, has a wall height of 9 m and a maximum height of 12.5 m. The waste is piled to 7.8 m height and the bottom of the vault is covered by a 0.3 m thick layer of gravel. On top of the gravel a concrete floor, 0.4 m thick, is placed.

In the vault ISO-containers will be stacked in rows of two containers side by side and three high. BLA will not be backfilled at repository closure.

The concrete bottom in BLA is reinforced. The quantity of reinforcement bars per m^3 of concrete is about 100 kg /Forsgren et al., 1996/. This gives about 90 tonnes of reinforcement bars.

2.4.2 Waste inventory

BLA is designed for approximately 12 000 m^3 of unconditioned and bitumenised waste. Most of the waste is unsolidified trash, about 87%, 4% is bitumenised ion exchange resins and 9% odd waste.

The waste allocated to BLA is packed in ISO-containers, steel drums in ISO-containers and steel drums in steel drums placed in ISO-containers. There are ISO-containers of different sizes, but here all ISO-containers are assumed to be 6 m long, 2.5 m wide and 1.3 m high. The drums have a diameter of about 0.6 m and a height of about 0.9 m.

The waste allocated to BLA can be divided into the following categories:

- ISO-containers with unsolidified trash.
- Steel drums with bitumenised ion-exchange resins.
- Steel drums with unsolidified trash in steel drum placed in an ISO-container.

In addition to the waste types specified above some ‘Odd waste’ will be allocated to BLA. Presently this waste is only defined in terms of metal content and it is assumed to have the same dimensions as an ISO-container.

About 76% of the waste volume consist of ISO-containers, 4% of steel drums in ISO-containers and 11% of steel drums in steel drums placed in ISO-containers. About 9% of the waste volume is odd waste.

Detailed information on quantity of materials and geometrical data for barriers, waste packages and gas generating materials are found in Appendix A.

3 Gas generation

3.1 Gas generating processes

Gas can be generated in the repository by hydrogen evolving corrosion of metals, by microbial degradation of organic materials and by radiolytic decomposition of water.

3.1.1 Metal corrosion

The major metal present in the repository is steel, but the waste also contains other metals such as aluminium and zinc.

Steel is present in all repository parts. Hydrogen evolving corrosion can occur only in the absence of dissolved oxygen. This implies that anaerobic corrosion will start when aerobic corrosion or another oxygen consuming reaction, such as microbial activity has consumed the oxygen initially present.

Under anaerobic conditions, the amount of hydrogen evolved can be estimated by the following overall reaction for corrosion of steel, for which the formation of magnetite is the end product /Höglund and Bengtsson, 1991/.

$$3Fe(s) + 4H_2O \rightarrow Fe_3O_4(s) + 4H_2(g)$$

Aluminium is present in the waste in all parts of the repository. Due to the large amount of concrete, the water in contact with the aluminium waste will be alkaline. Aluminium is not thermodynamically stable in water, but has a very dense protective oxide layer. However, in alkaline environments this oxide layer will dissolve and a rapid corrosion of aluminium yielding hydrogen can take place according to the reaction /Höglund and Bengtsson, 1991/:

$$2Al(s) + 2OH^- + 4H_2O \rightarrow 2AlO(OH)_2^- + 3H_2(g)$$

or alternatively

$$2Al(s) + 2OH^- + 2H_2O \rightarrow 2AlO_2^- + 3H_2(g)$$

A compilation has been made of corrosion rates for conditions similar to the SFR. The corrosion rates for iron and steel lie in the interval 0.1–10 μm/year (see Appendix B). In the calculations of the gas formation the corrosion rate for iron and steel has been assumed to be 1 μm/year, corresponding to a production of hydrogen gas of approximately 3 l/m^2,year and that total corrosion of a 5 mm slab takes 2 500 years. For aluminium and zinc, the corrosion rate has been assumed to be 1 mm/year, corresponding to corrosion of all material within a few years. In a status report from the European Commission on gas migration and two-phase flow for a deep repository an overview is given of studies and experiments published within the area of gas generation before 1999 /Rodwell et al, 1999/. The compiled gas formation rates for different materials and environments are in accordance with the rates assumed in the current study.

In calculating the gas formation rates due to corrosion all corroding parts, except reinforcements in concrete packages and concrete structures, are assumed to have a planar geometry. Gas generation by corrosion of reinforcement bars considers the shrinking surface, which is a function of the time.

3.1.2 Microbial degradation of organic materials

Organic materials are present in the waste in SFR. These materials may be digested by microorganisms. Examples of microbially degradable materials are cellulose, ion exchange resins with organic matrices, different scrap material and bitumen. The result of microbial degradation in SFR may be unwanted effects, such as the formation of gas.

The chemical environment significantly influences the rate of microbial degradation, where optimal conditions for most microorganisms are at a pH close to neutral, a temperature of 25–30°C, and absence of biotoxic substances. However, different microorganisms possess a remarkable ability to adapt to different environments. Therefore, microbial activity and gas generation cannot be excluded even if strongly alkaline conditions are expected in the waste packages after saturation of the repository.

Under aerobic conditions, microbial degradation of organics will consume oxygen and produce carbon dioxide. Aerobic corrosion of the large amounts of steel in the repository will also consume oxygen. Due to these processes, the rather small amounts of oxygen initially present after closure of the repository is assumed to be totally consumed a short time after the closure and anaerobic conditions will be established.

Under anaerobic conditions, other oxidants such as nitrate, sulphate and carbon dioxide will participate in the microbial degradation process. A simplified reaction formula for the degradation of an arbitrary organic compound can be written as /Höglund and Bengtsson, 1991/:

$$C_{org} + \text{Oxidant} \rightarrow C^{*}_{org} + H_2 + CO_2 + CH_4 + \text{Reducing agent}$$

Gas generation rates for microbial degradation of organic materials are relatively sparse. The type of organic substrate as well as the surface area available for microbial attack is important for the degradation rate. The organic material can be divided into two groups, cellulose material with a large surface to volume ratio and other organic materials with a low surface to volume ratio. Other organic material includes ion exchange resins, plastic, rubber etc.

Within the SAFE project, a study has been conducted by /Pedersen, 2001/ concerning the possibilities for microbial degradation of organic materials under conditions similar to what can be expected in SFR after closure. The study also refers to experiments conducted in England, where it is implied that the gas formation decreases after an initial formation period. Pedersen states that the environment in the SFR is not ideal for microbial degradation, but that even a pH as high as 12 is not an obstacle for microbial activity. The formation of gas in the SFR from microbial activity could be restricted by the supply of oxidants and nutrients and the removal of reaction products. A possibly beneficiary aspect for the total gas formation in the repository is that several microorganisms can use hydrogen gas as an energy source and could thereby reduce the amount of hydrogen gas formed by corrosion.

Based on data on the organic content in the waste /Riggare and Johansson, 2001/, the contribution to the total amount of gas from microbial degradation of cellulose has been calculated. Conservative estimations of the degradation of ion-exchange resins, bitumen and plastics have also been made. In the calculations, degradation rates for cellulose corresponding to complete degradation in a little less than 200 years is assumed. This results in a degradation rate of 0.2 mole/kg,year and a gas formation rate of about 2 l/kg,year, assuming that 50% of the gases are inert, see Table 3-1.

Table 3-1. Gas generation rates and maximum yields for microbial degradation of cellulose and other organics /Wiborgh et al., 1986/.

	Cellulose	Other organics
Rate, (mole gas/year, kg organic)	0.2	0.002
Maximum yield, (mole gas/kg organic)	37	30

In the literature, data on the microbial degradation of bitumen, ion-exchange resins and plastics are scarce. The few experiments found imply that these are very slow processes. In the calculations it is assumed that 0.002 mole/kg,year is degraded, corresponding to a degradation of all material in 15 000 years and a gas formation rate of 0.02 l/kg,year assuming that 50% of the gases are inert, see Table 3-1.

3.1.3 Radiolysis

The radiolytic decomposition of material in the repository may lead to the formation of gases and also species that can influence the speciation of radionuclides. In the present study, however, only the gas formation has been considered.

The irradiation of materials in the waste and conditioning material by alpha, beta and gamma radiation leads to the formation of excited and ionised species. These species can participate in a number of chemical reactions forming, for example, gaseous compounds such as hydrogen.

The water content in different materials determines the amount of hydrogen gas generated by radiolysis. For example, the amount of hydrogen produced by irradiation of concrete is influenced by the water/cement ratio as the cement minerals are stable and consequently only the water will decompose due to the irradiation.

Irradiation of water eventually leads to the formation of hydrogen gas. The first step is the formation of the following highly reactive intermediate reaction products /Möckel et al.,1980/:

$$H_2O \Rightarrow H\cdot, OH\cdot, e^-_{aq}, H^+$$

In pure water the final products will be hydrogen and hydrogen peroxide:

$$H\cdot + H\cdot \Rightarrow H_2$$

$$2H_2O + 2e^- \Rightarrow H_2 + 2OH^-$$

$$OH\cdot + OH\cdot \Rightarrow H_2O_2$$

If multivalent metal ions are present in the water, many researchers have noted a decrease in the hydrogen production.

Irradiation of certain types of spent ion exchange resins may produce different methyl-amines. However, they are fairly soluble in water and may, depending on the amount of water present, give different contributions to the gas pressurisation. Gas can also be produced by irradiation of organic hydrocarbons. When the bond between the carbon and hydrogen atoms breaks, hydrogen gas is formed as well as small amounts of carbon monoxide, carbon dioxide and methane. The major source of gas from radiolysis however, is water and no other process will be considered here.

The effect of irradiation is generally expressed as the radiolytic yield, the G-value. It is defined as the number of molecules produced per 100 eV of absorbed energy by the material. G-values can, for practical purposes, be converted into generation rates expressed as mole/Mrad,tonne. The conversion factor is close to unity. The amount of gas formed due to radiolysis of water during a time period, t, can be calculated as:

$$V_{gas} = A_0 \frac{3.15 \cdot 10^7}{\lambda}(1 - e^{-\lambda t})(E_\alpha G_\alpha + (E_\beta + E_\gamma)G_{\beta\lambda})\frac{V_0}{N_A}$$

where:

V_{gas}	is the amount of gas formed during the time period t, [m^3(STP)]
A_0	is the activity of the nuclide at the closure of the repository, (Bq)
λ	is the decay constant, (yr^{-1})
t	is the time, (yr)
$E_.$	is the alpha energy per transformation of the nuclide, (MeV/decay)
$E_.$	is the beta energy per transformation of the nuclide, (MeV/decay)
$E_.$	is the gamma energy per transformation of the nuclide, (MeV/decay)
$G_.$	is the radiolytic yield from alpha radiation, (molecules/MeV)
$G_{..}$	is the radiolytic yield from beta/gamma radiation, (molecules/MeV)
N_A	is Avogadros number, (molecules/mol)
V_0	is the molar volume of an ideal gas at 0°C and 1 atm, (m^3(STP)/mol)

The equation assumes unrestricted access to water, which may not be the case. If sufficient amounts of water are not available, the gas formation may be reduced. In Table 3-2 the chosen G-values for this study are given.

Table 3-2. Assumed G(H_2)-values for radiolysis of water /Warrant, 1989/.

	G-values (mol/Mrad/tonne)
Alpha irradiation	1.5
Beta and gamma irradiation	0.5

G-values for different materials and types of radiation gives the amount of released molecules formed by irradiation. The G-values are developed experimentally and can be found in the literature. The effect from the irradiation is proportional to the absorbed dose and depend on the structure and water content of the material. Inorganic materials are often more stable than organic. In the simplified calculations of the radiolysis, G-values for water have been assumed and that all the energy is absorbed in water present in the ion-exchange resins, the conditioning material and the surrounding material.

3.2 Gas generation in SFR due to metal corrosion

3.2.1 The Silo

The estimated gas generation rates in the Silo from corrosion of metals in waste packages and concrete structures are calculated using the amounts and dimensions of different materials in the Silo given in Appendix A. Quantities given as the sum of aluminium and zinc have been assumed to be aluminium. The results are given in Figures 3-1 and 3-2 and in Table 3-3.

Table 3-3. Initial gas formation rates and maximum theoretical gas volume that can be generated due to corrosion of metals in the Silo.

	Initial gas formation rate (Nm^3/year)		Maximum theoretical gas volume (Nm^3)	
Packaging		550		$1.2 \cdot 10^6$
Reinforcement		204		$6.1 \cdot 10^5$
Waste		1 080		$2.3 \cdot 10^4$
steel	*8*		*$2.0 \cdot 10^4$*	
aluminium	*1 080*		*$2.7 \cdot 10^3$*	
Structures		82		$2.4 \cdot 10^5$
Total		**1 920**		**$2.1 \cdot 10^6$**

The gas generation rates are calculated for packaging, reinforcement, waste and structures separately. Packaging includes metals in the packaging of the waste, excluding reinforcement bars in concrete packaging, which are shown separately. The category waste in the figures includes steel and aluminium in the waste. Structures include gas formed from corrosion of reinforcement bars in the concrete structures of the repository.

For the first 2.5 years corrosion of aluminium in the waste will dominate the gas formation, see Figure 3-1.

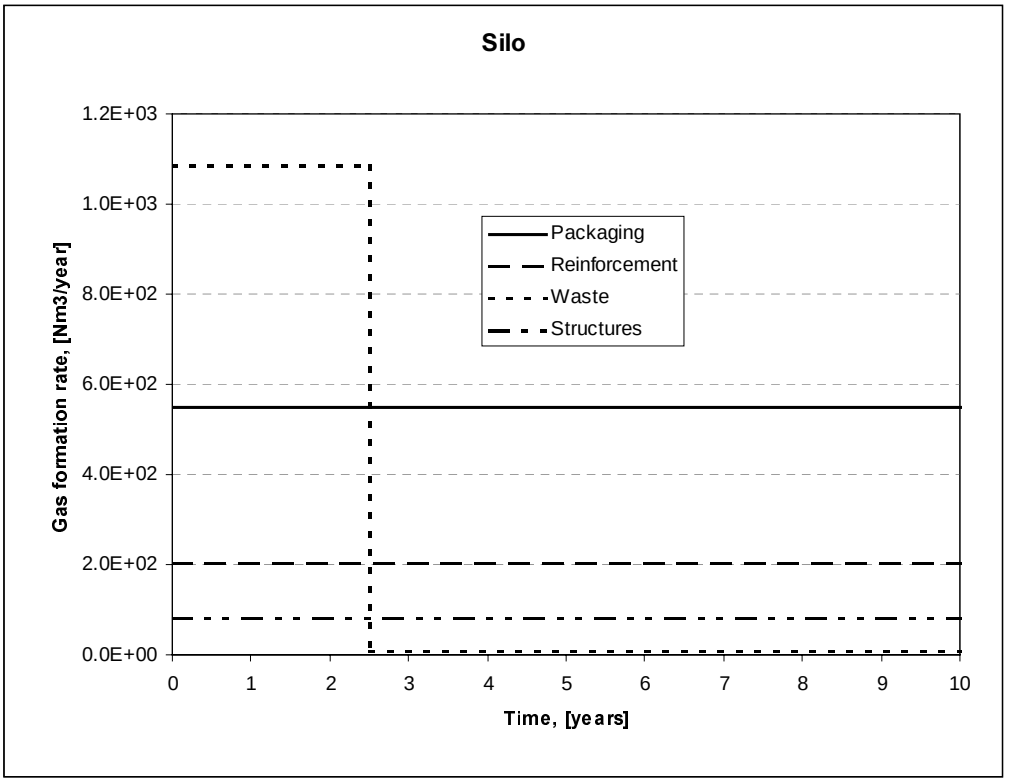

Figure 3-1. *Gas formation rates due to corrosion in the Silo, (Nm^3/year). 0–10 years.*

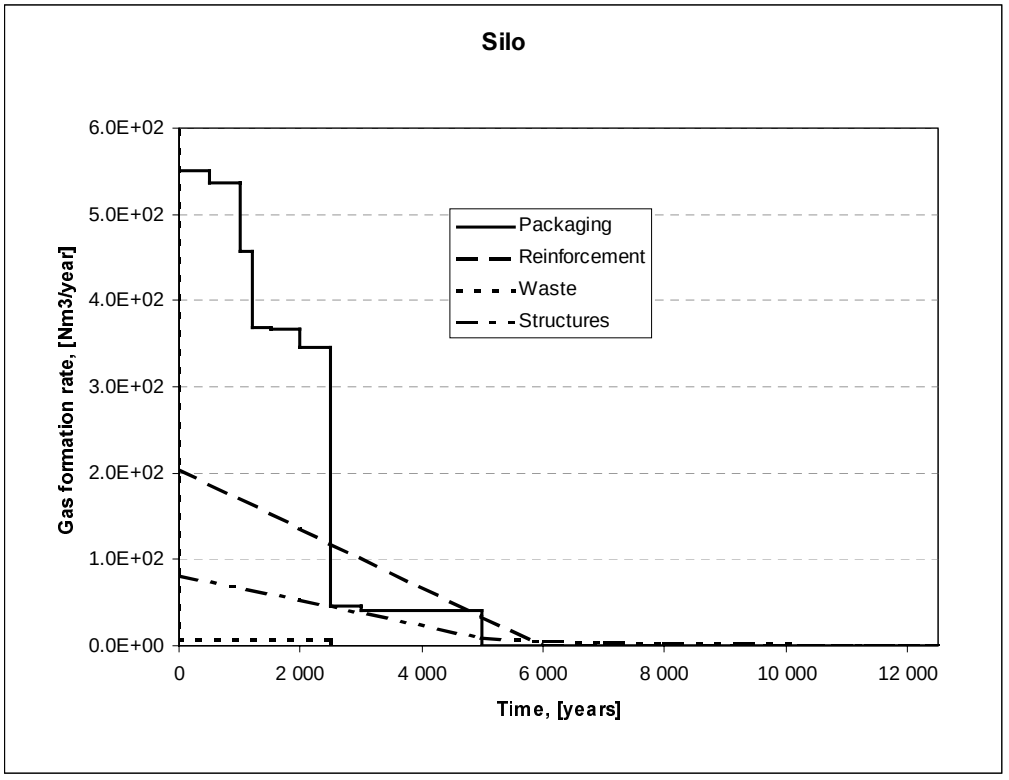

Figure 3-2. *Gas formation rates due to corrosion in the Silo, (Nm^3/year). 0–12 500 years.*

3.2.2 The BMA vault

The estimated gas generation rates in the BMA from corrosion of metals in waste packages and concrete structures are calculated using the amounts and dimensions of different materials in BMA given in Appendix A. Quantities given as the sum of aluminium and zinc have been assumed to be aluminium. The results are given in Figures 3-3 and 3-4 and in Table 3-4.

Table 3-4. Initial gas formation rates and maximum theoretical gas volume that can be generated due to corrosion of metals in BMA.

	Initial gas formation rate (Nm^3/year)	Maximum theoretical gas volume (Nm^3)
Packaging	346	$7.1 \cdot 10^5$
Reinforcement	178	$5.4 \cdot 10^5$
Waste	7 110	$3.3 \cdot 10^5$
steel	*96*	*$3.2 \cdot 10^5$*
aluminium	*7 020*	*$1.8 \cdot 10^4$*
Structures	54	$2.1 \cdot 10^5$
Total	**7 690**	**$1.8 \cdot 10^6$**

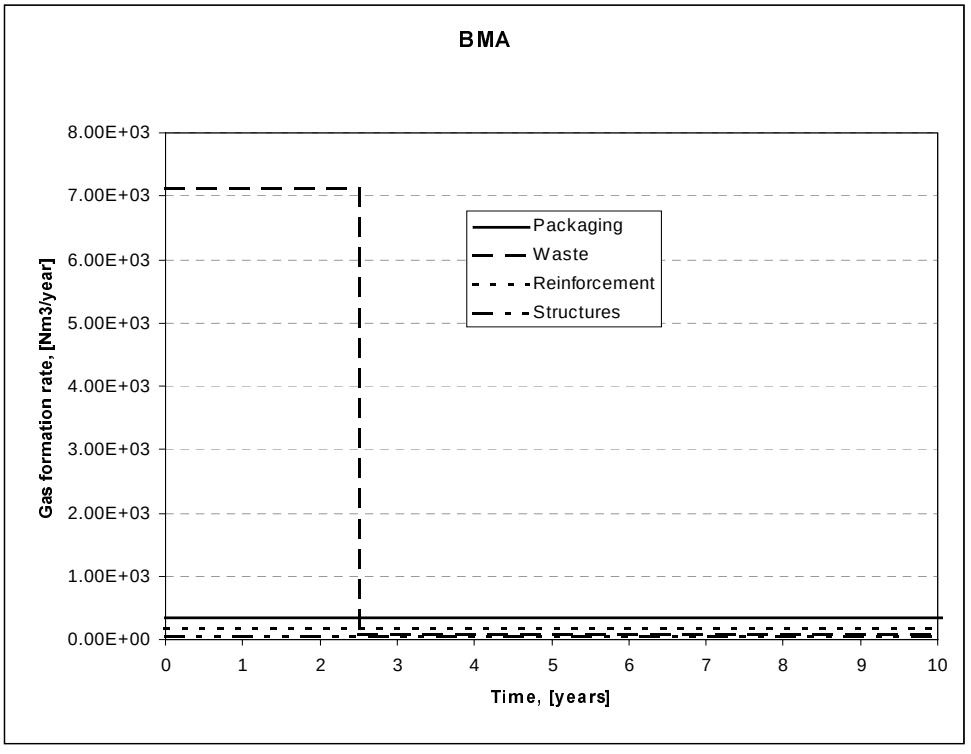

Figure 3-3. *Gas formation rates due to corrosion in BMA, (Nm^3/year). 0–10 years.*

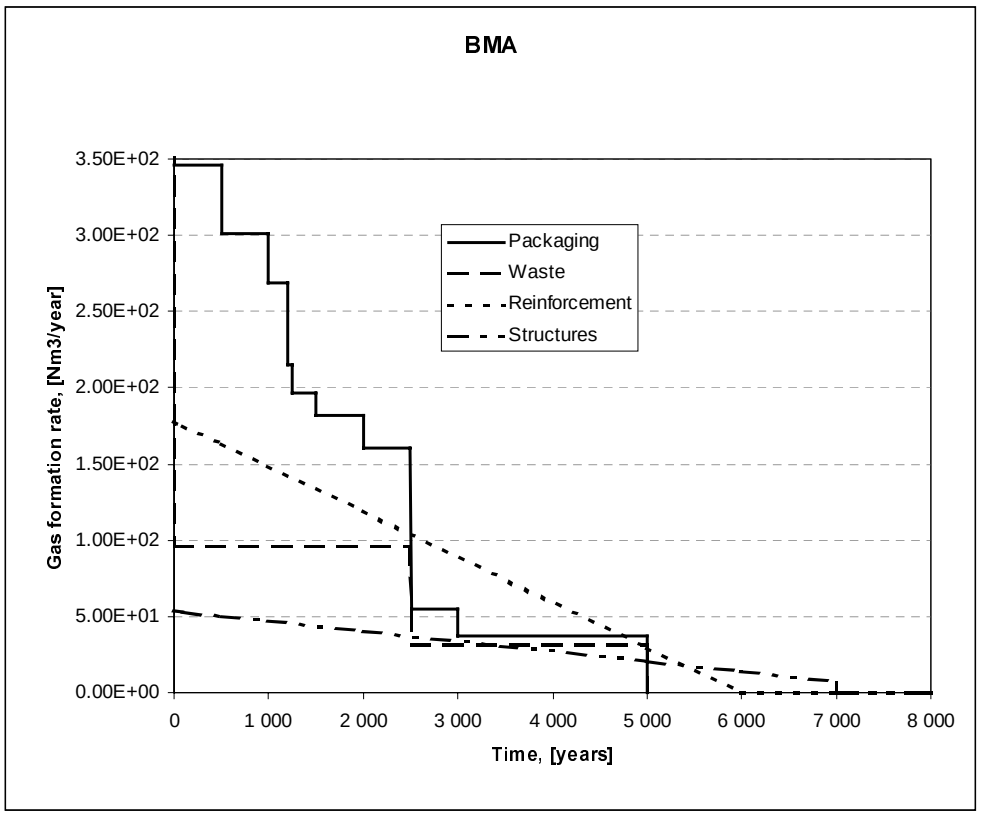

Figure 3-4. *Gas formation rates due to corrosion in BMA, (Nm^3/year). 0–8 000 years.*

3.2.3 The BTF vaults

The estimated gas generation rates in the BTF vaults, 1BTF and 2BTF from corrosion of metals in waste packages and concrete structures are calculated using the amounts and dimensions of different materials in BTF given in Appendix A. Quantities given as the sum of aluminium and zinc have been assumed to be aluminium. The results are given in Figures 3-5, 3-6, 3-7 and 3-8 and in Tables 3-5 and 3-6. In the BTF vaults the only concrete structures are the bottom and lids.

For 1BTF the gas generation rates are calculated for packaging (steel), reinforcement (in packaging), waste (steel and aluminium), ashes in waste (aluminium) and structures (reinforcement) separately. In 2BTF the only sources of metal are reinforcement bars in the waste packagings and concrete structures.

For the first years, the corrosion of aluminium in the waste will dominate the gas formation in 1BTF, see Figure 3-5.

To facilitate the comparison of gas formation rates, the spherical aluminium particles in the ashes have been approximated to slabs with the same thickness as the diameter of the spheres. The amount of aluminium corroded is the same and hence the same total amount of gas will be formed. Spherical particles would have resulted in a significantly higher initial formation rate, which would have decreased rapidly. However, the total corrosion time would have been the same.

Table 3-5. Initial gas formation rates and maximum theoretical gas volume that can be generated due to corrosion of metals in 1BTF.

	Initial gas formation rate (Nm^3/year)		Maximum theoretical gas volume (Nm^3)	
Packaging		200		$1.1 \cdot 10^5$
Reinforcement		42		$9.5 \cdot 10^4$
Waste (excl ashes)		556		$1.6 \cdot 10^6$
steel	*313*		*$1.6 \cdot 10^6$*	
aluminium	*243*		*$6.1 \cdot 10^2$*	
Ashes in waste (Al)		26 400		$5.3 \cdot 10^4$
Structures		26		$1.0 \cdot 10^5$
Total		**27** 300		**$1.9 \cdot 10^6$**

The high rate for gas generation from aluminium in ashes is explained by the large amount of aluminium present in the 1BTF vault. However, since the aluminium is completely depleted after a few years, the total gas volume generated is small, see Table 3-5.

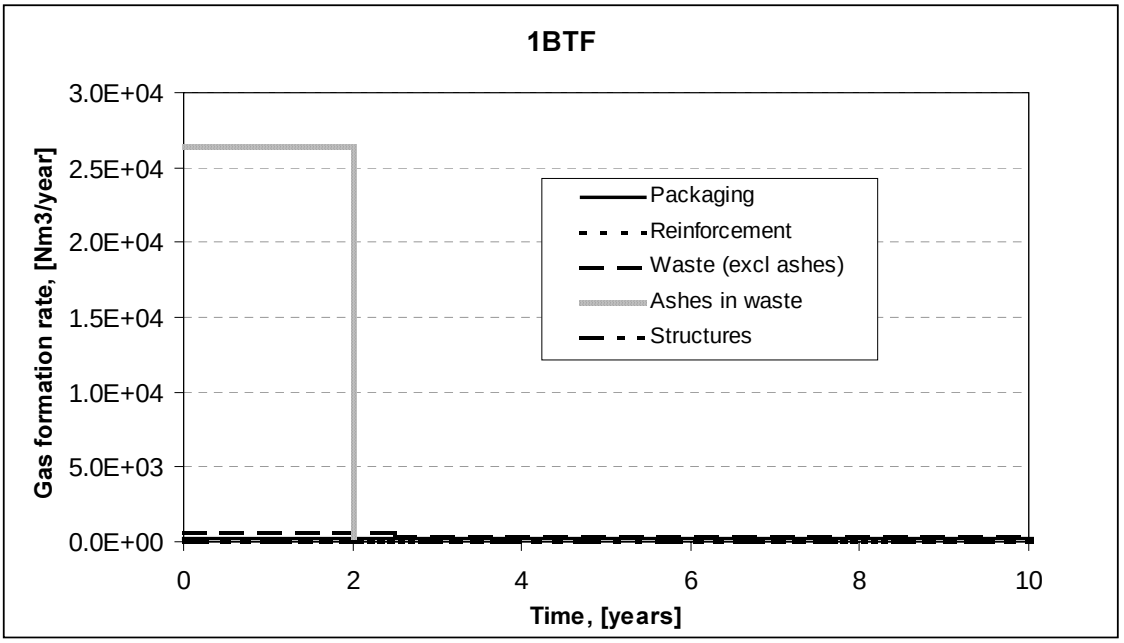

Figure 3-5. *Gas formation rates due to corrosion in 1BTF, (Nm^3/year). 0–10 years.*

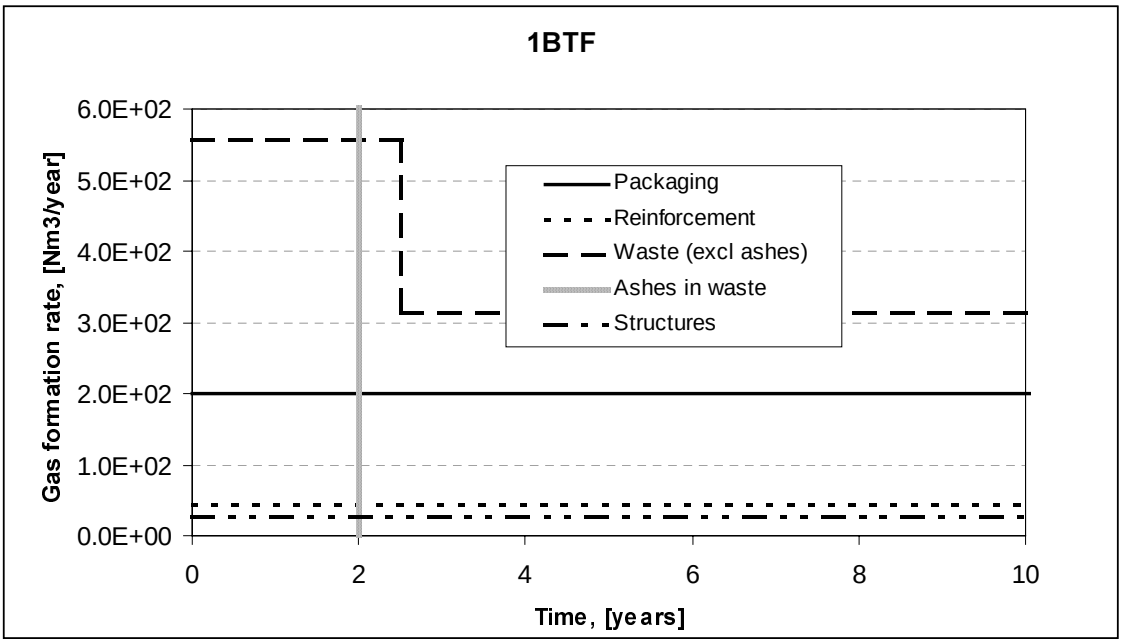

Figure 3-6. *Gas formation rates due to corrosion in 1BTF, (Nm^3/year). 0–10 years, 0–600 Nm^3/year.*

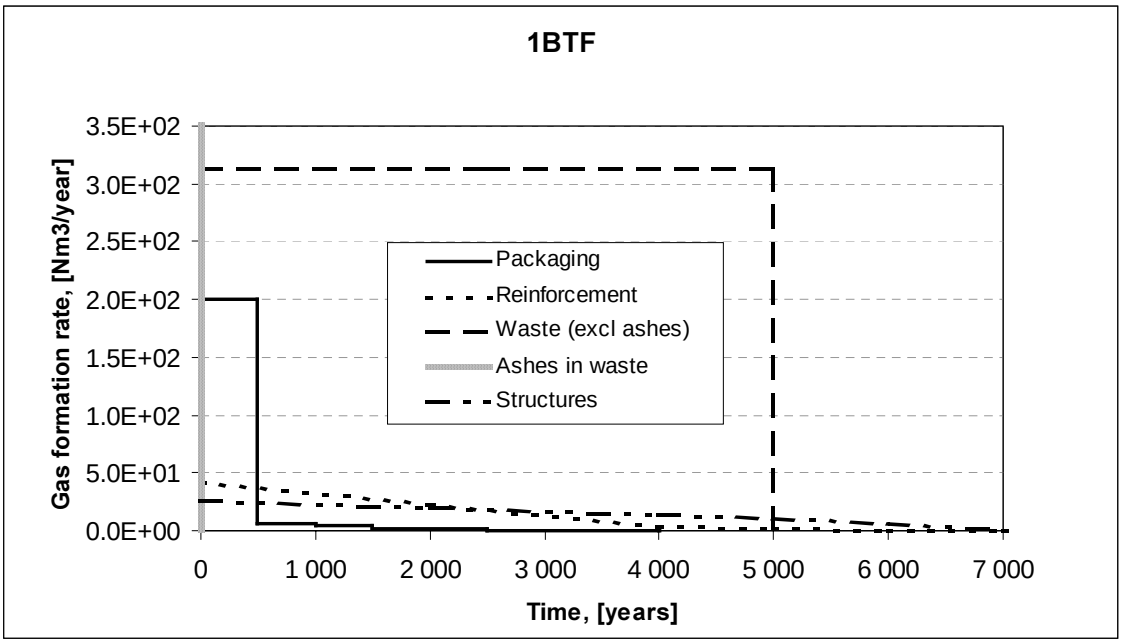

Figure 3-7. *Gas formation rates due to corrosion in 1BTF, (Nm^3/year). 0–7 000 years.*

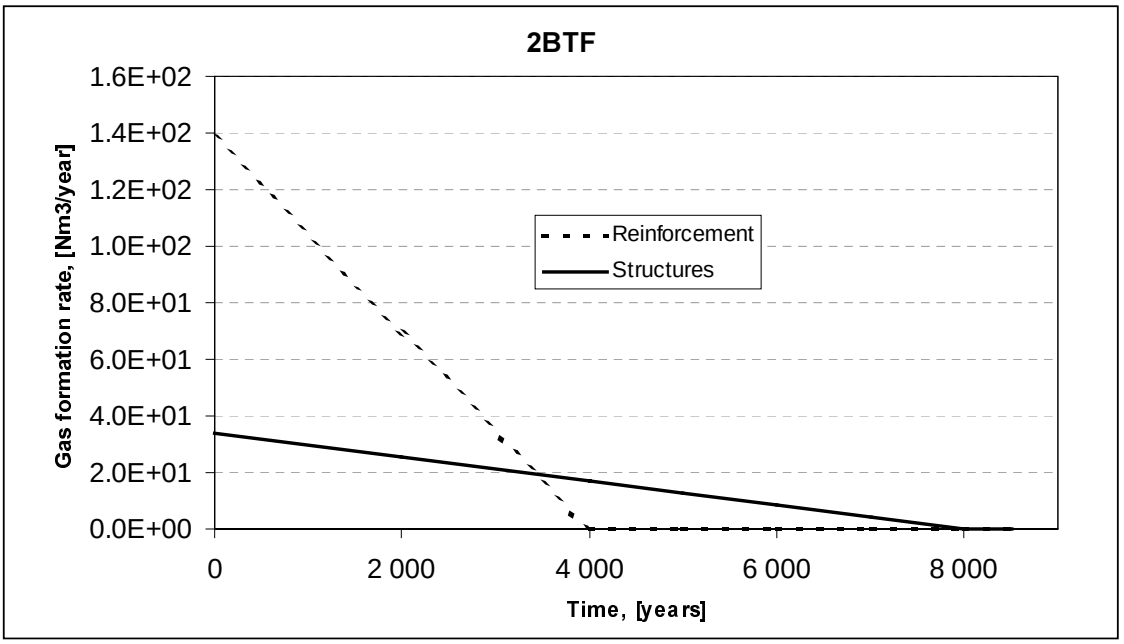

Figure 3-8. *Gas formation rates due to corrosion in 2BTF, (Nm^3/year). 0–9 000 years.*

Table 3-6. Initial gas formation rates and maximum theoretical gas volume that can be generated due to corrosion of metals in 2BTF.

	Initial gas formation rate (Nm^3/year)	Maximum theoretical gas volume (Nm^3)
Reinforcement	138	$2.8 \cdot 10^5$
Structures	34	$1.4 \cdot 10^5$
Total	**173**	**$4.1 \cdot 10^5$**

3.2.4 The BLA vault

The estimated gas generation rates in the BLA vault from corrosion of metals in waste packages are calculated using the amounts and dimensions of different materials in BLA given in Appendix A. Quantities given as the sum of aluminium and zinc have been assumed to be aluminium. The results are given in Figures 3-9 and 3-10 and in Table 3-7. In the BLA vault the only concrete structure is the bottom which is made of reinforced concrete.

The gas generation rates are calculated for packaging (steel), waste (steel and aluminium) and structures (reinforcement) separately. Gas from reinforcement is not found in the figures or the table below, since no concrete packagings are used in BLA.

For the first 2.5 years corrosion in BLA aluminium in the waste will dominate the gas formation, see Figure 3-9.

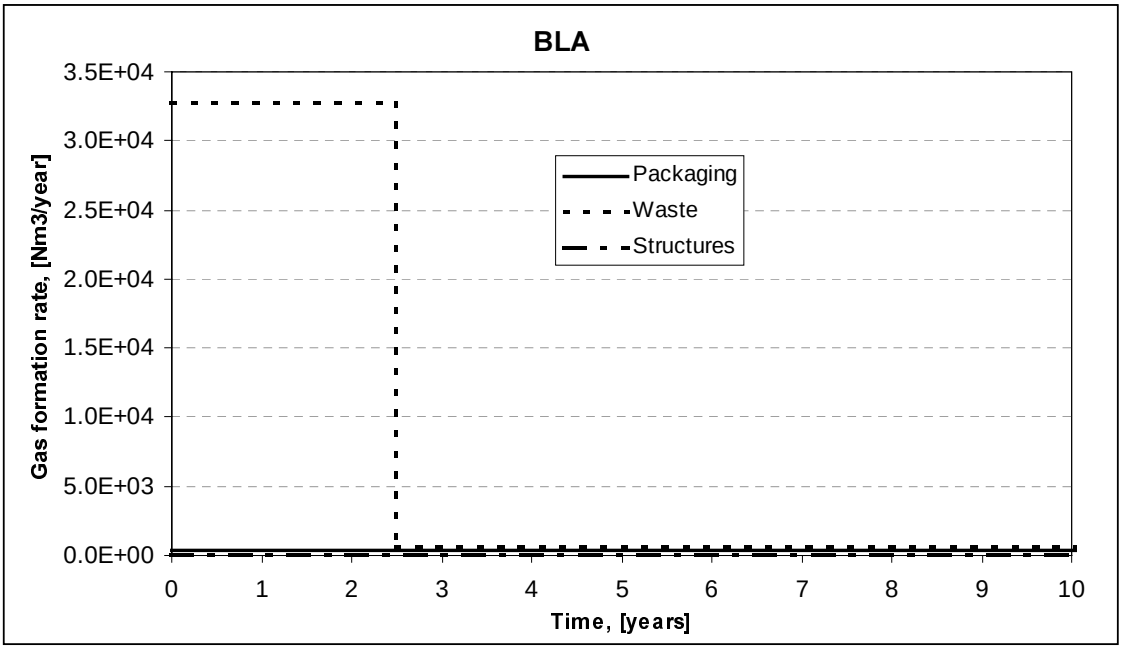

Figure 3-9. *Gas formation rates due to corrosion in BLA, (Nm^3/year). 0–10 years.*

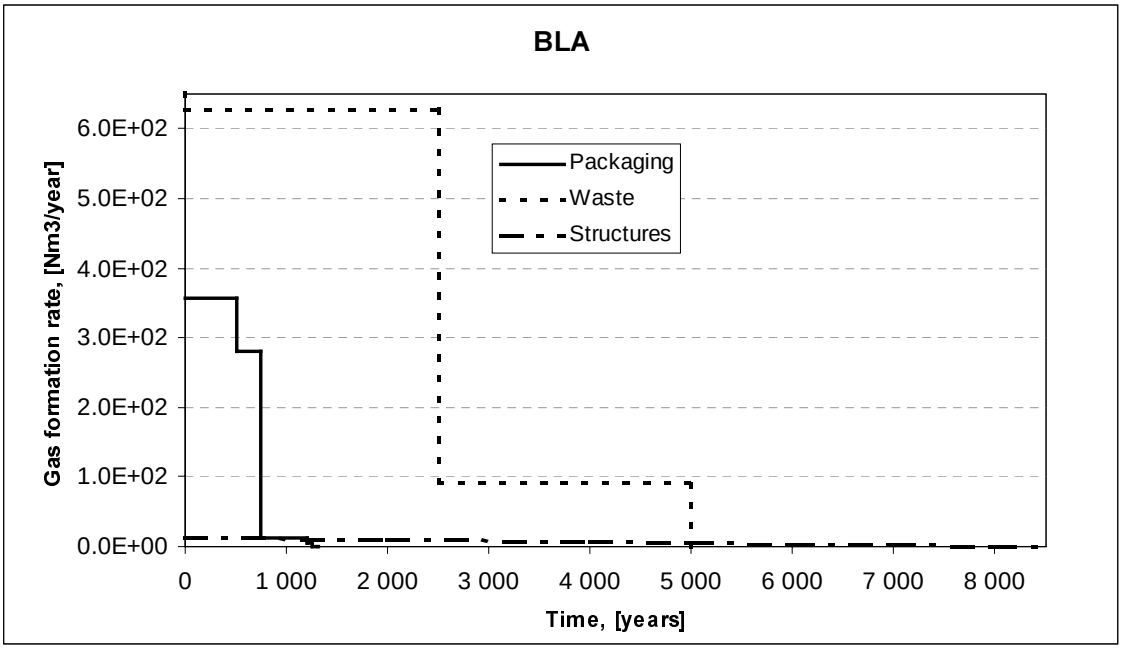

Figure 3-10. *Gas formation rates due to corrosion in BLA, (Nm^3/year). 0–8 500 years.*

Table 3-7. Initial gas formation rates and maximum theoretical gas volume that can be generated due to corrosion of metals in BLA.

	Initial gas formation rate (Nm^3/year)		Maximum theoretical gas volume (Nm^3)	
Packaging		358		$2.5 \cdot 10^5$
Waste		32 800		$1.9 \cdot 10^6$
steel	*628*		*$1.8 \cdot 10^6$*	
aluminium	*32 200*		*$8.0 \cdot 10^4$*	
Structures		13		$5.0 \cdot 10^4$
Total		**33 200**		**$2.2 \cdot 10^6$**

The high rate for gas generation from aluminium is explained by the large amount of aluminium present in the BLA vault. However, since the aluminium is completely depleted after 2.5 years, the total gas volume generated is small, see Table 3-7.

3.3 Gas generation in SFR due to microbial degradation of organic material

The initial gas formation rates and the maximum theoretical gas volumes that can be generated due to microbial degradation of organic material in the different repository parts in SFR are given in Table 3-8.

Table 3-8. Initial gas formation rates and maximum theoretical gas volume that can be generated due to microbial degradation of organic material in SFR.

	Initial gas formation rate (Nm^3/year)	Maximum theoretical gas volume (Nm^3)
Silo		
Cellulose	20.1	$3.7 \cdot 10^3$
Other organics	1.0	$1.5 \cdot 10^4$
Resins+bitumen	(98.6)	($1.5 \cdot 10^6$)
BMA		
Cellulose	235	$4.4 \cdot 10^4$
Other organics	6.1	$9.2 \cdot 10^4$
Resins+bitumen	(65.4)	($9.8 \cdot 10^5$)
1BTF		
Cellulose	0.2	32
Other organics	0.5	$8.0 \cdot 10^3$
Resins+bitumen	(5.6)	($8.4 \cdot 10^4$)
2BTF		
Cellulose	0	0
Other organics	2.1	$3.1 \cdot 10^4$
Resins+bitumen	(20.2)	($3.0 \cdot 10^5$)
BLA		
Cellulose	953	$1.8 \cdot 10^5$
Other organics	34.8	$5.2 \cdot 10^5$
Resins+bitumen	(4.7)	($7.0 \cdot 10^4$)

The gas generation rates have been calculated for cellulose and other organics, such as plastics, ion exchange resins and bitumen. However, material such as ion-exchange resins and bitumen are thought to degrade so slowly that the gas formation rate can be neglected. Therefore the rates for resins and bitumen are shown separated in Table 3-8 and in the tables given in the summary, see Section 3.5.

3.4 Gas generation in SFR due to radiolysis

The estimated gas generation rates and theoretical volumes of gas that can form in the different repository parts due to radiolysis of water in waste matrices and surrounding materials are given in Table 3-9.

Table 3-9. Calculated gas formation rates at 1 year and at 10 years after closure of the repository and theoretical gas volumes at 10 000 years.

	Gas formation rate at 1 year (Nm^3/year)	Gas formation rate at 10 years (Nm^3/year)	Theoretical gas volume at 10 000 years (Nm^3)
Silo	3.1	1.8	160
BMA	0.13	0.077	7.1
1BTF	0.010	0.0063	0.98
2BTF	0.016	0.010	0.75
BLA	0.0021	0.0014	0.27

The amount of gas formed in the different repository parts is governed by the activity of the radionuclides and the half-life of the radionuclides is a measure of the time during which gas will be formed.

In a short time perspective, the total amount of gas formed is dominated by the amount of gas formed from the decay of ^{60}Co in all the different repository parts, followed by ^{137}Cs. In a longer term, more than 1 000 years, different radionuclides dominate the amount of gas formed for different repository parts. The amount of gas formed in the Silo at 1 000 years is dominated by ^{241}Am followed by ^{60}Co. For BMA and 2BTF the gas formation at 1 000 years is dominated by irradiation of water by ^{60}Co and ^{137}Cs. In 1BTF the largest amount of gas at 1 000 years originates from ^{14}C (both organic and inorganic) and ^{137}Cs and finally in BLA the amount of gas formed at 1 000 years is dominated by ^{137}Cs and ^{240}Pu.

The gas generation rates due to radiolysis of water calculated for the different repository parts are negligible in comparison to the rates due to metal corrosion. The maximum theoretical gas volumes are calculated as the sum of gas volumes from irradiation of water by all radionuclides during 10 000 years. In comparison to the gas volumes formed due to corrosion, the volumes due to radiolysis are negligible for all repository parts.

3.5 Summary of gas generation rates and gas volumes

A summary of gas formation rates and total volumes of gas formed in the different repository parts in SFR due to different processes are given in Table 3-10 and 3-11. The dominating processes for gas formation are corrosion and microbial degradation of organic material. Radiolysis produces only negligible amounts of gas.

Table 3-10. Gas formation rates for different repository parts in SFR.

	Gas formation rates				
	Silo (Nm^3/year)	**BMA (Nm^3/year)**	**1BTF (Nm^3/year)**	**2BTF (Nm^3/year)**	**BLA (Nm^3/year)**
Corrosion					
Steel	840	670	580	170	1 000
Al + Zn	1 100	7 000	27 000	0	32 000
Microbially					
Cellulose	20	240	0.2	0	1 000
Other org.	1	6	0.5	2	30
Resins+bitumen	(100)	(65)	(6)	(20)	(5)
Radiolysis					
0–1 years	3	0.1	0.01	0.02	0.002
(10 years)	(2)	(0.08)	(0.006)	(0.01)	(0.001)

Table 3-11. Total gas volumes for different repository parts in SFR.

	Accumulated gas volumes				
	Silo (Nm^3)	**BMA (Nm^3)**	**1BTF (Nm^3)**	**2BTF (Nm^3)**	**BLA (Nm^3)**
Corrosion					
Steel	2 100 000	1 800 000	1 900 000	410 000	2 100 000
Al + Zn	2 700	18 000	53 000	0	80 000
Microbially					
Cellulose	3 700	44 000	30	0	180 000
Other org.	15 000	92 000	8 000	31 000	520 000
Resins+bitumen	(1 500 000)	(980 000)	(84 000)	(300 000)	(70 000)
Radiolysis					
0–10 000 years	< 200	< 10	≈ 1	< 1	< 1

3.6 Heat generation in SFR due to corrosion and radiolysis

Besides generating gas, processes occurring in the repository can also generate heat. Examples of such processes are corrosion of metals and radiolysis of water. The corrosion of aluminium is an exothermic process, which means that it generates heat. Since the aluminium in SFR is expected to be completely degraded in only a few years the amount of heat generated by corrosion of aluminium in a short time may be significant. Simplified calculations have been made to quantify the effect. The amount of heat generated from radiolysis of water has also been included.

The heat that can be generated from corrosion of aluminium can be estimated from the ΔH_f-value for the chemical reaction. The heat generated from radiolysis can be calculated using values for energy per transformation of the nuclides (alpha, beta and gamma radiation).

In the calculations the repository parts in SFR were approximated to cylinders and the volume of rock from the interface of the repository and 6 metres out was estimated. Data on dimensions of the repository was taken from Chapter 2 and Appendix A. Effects of uptake of heat by other materials in the repositories have not been considered. The heat generated has been assumed to be distributed in the water present in the vault and in the adjacent rock. All the void volumes in the structures and waste packages in the different repository parts are assumed to be filled with water.

Values of properties of water and rock used in the calculations are given in Table 3-12.

Table 3-12. Properties of water and rock used in the calculations.

	Heat capacity, (kJ/kg,K)	Density, (kg/m3)
Water	4.18	1 000
Rock	0.80	2 700

The results from the calculations are given in Table 3-13. Data on quantities of materials and void volumes in the waste packages and the structures from Appendix A have been used in the calculations. The results indicate that the temperature elevation due to heat generating processes does not exceed 5 degrees in any of the repository parts. The theoretical annual heat transport capacity for the rock adjacent to the repository has been concluded to exceed the heat produced. The effect of heat transport on the temperature elevation has not been included in the calculations, but would probably contribute to a lower increase in temperature. However, locally, the temperature increase could probably be significantly higher than Table 3-13 shows.

Table 3-13. Energy generated in the different repository parts and the resulting temperature elevation in the water in the repository and the adjacent rock.

	Energy from Al corrosion (J)	Energy from radiolysis, first 10 years (J)	Temperature elevation, (K)
Silo	$3.3 \cdot 10^{10}$	$1.6 \cdot 10^{11}$	1.7
BMA	$2.1 \cdot 10^{11}$	$6.9 \cdot 10^{9}$	1.2
1BTF	$6.4 \cdot 10^{11}$	$5.6 \cdot 10^{8}$	3.8
2BTF		$9.3 \cdot 10^{8}$	0.01
BLA	$9.6 \cdot 10^{11}$	$1.2 \cdot 10^{8}$	4.6

4 Conceptual model of gas escape and effects on radionuclide release

4.1 General

After the repository is sealed, the water pressure in the repository is restored to the same pressure as in the surrounding rock. During this period water flows into the repository vaults and concrete structures. The re-saturation of the Silo takes about 20 years, but for the other parts of the repository the re-saturation takes only a few years /Holmén and Stigsson, 2001a/. Due to the relatively short time required to re-saturate the repository, it is assumed that all pores and voids in the Silo become completely water-filled when the repository is sealed. This means that all the air initially present in the encapsulation has to be expelled, consumed or dissolved in the water. If air is even present in the concrete structure when the gas generation starts, the volume of water to be expelled in the initial period from the respective structures will be smaller.

Gas is generated in the SFR repository from different sources. The most important source for gas generation is the anaerobic corrosion of metals, mainly iron, aluminium and zinc. Gas may also be generated by degradation of organic materials, as for example cellulose, and by radiolysis. However, the gas generation rate from these two last sources is expected to be small, see Section 3.5.

Gas can not flow through water saturated concrete, therefore water is expelled from the concrete (concrete structure, backfill concrete and cement-conditioned waste) to create paths for the gas flow. Moreover, water may also be expelled from the encapsulation to equilibrate the inner overpressure with the pressure existing outside of the structure. When paths for the gas flow have been created and the pressures have been equilibrated, no more water will be expelled from the repository.

The impact of the gas production on the radionuclide release may be important in the Silo, BMA, and BTF. The gas production may result in potentially contaminated water being expelled into the gravel/sand around the concrete structure and finally into fractures in the rock surrounding the repository.

Here, we discuss the basic concepts upon which the models used in these calculations are based. The assumed gas generation rates in the calculations are given and the availability of water is firstly discussed. The conditions under which gas may flow through water saturated porous media are also discussed. Finally the conditions existing in the different parts of the repository are considered in detail.

4.2 Gas generation

The gas generation in the first years is very high and it is mainly caused by the anaerobic corrosion of aluminium. After the aluminium has been corroded, the gas generation is determined mainly by the corrosion of iron. As shown in Chapter 3 (in this report) for the Silo the initial gas generation rate will be about 1900 Nm^3/year. After 2.5 years,

when the aluminium has been depleted, this gas generation decreases to 800 Nm^3/year. The gas production will then be 250 and 100 m3/year measured at the pressure existing in the Silo (an average pressure of 750 kPa is considered).

For BMA the situation is more pronounced. The gas production rate is initially about 7700 Nm^3/year and decreases to 700 Nm^3/year when aluminium has been consumed after 2.5 years. For 1BTF, the initial gas generation is very high, about 27 000 Nm^3/year due to the corrosion of the ashes. Later the gas generation rate is maintained at about 600 Nm^3/year for a long time. For 2BTF the gas generation rate is small, about 200 Nm^3/year.

Another aspect that is interesting to discuss is the water availability. Water is needed for the hydrogen evolving corrosion of metals (iron, aluminium) to take place. However, the volume of water is quite small. For each Nm^3 of gas generated, only about one litre of water is required. This means that, in general, water availability is not a limiting factor for the gas generation. Even, when a certain volume of water has been expelled from the concrete (or cement-conditioned waste), there is enough water to continue the corrosion process. The volume of water that may be expelled from concrete to allow gas flow and to equilibrate the overpressure in the interior of the encapsulation is only a few percent of the total porosity.

Water availability may be a limiting factor, only during the initial stage before the repository has been re-saturated. This may be the case, for example, for the waste contained in steel packages, which could be kept dry for a certain period of time. However, due to the pressure difference and that they are not hermetically closed, it is expected that water penetrates them.

4.3 Gas transport through the concrete

Gas can not flow through a water saturated porous media, like concrete. A volume of water has to be expelled from the porous medium to create a network of connected pores to allow the gas to flow. This means that a volume of potentially contaminated water may be directly pushed out from the repository.

Regarding the gas flow, the capillary effects of the material must be accounted for, they become important in materials with very fine pore structures, such as bentonite and concrete. The finer pores will suck in water even against a considerable gas pressure in the pores. Thus an incompletely saturated bentonite or concrete will tend to suck up the water from the surroundings. The suction capillary pressures may be large (many tens of atmospheres). The process works the other way also. Once the material is filled with water, a considerable pressure is needed to expel the water from the pores. Once the gas starts to flow, only the larger pores will be purged of water because of their lower capillary pressure. If the gas generation rate is increased, more water will be purged to open more pores. For a given gas flow a steady state will be reached where just enough larger pores are empty to allow the gas to escape. Depending on the pore size distribution and the structure of the material the amount of water expelled may vary considerably.

Water expulsion occurs when gas starts to be produced and paths are opened in the concrete for the gas flow. The capillary forces decide the pressure that is needed to open these paths. The capillary pressure is a function of the capillary radius,

$$P_c = \frac{2 \cdot \sigma}{r_m}$$

where P_c is the capillary pressure (Pa), • is the surface tension (N/m) and r_m is the capillary radius (m).

The construction concrete has a very fine pore structure, this means that very high pressures are needed to expel water from the concrete and allow the gas to flow. For good construction concrete this pressure may be as high as 1.5 MPa /Möller et al., 1981/. The concrete structures in SFR are not designed for these high pressures and they will be damaged if gas can not escape from the encapsulation. For this reason evacuation pipes were installed in the concrete lid of the Silo. However, if the concrete has small fractures, gas flow may be established through these fractures at a lower pressure. For example for fractures with apertures of 10 μm the gas flow may be established with an overpressure of only 15 kPa.

Neglecting the capillary effects, the gas flow through a fracture may be calculated from the flow through a slit,

$$Q = \frac{b^3 \cdot W}{12 \cdot \mu} \frac{\Delta P}{\Delta L}$$

where Q is the gas flow (m^3/s), b is the fracture aperture (m), W is the length of the fracture, μ is the dynamic viscosity (Ns/m^2), L is the thickness of the wall and P is the pressure (Pa).

One fracture of 10 μm per m of concrete wall corresponds to the hydraulic conductivity assumed for concrete in SFR. Figure 4-1 shows the gas flow rate as a function of the fracture aperture for 15 and 50 kPa of overpressure. A thickness of 0.50 metre is assumed for the concrete wall. A larger fracture or slit would result in a lower capillary pressure and thereby the internal overpressure necessary for initiating gas release would be lower.

The capacity of the fractures in the rock surrounding the repository to transport the gas has been calculated. The results show that the fracture system that usually exist in the rock has a large transport capacity for the gas and that only a few fractures are required to transport away the gas generated in the repository /Braester and Thunvik, 1988/. Gas breakthrough occurs very fast and the gas is transported through the most permeable fractures while the water in the fractures with lower permeability is almost stagnant /Thunvik and Braester, 1990; Berger and Braester, 2000/.

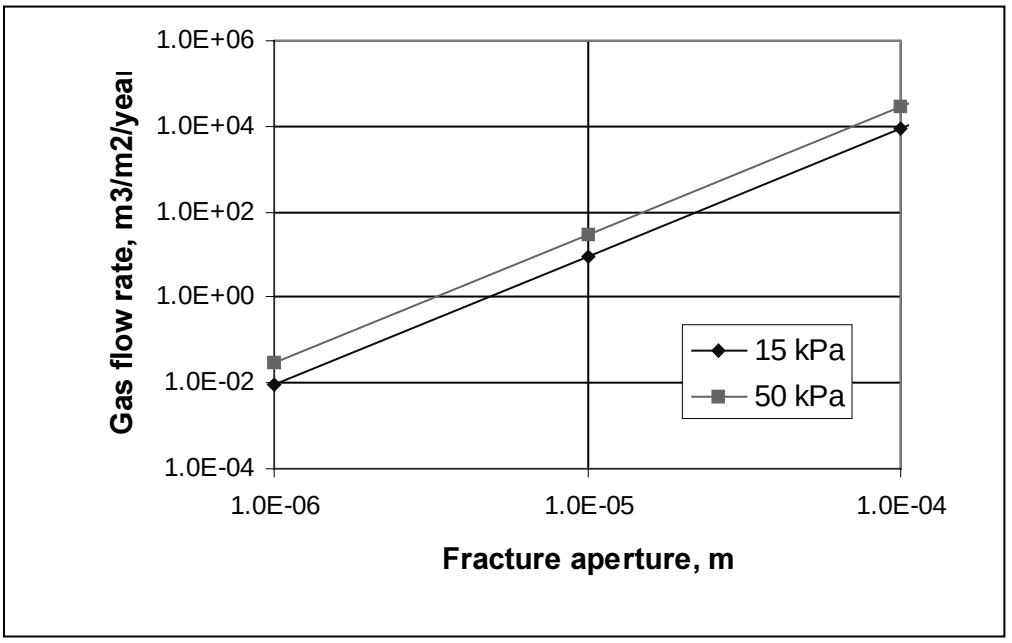

Figure 4-1. *Gas flow rate as a function of the fracture aperture for two different internal overpressures.*

4.4 Silo

The gas generated in the interior of the Silo (waste packages and inner Silo walls) firstly flows through the porous concrete and reaches the evacuation pipes located at the Silo lid. Through the evacuation pipes, the gas reaches the sand and sand-bentonite layers located on the top of the Silo and the gravel/sand filling above them. Finally the gas flows into fractures in the rock surrounding the Silo vault.

At the beginning, the activity in the Silo is situated only in the interior of the waste packages. With time, the walls of the concrete moulds and the porous concrete surrounding the moulds become contaminated by diffusion. Radionuclides may be also transported into the porous concrete with the water expelled from the moulds or drums containing the waste. If the gas generation starts very early, very little or negligible contamination will be expelled from the Silo since the activity of the pore-water in the porous concrete is small.

With the time the pore-water in the porous concrete will be contaminated by radionuclides. The time to reach, a certain concentration in the porous concrete is dependent upon the nuclide properties. Two cases may be distinguished: before the start of the anaerobic corrosion and after it.

Before the start of the anaerobic corrosion, it is expected that the steel packages (moulds and drums) are intact and no contamination escapes through the steel wall. Activity into the porous concrete is only transported by diffusion through the concrete walls of the concrete moulds. In this case the time to reach a significant concentration in the porous concrete is expected to be of the order of a few years for non-sorbing species. But, even for weakly sorbing radionuclides, this time is expected to be quite long.

Due to the presence of waste containing aluminium, it is expected that the corrosion of metals and gas generation start early and that during the first year, enough water is expelled from the porous concrete to allow the gas flow. In the model, it is assumed that after the initial period (about one year) the steel packages are totally corroded and they can not prevent the migration of radionuclides contained in the waste into the porous concrete. For the steel packages with cement-conditioned waste, the diffusion resistance through the cement-waste mixture is small and the transport of radionuclides into the porous concrete is important. The situation is different for the steel packages with the bitumen-conditioned waste. In this case, even if the steel wall of the package has been totally corroded the radionuclides in the bitumen mixture are not available for dissolution in the water in the package. These radionuclides are dissolved only when the bitumen matrix has been degraded. It is assumed that they are released from the bitumen matrix over a 100-year time scale /Pettersson and Elert, 2001/.

4.4.1 Processes during opening of gas pathways

When the gas production starts all pores and voids in the Silo are completely water-filled. To allow gas escape from the Silo, paths for the gas flow have to open in the interior of the Silo. Therefore, water is expelled from the concrete until a network of gas-filled pores is formed which allow the gas escape from the evolution sites to the top of the Silo. If the gas generation rate is increased, more water has to be expelled in order to open more pores.

The water expelled from the Silo during the pressure build up period may escape through the evacuation pipes or through the Silo walls. The water distribution between these paths is determined by the hydraulic conductivity of the concrete, bentonite and sand-bentonite. The fresh concrete may have a very low hydraulic conductivity leading to a very high resistance to flow. For this reason in these calculations, the situation where all this water volume is expelled through the evacuation pipes is addressed.

The water expelled through the gas evacuation pipes enters the sand layer and sand-bentonite sealing on top of the Silo and pushes out an equivalent volume of non-contaminated water. Since the expected water flow through the sand layer and sand/bentonite layers is small, less than one metre per year, it is expected that the dispersion is negligible. Diffusion and sorption on the sand and sand-bentonite are considered.

4.4.2 Decreasing water level due to pressure build up

The gas expelled through the evacuation pipes enters the sand layer on top of the Silo. Since the sand layer is covered with a sealing layer of sand mixed with bentonite, overpressure is needed to open up flow pathways through the sealing layer. Push and Hökmark /1987/ found that overpressure of about 15 kPa is needed to open the sand-bentonite layer to the gas flow. However, in these calculations it is conservatively assumed that an overpressure of 50 kPa is needed. When an overpressure in the interior of the Silo has built up, the water not bound by capillary forces is expelled from the Silo. Water is expelled through the outer wall and the bottom, until equilibrium is reached between the pressure inside the Silo and the pressure at the surroundings. The voids in the Silo below the water level are then completely water saturated except for the gas-filled paths needed for the gas flow. The porosity above the water level still contains water bound by capillary forces. For an overpressure of 50 kPa, the water level is lowered by 5 m.

When the overpressure and water level in the Silo balance each other, equilibrium is reached and water is no longer pushed out from the Silo. After this, radionuclides are released from the Silo by diffusion through the Silo wall, top and bottom.

Once that the initial processes are completed, a volume of potentially contaminated water has been pushed out into the concrete in the outer Silo wall and the bottom. If the volume of water expelled into the Silo walls is larger than the sorption capacity (pore volume for non-sorbing species) of the concrete walls and bottom, some contaminated water may flow into the bentonite or sand-bentonite. The water expelled through the evacuation pipes is located in the sand and sand-bentonite, at the top of the Silo.

4.5 BMA

The gas generated in the waste packages and in the concrete structure flows into the water filled space in the interior of the encapsulation. The gas will reach the top of the encapsulation and it is expected to escape through gaps between the concrete lid and the walls of the structure reaching the sand/gravel at the top.

The waste in BMA is conditioned with cement or bitumen and deposited in concrete moulds or steel packages (moulds and drums). The activity is initially located only in the waste and subsequently in the water in the waste packages. With time, the walls of the concrete moulds, and finally the water that filled the void between the waste packages will be contaminated. The transport of the radionuclides from the waste occurs mainly by diffusion. A fraction of the activity in the interior of the waste packages may be transported with the water expelled by the effect of the gas generation.

If the gas generation starts early, very little or negligible contamination will be expelled from BMA since the activity of the water surrounding the waste packages is small. With time this water will be contaminated by radionuclides. The time to reach a significant concentration of the dissolved radionuclides depends on nuclide properties. It is expected that before the start of the corrosion, the steel containers are intact and no contamination escapes from them. Activity into the water surrounding the waste packages is only transported by diffusion through the concrete walls of the concrete moulds. In this case the time to reach a significant concentration in the porous concrete is expected to be of the order of a few years for non-sorbing species and longer times for the sorbing radionuclides

Due to the presence of waste containing aluminium, it is expected that the corrosion of metals and gas generation start early and that during the first year enough water is expelled from the porous concrete to allow the gas flow. After the start of the gas production (about one year) it is assumed that the steel packages are totally corroded and they can not prevent the transport of radionuclides contained in the waste into the porous concrete. The diffusion resistance for the cement-conditioned waste is small and therefore the transport of radionuclides into the water surrounding the waste packages is fast. For the bitumen-conditioned waste, even if the steel wall of the package has been totally corroded the radionuclides in the bitumen mixture are not available for dissolution in the water around the waste packages. They are available only when that the bitumen has been degraded. It is assumed that they are released from the bitumen matrix over a 100-year period /Pettersson and Elert, 2001/.

4.5.1 Processes during opening of gas pathways

It is assumed that all pores and voids in the repository are completely water-filled when gas production starts. To allow gas to escape from the waste packages and the concrete structure walls, gas filled paths must be created in the concrete. Therefore, water is expelled from the concrete until a network of empty pores is created. If the gas generation rate is increased, more water has to be expelled in order to open more pores.

When the gas generation starts and water is expelled from the waste packages, water escapes through the lateral walls, the bottom and the lid on the top of the concrete structure. The distribution between the different paths is determined by the relative thickness of the walls. In this case is assumed that all the water escapes through gaps between the lid and the walls in the top of the encapsulation.

The gas generated in the interior of the concrete encapsulation has to escape from the encapsulations into the gravel/sand filling surrounding the concrete construction. It is expected that the gas generated in the interior of the encapsulation escapes through gaps between the lid and the walls. In this case no overpressure is created in the interior of the encapsulation.

If there are no gaps between the lid and the walls the gas has to escape through the concrete. However, intact concrete has a very fine pore structure and this implies that a high pressure is required to allow gas to flow through it. The concrete construction is not designed to support such a high pressure and fractures will be created in the concrete walls through which the gas may then escape.

4.5.2 Decreasing water level due to pressure build up

If the gas escapes through gaps between the lid and the walls, no overpressure is created in the interior of BMA and no more water need be expelled. However, if gaps do not exist, an overpressure will be created in the BMA encapsulation. In this case a certain overpressure is required to expel the gas generated in the interior of the concrete structure. For poor concrete with small fractures (e.g., with apertures of 10 μm), this overpressure is about 15 kPa. The pressure in the interior of the concrete construction has to be equilibrated with the pressure in the surroundings, and a certain volume of water is expelled from BMA to lower the water level. The water level needs to be lowered by 1.5 m in order to compensate the overpressure of 15 kPa. Water is expelled through the lateral walls and the bottom, until equilibrium is reached. The porosity above the water level still contains water bound by capillary forces.

When the overpressure and water level in BMA balance each other, equilibrium is reached and water is no longer pushed out from BMA. After this, radionuclides are released by diffusion through the walls.

4.6 BTF

There are mainly three types of packages in 1BTF, concrete moulds, concrete tanks and steel drums. The steel drums will be deposited in six fictitious sections in 1BTF. In each section, the steel drums occupy the central part of a room. The concrete tanks (1.2 x 3.3 m and 2.2 m in height) are used to form the lateral walls and the concrete moulds

(1.2 x 1.2 x 1.2 m) form the walls between the sections. The remainder of 1BTF is mainly filled with concrete tanks. In this last part, gas is mainly generated by corrosion of the iron used as reinforcement in the concrete tank walls.

In 2BTF there are only concrete tanks with unsolidified resins. In this case the gas generation is small and mainly due to corrosion of the iron used as reinforcement. It is expected that the effect of the gas generation from 2BTF is much less than from 1BTF. For this reason the effect of the gas generation on the radionuclide release is only calculated for 1BTF.

The activity is initially located only in the waste and in the water in the interior of the respective package. With time, the walls of the concrete moulds and tanks and the concrete filling between the waste packages will be contaminated. The transport of the radionuclide from the waste occurs mainly by diffusion. A fraction of the activity in the interior of the packages may be transported out from the packages with the water expelled by effect of the gas generation.

The activity contained in the steel drums can not be transported out through the steel walls. It is expected that the steel will be intact for some years. The backfill concrete will be contaminated initially by radionuclides diffusing from the concrete moulds and tanks and by the water expelled from the waste packages.

4.6.1 Processes during opening of gas pathways

The potential gas production rate of the ashes contained in the steel drums is very high initially. The steel drums actually consist of two steel drums, the drum containing the ashes is deposited in another steel drum and the space between them is filled with concrete. The gas generation may start after water has penetrated the waste (ashes). It is expected that water may reach the waste owing to that the steel drums are not hermetically closed.

Due to the presence of ashes containing aluminium, it is expected that the gas generation starts early in the sections where the steel drums with the ashes are located. It is also assumed that during the first year enough gas is generated to expel the pore water from the concrete backfill needed to allow the gas flow. If the gas generation from the ashes starts simultaneously in many drums, the water flow may be quite high and a large overpressure may be created in the backfill concrete surrounding the steel drums. Fractures will then be created in the concrete to release the overpressure. This may increase the water flow through the backfill.

The gas generated in the waste flows through the backfill concrete into the sand/gravel located at the top and bottom of the structure. Gas may also flow directly into the rock surrounding the 1BTF vault.

4.7 BLA

Most of the waste allocated to BLA is unsolidified trash in ISO-containers. Moreover there are some steel drums with bituminised resins and odd waste. BLA is not foreseen to be backfilled at repository closure. The gas generation potential is very large.

The activity is initially located in the interior of the containers. It is, however, expected that the radionuclides will be dissolved in the water in the vaults very soon after closure of the repository. The radionuclides will be transported from the vault by the water flowing through it.

It is also expected that the gas generated in BLA and others vaults may escape through the fractures in the rock without any significant build-up of pressure inside the vaults /Braester and Thunvik, 1988; Thunvik and Braester, 1990; Berger and Braester, 2000/. This means that only a small volume of water will be expelled from BLA when gas generation starts. For this reason the effect of the gas generation on the radionuclide release in BLA is not calculated.

5 Data

To study the consequences of gas generation in the repository on the radionuclide release, gas and water flows have to be calculated. Since gas can not flow through water saturated porous media, a certain volume of water has to be expelled from the porous media to allow the gas flow. Moreover, due to overpressures in the interior of the encapsulations some volumes of water are also expelled. Here, data about the capillary pressure and permeability of the different materials are presented. In addition, sorption, diffusivity and other physical data are also shown.

5.1 Capillary pressure and capillary bound water

Capillary forces bind the water in porous media and they must be accounted for. The capillary effects are important in materials with a fine porous structure such as construction concrete and bentonite. This means that to expel water from porous media with a fine porous structure considerable pressures may be required.

For bentonite it is expected that the capillary pressure is very high, and no gas flow is possible. For intact construction concrete, the capillary pressure is about 1.5 MPa /Möller et al, 1981/, therefore very high pressures are needed to press the gas through intact construction concrete. But, the Silo and the encapsulations in the other storage tunnels are not designed to support such a high pressure and the walls will be damaged. Small fractures in concrete crossing the entire wall thickness, are sufficient to reduce significantly the capillary pressure required to start the gas flow. The capillary pressure for fractures of 10 μm is 15 kPa (See Chapter 4). The capillary pressures for the porous concrete used as backfill in the Silo, BMA, and 1BTF are quite low.

To allow gas flow through porous materials water has to be expelled from the largest pores to create a network of gas filled channels. The volume of water to be expelled is determined by the pore structure of the porous medium. In experiments, it was found that the volume of water to be expelled from the porous concrete is at most about 2% of the water content in the sample /Björkenstam, 1996, 1997/. These measures were performed using a gas flow of about 100 m^3/m^2year, which is several times larger than the gas flow found in the Silo and BMA (See Appendix C). The pressures used in these experiments were about 10 kPa.

For construction concrete, it is expected that the value is lower, however the same value of 2% of the water is considered.

5.2 Hydrological data

The water flow rate through the different repository parts of SFR has been estimated and is discussed in detail elsewhere /Holmén and Stigsson, 2001b/. The total water flow rate through the different repository parts of SFR as estimated in the detailed hydrology

modelling is given in Table 5-1. The values and directions of the water flows were simplified when they were introduced into the migration model.

Table 5-1. Total flow through different repository parts /Holmén and Stigsson, 2001b/.

Repository part	Total flow (m^3/yr) at 2000 AD
BTF1: Encapsulation	2.4
BTF1: Whole tunnel	7.5
BTF2: Encapsulation	2.4
BTF2: Whole tunnel	6.7
BMA: Encapsulation	0.07
BMA: Whole tunnel	8.7
SILO: Encapsulation	0.23
SILO: Filling at the top	0.53

To calculate the water flow rate through the different parts of the repositories, the hydraulic conductivity is required. Hydraulic conductivity of the different materials used in the repositories is shown in Table 5-2.

Table 5-2. Hydraulic conductivity of the materials /SKB, 2001/.

Materials	Hydraulic conductivity m/s
Structural concrete	$8.3 \cdot 10^{-10}$
Concrete backfill in Silo and BMA (Porous concrete)	$3 \cdot 10^{-08}$
Concrete backfill in BTF	$3 \cdot 10^{-09}$
Cement mortar used as waste conditioning	–
Bentonite in Silo, upper part	$2 \cdot 10^{-10}$
Bentonite in Silo, lower part	$2 \cdot 10^{-12}$
10/90 sand/bentonite	$1 \cdot 10^{-09}$
Sand/gravel	High

5.3 Physical and chemical data

Values on density, porosity and effective diffusivity for the materials modelled in SFR are given in Table 5-3. Sorption coefficients used are compiled in Table 5-4. No sorption on bitumen has been accounted for.

Table 5-3. Physical data for materials used in SFR /SKB, 2001/.

Material	Bulk density (kg/m^3)	Effective diffusivity (m^2/s)	Porosity (m^3/m^3)
Structural concrete	2300	$1 \cdot 10^{-11}$	0.15
Porous concrete	2000	$1 \cdot 10^{-10}$	0.30
Gravel and sand	2190	$6 \cdot 10^{-10}$	0.30
Cement in conditioning	2300	$1 \cdot 10^{-10}$	0.20
Bentonite (dry)	1050	$1 \cdot 10^{-10}$	0.61
Sand/bentonite 90/10 (dry)	2000	$1 \cdot 10^{-10}$	0.25
Bitumen	1030	–	0
Water	1000	$2 \cdot 10^{-9}$	1

The equivalent water flow rate, Q_{eq}, used for representing the diffusive transport of radionuclides from the bentonite wall of the silo to the far field (host rock) is estimated to be 0.043 (m^3/year) /Romero et al., 1995/.

Table 5-4. Sorption coefficients K_d (m^3/kg) /SKB, 2001/.

Element	Concrete and cement	Gravel and sand	Bentonite	Bentonite/sand 10/90
H	0	0	0	0
C (inorganic)	0.2	0.0005	0	0.0005
C (organic)	0	0	0	0
Cl	0.006	0	0	0
Co	0.04	0.01	0.02	0.01
Ni	0.04	0.01	0.02	0.01
Se	0.006	0.0005	0	0.0005
Sr	0.001	0.0001	0.001	0.0002
Zr	0.005	0.005	0.0005	0.005
Nb	0.005	0.005	0	0.005
Mo	0.006	0	0	0
Tc	0.005	0.003	0.0001	0.003
Pd	0.04	0.001	0	0.0009
Ag	0.001	0.01	0	0.009
Cd	0.004	0.001	0.002	0.001
Sn	0.005	0	0.0001	0.00001
I	0.003	0	0	0
Cs	0.001	0.01	0.005	0.01

5.4 Radionuclide inventory

The estimated inventory of radionuclides in SFR at repository closure /Riggare and Johansson, 2001/ includes 60 radionuclides, Table 5-5 shows the inventory of the radionuclides that may be of importance when the gas consequences are studied.

Table 5-5. Radionuclide inventory (Bq) in SFR at repository closure (2030) /Riggare and Johansson, 2001/.

Nuclide	Half-life (years)*	Silo	BMA	1BTF	2BTF	BLA
^{3}H	12.3	$5.8\cdot10^{11}$	$3.3\cdot10^{10}$	$3.3\cdot10^{9}$	$5.3\cdot10^{9}$	$6.6\cdot10^{8}$
^{14}C inorg	5730	$2.0\cdot10^{13}$	$1.9\cdot10^{12}$	$2.3\cdot10^{12}$	$2.7\cdot10^{11}$	$3.9\cdot10^{10}$
^{14}C org	5730	$1.8\cdot10^{12}$!	$1.7\cdot10^{11}$	$1.8\cdot10^{11}$	$3.0\cdot10^{10}$	$3.3\cdot10^{7}$
^{36}Cl	301000	$4.7\cdot10^{10}$	$3.4\cdot10^{9}$	$3.0\cdot10^{8}$	$5.4\cdot10^{8}$	$8.2\cdot10^{7}$
^{60}Co	5.27	$1.8\cdot10^{15}$	$7.1\cdot10^{13}$	$5.4\cdot10^{12}$	$9.1\cdot10^{12}$	$1.0\cdot10^{12}$
^{59}Ni	76000	$2.1\cdot10^{13}$	$2.1\cdot10^{12}$	$1.8\cdot10^{11}$	$3.0\cdot10^{11}$	$3.9\cdot10^{10}$
^{63}Ni	100.1	$3.6\cdot10^{15}$	$3.2\cdot10^{14}$	$2.9\cdot10^{13}$	$4.7\cdot10^{13}$	$6.2\cdot10^{12}$
^{79}Se	1130000	$1.9\cdot10^{10}$	$1.4\cdot10^{9}$	$1.2\cdot10^{8}$	$2.2\cdot10^{8}$	$3.3\cdot10^{7}$
^{90}Sr	28.8	$2.4\cdot10^{14}$	$1.4\cdot10^{13}$	$1.3\cdot10^{12}$	$2.3\cdot10^{12}$	$3.6\cdot10^{11}$
^{93}Zr	1530000	$2.1\cdot10^{10}$	$2.1\cdot10^{9}$	$1.8\cdot10^{8}$	$3.0\cdot10^{8}$	$3.9\cdot10^{7}$
^{93m}Nb	16.1	$7.6\cdot10^{12}$	$4.9\cdot10^{11}$	$4.7\cdot10^{10}$	$7.6\cdot10^{10}$	$9.7\cdot10^{9}$
^{94}Nb	20300	$2.1\cdot10^{11}$	$2.1\cdot10^{10}$	$1.8\cdot10^{9}$	$3.0\cdot10^{9}$	$3.9\cdot10^{8}$
^{93}Mo	4000	$1.1\cdot10^{11}$	$1.0\cdot10^{10}$	$9.1\cdot10^{8}$	$1.5\cdot10^{9}$	$1.9\cdot10^{8}$
^{99}Tc	211000	$2.4\cdot10^{13}$	$1.7\cdot10^{12}$	$1.5\cdot10^{11}$	$2.7\cdot10^{11}$	$4.1\cdot10^{10}$
^{107}Pd	6500000	$4.7\cdot10^{9}$	$3.4\cdot10^{8}$	$3.0\cdot10^{7}$	$5.4\cdot10^{7}$	$8.2\cdot10^{6}$
^{108m}Ag	418	$1.2\cdot10^{12}$	$1.2\cdot10^{11}$	$1.0\cdot10^{10}$	$1.7\cdot10^{10}$	$2.2\cdot10^{9}$
^{113m}Cd	14.1	$8.2\cdot10^{11}$	$3.6\cdot10^{10}$	$3.6\cdot10^{9}$	$6.4\cdot10^{9}$	$1.0\cdot10^{9}$
^{126}Sn	100000	$2.4\cdot10^{9}$	$1.7\cdot10^{8}$	$1.5\cdot10^{7}$	$2.7\cdot10^{7}$	$4.1\cdot10^{6}$
^{129}I	$1.6\cdot10^{7}$	$1.4\cdot10^{9}$	$1.0\cdot10^{8}$	$9.1\cdot10^{6}$	$1.6\cdot10^{7}$	$2.5\cdot10^{6}$
^{135}Cs	2300000	$2.4\cdot10^{10}$	$1.7\cdot10^{9}$	$1.5\cdot10^{8}$	$2.7\cdot10^{8}$	$4.1\cdot10^{7}$
^{137}Cs	30.1	$2.5\cdot10^{15}$	$1.4\cdot10^{14}$	$1.4\cdot10^{13}$	$2.4\cdot10^{13}$	$3.7\cdot10^{12}$

*) /Firestone, 1998/

6 Calculation cases

6.1 General

As discussed earlier, the gas generated in the interior of the encapsulation has to escape from the waste packages and concrete structures otherwise a large local pressure will be created in the repository. Once that the gas escapes from the repository, it will flow through the fractures in the rock surrounding the repository to the biosphere.

However, gas can not flow through a water-saturated medium (for example concrete). Gas flow can only be established in a porous medium if previously a network of gas filled connected paths has been created. This means that a certain volume of water has to be expelled from the concrete. The capillary forces determine the overpressure required for pushing the water out from the concrete. For good construction concrete a very high pressure is required. However, the concrete constructions in the repository are not designed to support high pressures and fractures (micro-fractures) will be formed in the concrete walls and gas can then flow through the concrete. Therefore, the way the gas generated in the interior of the concrete construction escapes from the repository is a very important issue in determining the behaviour of the barriers.

The conditions under which the gas is expelled from the repository are determined by the quality of the construction concrete. Since fractures may be created by the effects of pressure or other stresses, there is a certain uncertainty about the quality of the construction concrete. For this reason the radionuclide release from the repository is calculated here for two types of concrete; a high quality concrete with low hydraulic conductivity and a poor quality concrete (damaged concrete). A difference of two orders of magnitude in the hydraulic conductivity is used in the calculations. Gas flow is not possible through the high quality concrete, since very high pressures are needed to expel water from the pore structure. For the poor quality concrete, it is assumed that there are small fractures (apertures of 10 μm) through which gas flow can be established with a moderate pressure (15 kPa).

A very important issue is the volume of water that will be expelled from the encapsulation under the influence of the gas generation. If the volume of this potentially contaminated water is small, the contamination may be kept within the repository barriers and the impact on the radionuclide release will be small. On the other hand, if a large volume of water is expelled, a fraction of this potentially contaminated water may be directly released into the water flowing in the fractures around the repository. This may strongly increase the release of radionuclide from the repository.

Radionuclide release is calculated for several cases. For all the vaults in the repository, a base scenario is calculated, where the behaviour of the repository is as expected. For the Silo, for example, it signifies that the gas escapes through the evacuation pipes. A critical case is also calculated, the so-called Initial Defect (ID) in which it is assumed that the repository is initially defective. For the Silo and BMA, it is assumed that an initial fracture exists at the concrete bottom and that gas can not escape from the repository through the top (evacuation pipes for the Silo and gaps between lid and concrete walls for BMA). This means that all the free water in the repository is expelled.

Moreover other cases are also addressed regarding specific functions of each part of the repository. For the Silo, for example, the case where evacuation pipes are not installed in the Silo lid was studied. For BMA, the addition of porous concrete as backfill between the waste containers was addressed.

In the next section, the calculated cases for each part of the repository (Silo, BMA and 1BTF) are described.

6.2 Silo

Several cases are calculated for the Silo repository. They are based on the way the gas escapes from the Silo and the buildup of overpressure in the interior of the Silo. The following cases are studied.

- Case B1. Gas escapes through the evacuation pipes in the concrete lid. Two situations are distinguished regarding the permeability of the construction concrete: hydraulic conductivity of $8 \cdot 10^{-12}$ m/s (Case B1a) and $8 \cdot 10^{-10}$ m/s (Case B1b).

- Case ID1. Initial fracture in the bottom of the Silo and gas escape through the evacuation pipes in the concrete lid. Hydraulic conductivity of the concrete is of less importance since water escapes through the fracture.

- Case ID2. Initial fracture in the bottom and no evacuation pipes in the concrete lid. Hydraulic conductivity of the concrete is of less importance since water escapes through the fracture.

- Case E1. Concrete lid without evacuation pipes. Two situations are also calculated. The hydraulic conductivity is assumed to be $8 \cdot 10^{-12}$ m/s (Case E1a) and $8 \cdot 10^{-10}$ m/s (Case E1b).

6.2.1 Gas escape through evacuation pipes in the concrete lid (Case B1)

In the Silo repository gas is generated from the iron used as reinforcement, the steel packages containing the waste and the waste. Therefore, gas flow will be established through the waste, the packaging, the concrete walls, and finally through the porous concrete to the evacuation pipes. During the initial period, a volume of water is expelled from the concrete, porous concrete and cement-conditioned waste to allow the gas flow. Since the expulsion of the water occurs over a short time (few years) only a small part of this water escapes through the Silo walls, the most part escaping through the evacuation pipes in the Silo lid. In the calculations, it is assumed that all the water escapes through the evacuation pipes.

The gas produced in the interior of the Silo escapes through the evacuation pipes. The overpressure in the Silo will be about 15 kPa, which is the pressure that the gas requires to flow through the sand-bentonite layer at the top of the Silo /Push and Hökmark, 1987/. However, in the calculations, it is conservatively assumed that a pressure of 50 kPa is needed to open the sand-bentonite layer for gas flow. In order to equilibrate the overpressure in the interior of the Silo the water level has to then be lowered by

5 metres. The volume of water to then be expelled from the Silo comprises all the free water in five metres of the Silo height.

This water volume will flow out from the Silo through the outer Silo wall and the bottom. The distribution of the water flow is determined by the hydraulic conductivity of the concrete walls, of the bentonite around the Silo and the sand-bentonite at the bottom. Two sub-cases will be considered, where the concrete in the construction has a hydraulic conductivity of $8 \cdot 10^{-12}$ m/s (case B1a) and $8 \cdot 10^{-10}$ m/s (Case B1b).

In the first case, where the hydraulic conductivity of the construction concrete is lower ($8 \cdot 10^{-12}$ m/s), the water will be expelled over a longer time. The expulsion of this water takes place through both the bottom and the Silo wall, because the resistance to the water flow is mainly determined by the hydraulic conductivity of the concrete and the low resistance in the sand-bentonite is of less importance.

For the other case, where the hydraulic conductivity of the construction concrete is higher ($8 \cdot 10^{-10}$ m/s), the water expulsion to equilibrate the overpressure in the Silo will require a shorter time. This water volume will be pushed out mainly through the bottom of the Silo, since the sand-bentonite layer has a higher hydraulic conductivity than the bentonite around the Silo wall. The maximum flow rate with which the water can be expelled from the Silo is the gas generation rate, expressed at the actual pressure.

6.2.2 Initial fracture in the bottom and gas escapes through the evacuation pipes in the concrete lid (Case ID1)

This case is similar to the Case B1. The only difference is that the overpressure in the interior of the Silo pushes the water out through a fracture at the bottom of the Silo. The overpressure in the Silo is 50 kPa and all the free water in the upper five-metre section is expelled. In this case, the conductivity of the construction concrete is of less concern due to that the water escapes mainly through the fracture at the bottom. In this case the sorption capacity (or pore water volume) of the concrete at the bottom is not used and the potentially contaminated water flows directly into the sand-bentonite layer under the Silo.

6.2.3 Initial fracture in the concrete bottom and no or clogged evacuation pipes in the lid (Case ID2)

This case is similar to the Case E1, which is described below, with the difference that the pressure in the Silo pushes out all the free water through the fracture at the bottom. The water escapes from the Silo with a rate determined by the gas generation. In this case, the hydraulic conductivity of the concrete is of less importance since the water escapes through the fracture at the bottom.

6.2.4 Concrete lid without evacuation pipes (Case E1)

In these cases the hydraulic conductivity of the construction concrete is very important. Two cases are actually considered, construction concrete with a hydraulic conductivity of $8 \cdot 10^{-12}$ m/s (Case E1a) and a concrete with a hydraulic conductivity of $8 \cdot 10^{-10}$ m/s (Case E1b). The hydraulic conductivity of $8 \cdot 10^{-10}$ m/s may correspond to a concrete with one fracture per metre, where the fractures have an aperture of 10 μm.

The Case E1b is similar to the Case B1b, since the pressure in the Silo is determined by the overpressure required for the gas to flow through the sand-bentonite layer. The pressure to force the gas through the concrete lid is only 15 kPa. The water initially expelled to create paths for the gas flow may be expelled through the concrete lid, the bottom and the outer Silo wall instead of only through the evacuation pipes. The water expelled to equilibrate the pressure in the Silo will escape through the outer Silo wall and the bottom. The only difference with the Case B1b is that the water expelled through the Silo lid is pushed out through the concrete lid instead of the evacuation pipes. In this case, the sorption capacity of the concrete lid is taken into account.

For the Case E1a, the gas can not initially escape from the Silo through the concrete walls, the pressure increases with the gas generation until fractures will be created in the Silo walls to allow the gas to escape. The pressure in the Silo is determined by the strength of the concrete construction and the rate that the gas is generated. Here, it is assumed that all the free water in the Silo is expelled before fractures are created in the Silo walls. This means that the pressure in the interior of the Silo will be greater than 500 kPa. However, this situation is not probable, since the Silo is not designed for excessively high pressures. Due to this high pressure, fractures will be created on the Silo walls. If the fractures occur in the upper part of the Silo, the gas will escape through these fractures and the pressure will decrease and no more water will be expelled. If the fractures are created in the bottom of the Silo a situation similar to the case with a fracture at the bottom originates.

The water expelled from the Silo is distributed between the outer Silo wall and the bottom in relation to the respective flow resistance. The gas generation rate and the hydraulic conductivity of the walls determine the rate at which the water is pushed out. Since the gas generation rate in the Silo during the initial period is expected to be high, it is probable that fractures will be created in the Silo walls before all the free water has the time to escape from the Silo. In these calculations, it is assumed that fractures in the Silo walls are created after all the free water has been expelled from the Silo. This means that no water will escape through fractures. The situation where a fracture is created at the bottom of the Silo is discussed in a special case (initial defect).

6.3 BMA

The cases calculated for BMA are based on the different ways the gas escapes from the repository and its potential impact on the radionuclide release. The following cases are defined:

- Case B1. Gas escapes through gaps between the concrete walls and the lid.
- Case ID1. Initial fracture at the concrete bottom. Only the case with a hydraulic conductivity of the construction concrete of $8 \cdot 10^{-12}$ m/s will be studied.
- Case E1. No existing gaps between the concrete walls and the lid. Two values are considered for the hydraulic conductivity of the construction concrete, $8 \cdot 10^{-12}$ m/s (Case E1a) and $8 \cdot 10^{-10}$ m/s (Case E1b).
- Case E2. The space between the waste containers is filled with porous concrete.

For the sake of simplicity, the modelling of BMA is done for a storage room with an average waste composition.

6.3.1 Gas escape through gaps between the concrete walls and lid (Case B1)

During the operational phase, a concrete lid is put in position as soon as a room is filled and after that a 5 cm thick concrete layer is cast on top of the lid to prevent water intrusion. At repository closure, an additional 0.5 m thick reinforced concrete lid will be cast on top of the compartments. Since the lid is not hermetically sealed gaps are expected to exist between the lid and the walls through which the gas may escape from the encapsulation. In this case the gas escapes from the BMA structure and no over-pressure is created in the interior. The only effect on the radionuclide release is the expulsion of water to open paths for the gas flow through the waste and concrete walls.

Due to the large gas production of gas in BMA and the rather small water volume to be expelled from the repository to allow the gas flow, it is assumed that this water volume is expelled over the course of one year. Moreover, since the gas generation is expected to start very early, it is assumed that the walls of the steel containers are intact during this first year. However, it is assumed that they are not hermetically sealed and that water intrudes into the waste containers whereby the gas generated in its interior may escape through these openings. The same situation is considered for the concrete moulds, but in this case the water can also penetrate into the waste through the concrete walls.

The radionuclides are transported into the water surrounding the waste packages by diffusion through the concrete walls of the concrete moulds and by the water expelled from the interior of the waste packages. No diffusion through the walls of the steel moulds and drums is considered during this period (one year). After that, it is assumed that the steel walls are totally corroded and that they do not have any barrier function. Transport by diffusion from the waste is then considered.

6.3.2 Initial fracture in the concrete bottom and no existing gaps between the walls and lid (Case ID)

The volume of water expelled from BMA through the fracture at the bottom is determined by the hydraulic conductivity of the concrete used in the structure. If the concrete in the structure walls is of a high quality, with a hydraulic conductivity of $8 \cdot 10^{-12}$ m/s gas can not escape through the concrete walls and all the free water will be expelled through the fracture at the bottom. If the concrete used in the walls of the structure is of a poor quality, gas can then escape through the concrete walls with a moderate overpressure, for example 15 kPa if the fractures have an aperture of 10 μm.

Here, the situation is only calculated where the concrete hydraulic conductivity is assumed to be $8 \cdot 10^{-12}$ m/s and all the free water is expelled. It is also assumed that this water volume is expelled during one year. The total volume of free water (water not bound by capillary forces) in the encapsulation is very large (about 2 000 m^3). The most part of this water volume corresponds to the water in the space between the waste containers.

6.3.3 No existing gaps between concrete walls and lid (Case E1)

Regarding the hydraulic conductivity of the concrete, two cases may be distinguished. In the first case, the concrete in the walls is a high quality concrete with a hydraulic conductivity of $8 \cdot 10^{-12}$ m/s. In the second one, the concrete in the wall of the construction is of a less quality with a hydraulic conductivity of $8 \cdot 10^{-10}$ m/s.

For the case where the concrete walls have a hydraulic conductivity of $8 \cdot 10^{-12}$ m/s, gas flow through the concrete walls is only possible if there exists a very high overpressure. The construction is not designed to support such a high overpressure. A possible situation is that fractures are formed in the concrete walls and the hydraulic conductivity increases. We have then the same situation as in the case with a higher hydraulic conductivity (for example $8 \cdot 10^{-10}$m/s). Another alternative is that the pressure in the interior of the encapsulation is enough to lift the concrete lid and the sand on the top. In this case, all the free water will be expelled from the encapsulation. This water volume will be expelled during a long interval of time and with a low flow rate, a few cubic metres per year, due to the lower hydraulic conductivity. This case is, however, not probable, since BMA is not designed for high pressure and the probable situation is that the walls will be damaged and fractures created. If the fractures are created in the upper part of the walls, gas can escape from the encapsulation, the pressure decreases and no more water will be expelled from BMA. If the fractures occur at the bottom, water will be expelled through the bottom. This is discussed in the case ID1.

The case with a hydraulic conductivity of $8 \cdot 10^{-10}$ m/s may correspond to the situation where micro-fractures are created in the concrete walls. If the fractures have an aperture of 10 μm, gas may escape through these small fractures with an overpressure of 15 kPa and the water level will be lowered by 1.5 m to equilibrate the pressure. The water will be expelled through the lateral walls and the bottom over a period of a few years.

6.3.4 The space between the waste containers filled with concrete (Case E2)

As discussed above a large volume of water is free in the interior of the encapsulation and can be expelled if the pressure increases in the encapsulation. To reduce the volume of free water and increase the sorption capacity, it is proposed that the space between the waste containers will be backfilled with concrete with high hydraulic conductivity similar to that used in the Silo. This reduces considerably the volume of free water. In this case the only free water will be found in the interior of the moulds and drums.

The calculations will be made only for the case with an initial fracture at the bottom and no gaps between the lid and the walls. In this case all the free water is expelled through the fracture at the bottom. The addition of backfill concrete reduces the volume of free water and also decreases the flow rate with which the water is pushed out through the fracture at the bottom. The water flow rate is determined by the hydraulic conductivity of the backfill and the fracture aperture.

6.4 1BTF

The waste allocated to BTF is mainly packed in concrete tanks, steel moulds, and steel drums. In 2BTF only concrete tanks are located. Here, only the section of 1BTF containing the steel drums with ashes is modelled. The radionuclide release is calculated for two cases:

- Case B1. Gas escape through the backfill concrete
- Case ID. Initial transversal fracture crosses all the section

6.4.1 Gas escape through the backfill concrete (Case B1)

In this case, The water expelled to open paths for the gas flow is pushed out through the backfill concrete around the waste containers. A part of the water flows into the gravel located at the top and bottom of the concrete structure and from the gravel into the rock surrounding the vault at the ceiling and floor. Another volume of water flows directly from the concrete structure into the rock located at the sides of the structure. The flow rate distribution is assumed to be proportional to the respective cross sectional area through which the water flows.

Once paths have been opened for the gas flow, no more water is expelled from the concrete.

6.4.2 Initial transversal fracture crosses all the section (Case ID)

The location of the fracture is shown in Figure 6-1. When water is expelled from the repository to create paths for the gas flow, the situation is similar to the Case B1. The only difference is that a fraction of the water does not flow through the concrete located at the top, bottom and sides of the concrete volume. This means that the sorption capacity (or water volume) of the concrete located in these zones is not used in retarding the transport of the radionuclides. The distribution of the flow rate between the ceiling, floor and sides is the same than that used in the former case.

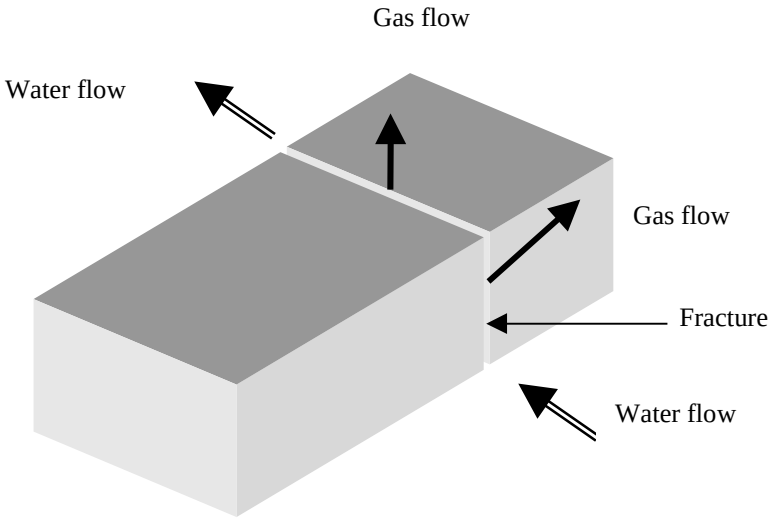

Figure 6-1. *Schematic picture showing the location of the fracture.*

After paths have been created for the gas flow, no more water is expelled and the hydraulic gradient and the geometry of the fracture determine the flow rate. For the case with a fracture crossing the modelled section transversally, the water flow rate is increased by a factor about 6 /Holmén and Stigsson, 2001b/.

7 Results for the Silo

7.1 Water expelled from the Silo

The generation of gas from corrosion in the Silo is very unevenly distributed between the different waste containers. The initial gas generation rate is about 2000 Nm^3/year (see Table 3-2). The largest volume of gas formed per year initially is produced from waste containing aluminium and/or zinc, which is deposited in steel moulds and conditioned with cement. For this waste, the gas generation rate is initially larger than 1000 Nm^3/year. Another large source is the steel used as packing in the steel moulds and drums, about 550 Nm^3/year. Finally the iron used as reinforcement in the concrete moulds and structures contributes with about 300 Nm^3/year to the gas generation rate.

7.1.1 To establish flow paths for gas

Gas can not flow through a water saturated porous medium. Gas flow may be established only if water is expelled from the porous medium and a network of gas-filled pores is created. Experimental tests /Björkenstam, 1996; 1997/ showed that the volume of water expelled from the porous concrete is less than 0.7% of the volume of the porous concrete. This value was obtained using larger gas flow rates than the flow rate expected to take place in the porous concrete in the Silo. If the porosity of the porous concrete is taken to be 0.30, about 2% of the water in the porous concrete may be expelled when the gas flow starts. For the normal concrete, it is expected that the volume of water to be expelled will be lower /Jacobsson and Forsberg, 1986/. However, a value of 2% of the pore water volume is assumed for the normal concrete.

The volumes of water expelled from the Silo to allow the gas flow are shown in Table 7-1. About 40 m^3 of water are expelled from the porous concrete around the containers with the waste to allow the gas flow up to the top. Another important water volume is expelled from the inner concrete walls and from the outer Silo wall, the bottom and the lid (about 28 m^3). This water volume is estimated assuming that all the water expelled from the outer Silo wall, bottom and lid flows into the Silo. A volume of water is also expelled from the concrete walls of the concrete moulds (about 8 m^3). Finally, a small volume of water is expelled from the waste containing potentially gas-generating materials. All this water volume escapes through the evacuation pipes into the sand-bentonite on the top the Silo.

The moulds and drums have a free volume inside the waste packages that could become water filled at the sealing of the Silo. For the drums and moulds made of steel, it is assumed that the walls are intact when the gas generation starts and the gas produced in its interior escapes through the top of the containers and water is not expelled. For the concrete moulds, it is also expected that the gas escapes through the top. If the gas can not escape through the top, fractures could be created in the concrete walls and a part of the free water could be pushed out. However, the gas generation from the waste deposited in the concrete moulds is very small, the only exceptions are the steel drums with aluminium containing waste.

Table 7-1. Volumes of water expelled from different parts of the Silo to allow the gas flow.

Part	Volume m^3	Porosity	Pore water volume m^3	Expelled water to allow gas flow m^3
Outer Silo wall	3662	0.15	549	11.0
Bottom and lid	1172	0.15	176	3.5
Inner walls	4301	0.15	645	13.0
Porous Concrete	6254	0.30	1876	37.5
Concrete mould walls	2557	0.15	383	7.5
Total				**72.5**

7.1.2 Due to pressure induced lowering of the internal water level

The water volume to be expelled from the Silo to lower the water level and equilibrate the pressure was estimated to be 200 m^3, since the total volume of free water is about 2000 m^3 and the level is lowered by 5 metres. This is calculated assuming that the pressure needed to open the sand-bentonite layer for gas flow is 50 kPa. The distribution of the free water in the Silo is shown in Table 7-2. The most important fraction is the water contained in the voids of mould and drums (1334 m^3). The other fraction is the easy to remove water contained in the cement-conditioned waste and the porous concrete surrounding the waste packages. It is assumed that 20% of the pore water may be expelled when the water level is lowered, in addition to the fraction expelled to allow the gas flow.

Table 7-2. Volumes of free water within the Silo that may be expelled when the water level is lowered.

Part	Pore water volume m^3	"Free water" m^3	Internal void m^3	Water possible to expel m^3
Concrete mould (cement conditioned waste)	659	132	638	770
Steel mould (cement conditioned waste)	802	160	325	485
Steel drum (cement conditioned waste)	7	1	4	5
Steel mould (bitumen conditioned waste)	–	–	160	160
Steel drum (bitumen conditioned waste)	–	–	207	207
Porous concrete	1876	375	–	375
Total		668	1334	2002

This water volume is expelled from the Silo through the lateral wall and the bottom. The distribution of the water flow depends on the hydraulic conductivity of the barriers (concrete walls, sand-bentonite, and bentonite).

7.2 Radionuclide release by expelled water

The radionuclide release is calculated for several cases. The description of the cases is given in Section 6.2 and the following cases are studied.

- Case B1. Gas escapes through the evacuation pipes in the concrete lid. Hydraulic conductivities of the construction concrete of $8 \cdot 10^{-12}$ (Case B1a) and $8 \cdot 10^{-10}$ m/s (Case B1b).

- Case ID1. Initial fracture in the bottom and gas escape through the evacuation pipes in the concrete lid.

- Case ID2. Initial fracture in the bottom and no evacuation pipes in the concrete lid.

- Case E1. Concrete lid without evacuation pipes. Hydraulic conductivities of $8 \cdot 10^{-12}$ (Case E1a) and $8 \cdot 10^{-10}$ m/s (Case E1b).

In the calculations, the relative radionuclide release is only determined since we are more interested in the impact of the gas generation on the release than in the absolute value of the release. For this reason the release is only calculated for a few generic radionuclides.

- Non-sorbing nuclide with rather long half-life (organic ^{14}C).
- Non-sorbing nuclide with short half-life (^{3}H).
- Slightly sorbing radionuclide with short half-life (^{90}Sr).
- Slightly sorbing radionuclide with very long half-life (^{36}Cl).

In the specific case of the Silo, the release was also calculated for two other radionuclides, ^{108m}Ag and ^{137}Cs. The release of ^{108m}Ag was calculated due to that this radionuclide contributes significantly to the total release in the first 1000 years. The release for ^{137}Cs was calculated due to its large inventory in the Silo and rather small K_d in the concrete. The calculations are done only for the first 1000 years. The results are presented as the maximum relative release. This is calculated as the ratio between the maximum release for the case with gas generation and the maximum release without gas generation reached in the first 1000 years.

The calculations are done in three steps. In the first step, water is expelled from the Silo to allow the gas flow. The duration of this step is, in general, one year. At the second step water is expelled from the Silo to compensate the pressure in the interior of the Silo. The duration of this step depends on the hydraulic conductivity of the concrete in the outer Silo wall and the bottom. Once the water has been expelled to allow the gas flow and the water level has been lowered to compensate the pressure in the Silo, no more water is expelled from the Silo. Then, the water that flows through the Silo from the bottom to the top is determined by the hydraulic gradient in the rock around the Silo. The calculations are carried out to 1000 years.

7.3 Gas escape through evacuation pipes in the concrete lid (Case B1)

In this case, 72.5 m^3 of water are expelled from the Silo to allow the gas flow. Due to the presence of waste containing aluminium, it is expected that the gas generation starts early and that during the first year, enough gas is generated to expel the 72.5 m^3 water. The gas production at the first year is estimated to about 270 m^3/year, considering a pressure of 750 kPa. Therefore, the duration of this step is assumed to be one year.

At the second step, 200 m^3 of water are expelled from the Silo to equilibrate the over-pressure of 50 kPa in the interior of the Silo, since the total volume of free water in the Silo is 2000 m^3 (Table 7-2). The pressure in the interior of the Silo is determined by the overpressure needed to open paths on the sand-bentonite at the top of the Silo for gas flow. For a hydraulic conductivity of the concrete of $8 \cdot 10^{-10}$ m/s the overpressure required to allow gas flow is only 15 kPa, but the gas can not escape through the outer Silo wall due to the presence of the bentonite surrounding the Silo. The water is expelled from the Silo through the outer Silo wall and the bottom. For this case, the water escapes in 10 years and the most of the flow occurs through the bottom. This is due to the low hydraulic conductivity of the bentonite surrounding the Silo. When the hydraulic conductivity of the concrete is low, $8 \cdot 10^{-12}$ m/s, the water is expelled in 50 years and most of the flow takes place through the cylindrical wall. Finally no more water is expelled from the Silo and the water flow through the Silo is about 0.25 m^3/year from the bottom to the top.

Figure 7-1 shows the release of organic ^{14}C as a function of time. The release is expressed as the fraction of the initial activity released in one year. The first peak, for the expulsion of water to allow the gas flow is very small. This is due to that the concentration of the water expelled from the Silo is low and that a large volume of water stays in the sand and sand-bentonite layer on the top of the Silo. The second peak corresponds to the activity released with the water expelled to lower the water level in the interior of the Silo. Here, the volume of water is larger and the activity higher. This peak is slightly smaller than the release occurring at 1000 years when no water is expelled by gas.

The breakthrough curve for ^3H is shown in Figure 7-2. The impact of gas generation on the release is significant since the maximum release without gas generation is quite small. This is due to the short half-life of this radionuclide. The maximum peak with gas generation is some orders of magnitude higher than the corresponding peak without gas generation. Fortunately in this period the recipient is the Baltic Sea and the doses for ^3H are very small. The relative release for ^{90}Sr, which has a slight sorption and a rather short half-life, is similar to the release for ^3H. This is shown in Figure 7-3.

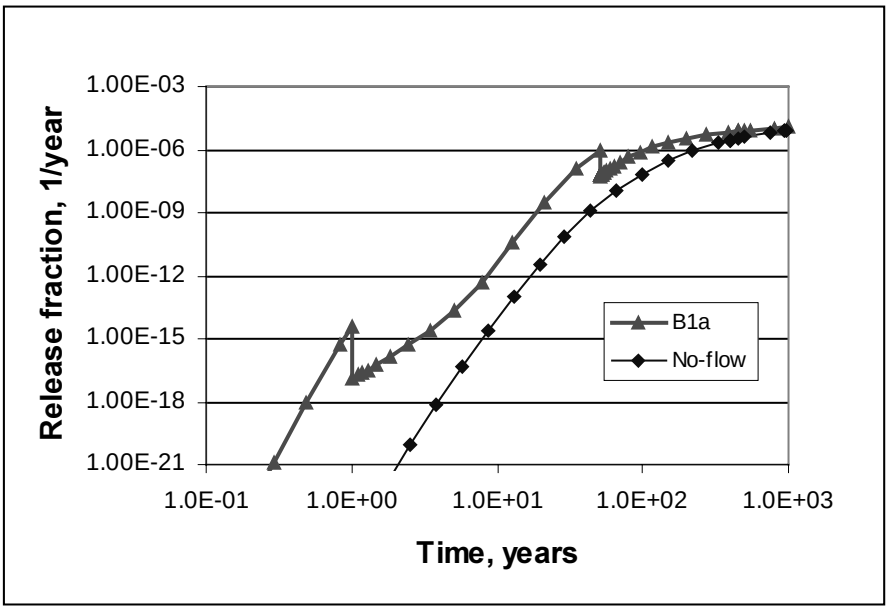

Figure 7-1. *Release of organic ^{14}C from the Silo as a function of time for the Case B1a, gas escapes through the evacuation pipes and concrete with low hydraulic conductivity ($8 \cdot 10^{-12}$ m/s). The release is expressed as the fraction of the initial activity per year.*

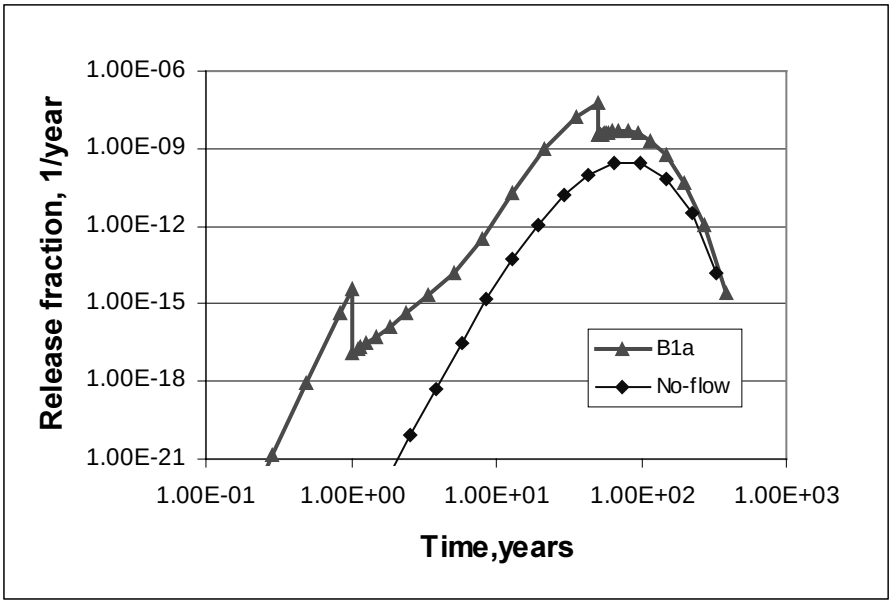

Figure 7-2. *Release of ^{3}H from the Silo as a function of time for the Case B1a, gas escapes through the evacuation pipes and concrete with low hydraulic conductivity ($8 \cdot 10^{-12}$ m/s). The release is expressed as the fraction of the initial activity per year.*

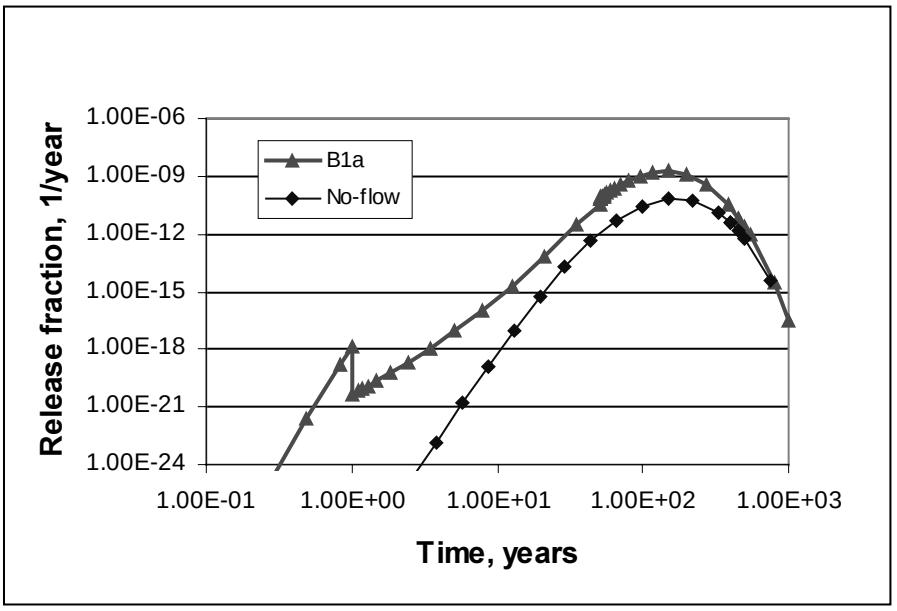

Figure 7-3. *Release of ^{90}Sr from the Silo as a function of time for the Case B1a, gas escapes through the evacuation pipes and concrete with low hydraulic conductivity ($8 \cdot 10^{-12}$ m/s). The release is expressed as the fraction of the initial activity per year.*

The impact of the gas generation is dependent on the sorption properties of the radionuclides and their half-lives. For the two long-lived radionuclides the impact of the gas generation is small. In both cases, the maximum release (without gas generation) occurs after 1000 years or more. The difference between the release of organic ^{14}C and ^{36}Cl may be explained by the sorption of ^{36}Cl on the concrete. For short-lived radionuclides the impact of the gas generation is important, especially for the ^{3}H due to its too short half-life.

Figure 7-4 shows the relative releases for the calculated nuclides. The relative release is calculated as the ratio between the maximum release with and without gas generation during the first thousand years. For the Case B1b, where the concrete has a higher hydraulic conductivity ($8 \cdot 10^{-10}$ m/s), the increase in the release is larger for the non-sorbing radionuclides. The impact on ^{3}H is very large, the maximum release is increased by five orders of magnitude, compared to the case without gas generation. Fortunately in this period the recipient is the Baltic Sea and the expected doses for ^{3}H are very small.

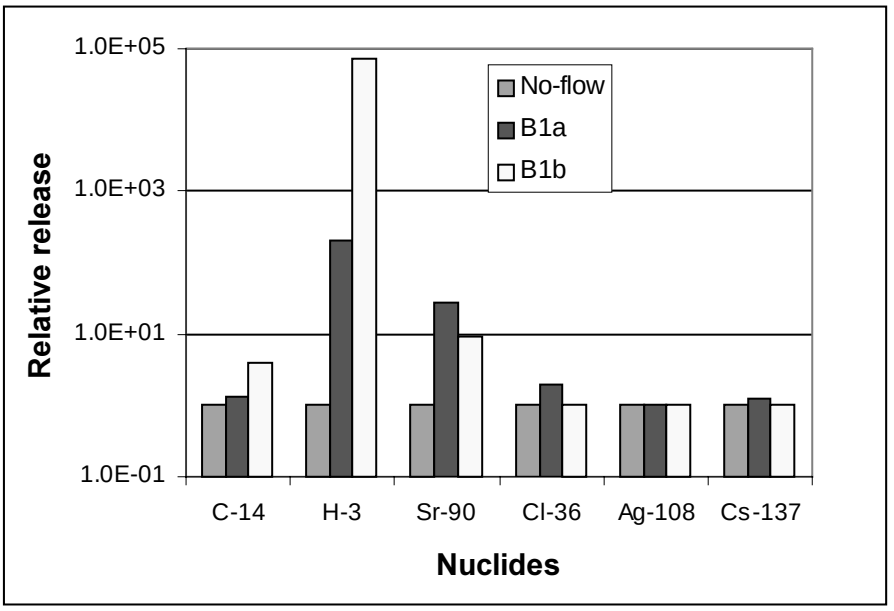

Figure 7-4. *Relative release for the Case B1, gas escapes through the evacuation pipes. Case B1a corresponds to concrete with low hydraulic conductivity ($8 \cdot 10^{-12}$ m/s) and B1b to concrete with high hydraulic conductivity ($8 \cdot 10^{-10}$ m/s). The Case without gas generation is also shown.*

7.4 Initial fracture in the bottom

7.4.1 Initial fracture in the bottom and gas escapes through the evacuation pipes in the concrete lid (Case ID1)

In this case the water is expelled through a fracture in the bottom of the Silo. In this case, the capacity of the concrete bottom (porosity and sorption) is not used, since the water expelled bypasses the concrete at the bottom. The pressure in the Silo is maintained at 50 kPa and the hydraulic conductivity of the concrete is not important since water does not flow through construction concrete. The water level is lowered by 5 metres and all the water (272 m^3) expelled flows out through the fracture at the bottom

The results in Figure 7-5 show that the release is strongly increased when a fracture exists at the bottom of the Silo. For the Case ID1, i.e., gas escaping through the evacuation pipes, the release is at least one order of magnitude greater than the value found for the Case B1a. For the radionuclides with a short half-life the increase is much larger. This is due to the fact that the sorption capacity of the concrete at the bottom is not used.

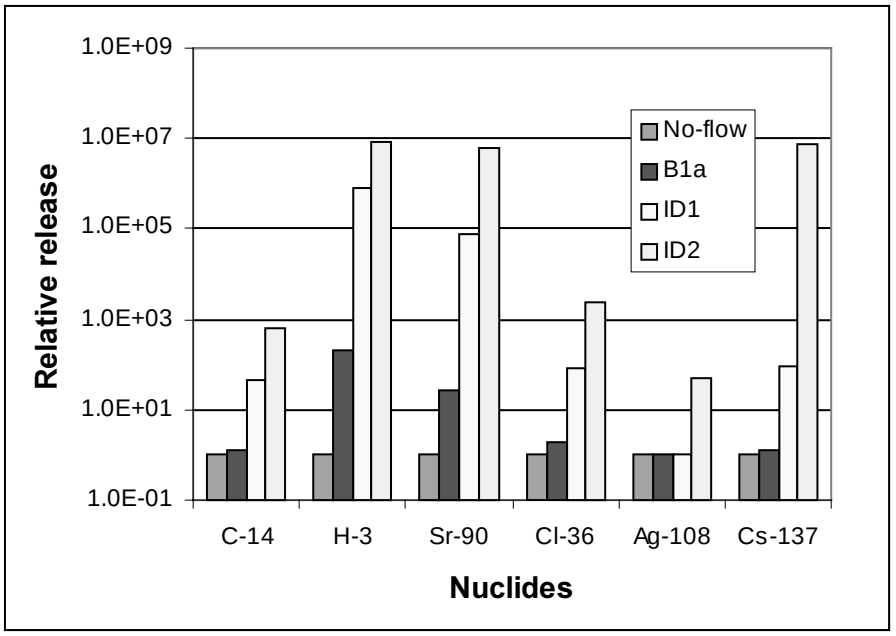

Figure 7-5. *Relative release for the Cases ID1 (initial fracture at the bottom and gas escaping through the evacuation pipes) and ID2 (initial fracture at the bottom and no evacuation pipes). The values for the cases without gas generation and Case B1a are also included.*

7.4.2 Initial fracture in the concrete bottom and no or clogged evacuation pipes in the lid (Case ID2)

The situation is more critical in this case where the evacuation pipes do not exist or are clogged. In this case all the free water is expelled from the Silo at the same rate that gas is generated. The hydraulic conductivity of the concrete is of less importance since the water escapes through the fracture at the bottom. The results are shown in Figure 7-5. Large releases are observed for ^{3}H, ^{90}Sr and ^{137}Cs. The impact of a fracture at the bottom is smaller for the long-lived radionuclides.

7.5 Concrete lid without evacuation pipes (Case E1)

The hydraulic conductivity of the construction concrete is very important in this case. For the case with poor concrete (Case E1b), a moderate pressure is required to create paths for the gas flow, since gas may flow through micro-fractures in the concrete. In the calculations, it is assumed that the concrete has a network of micro-fractures with an aperture of 10 μm, this implies that a pressure of 15 kPa is needed to push out the gas through the concrete lid. However, a pressure of 50 kPa is required to create gas flow through the sand-bentonite at the top of the Silo.

During the initial step, when water is expelled to allow the gas flow, water flows out from the Silo through the lid, the outer Silo wall and bottom. Later when the water level is being lowered, the water flow takes place only through the outer Silo wall and the bottom. The ratio between the water flow rates is determined by the relative hydraulic conductivity of the different barriers. In this case the water flow rate through the bottom is about 6 times larger than the flow rate through the cylindrical Silo wall.

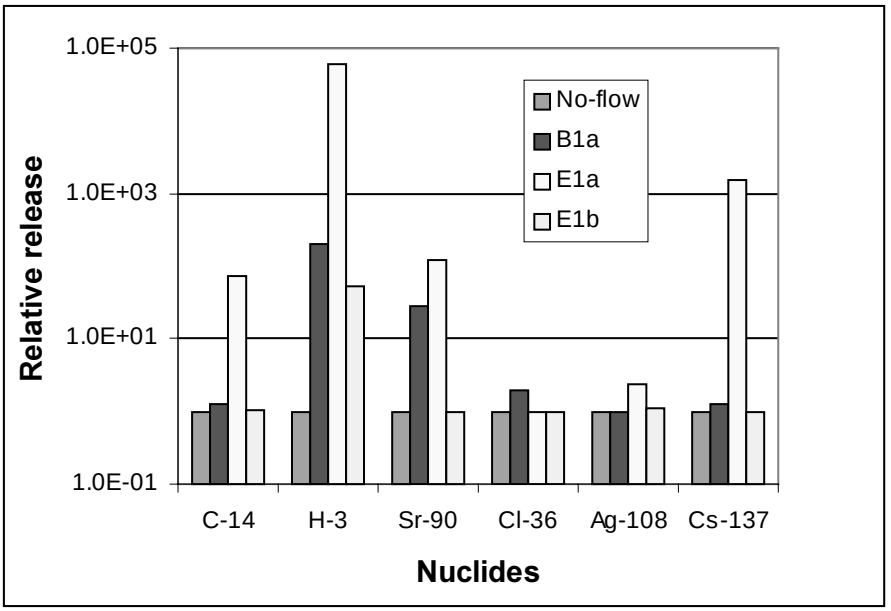

Figure 7-6. *Relative release for the Case E1. The values for the cases without gas generation and Case B1a are also included.*

In the other case, for concrete with a hydraulic conductivity of $8 \cdot 10^{-12}$ m/s (Case E1a), the pressure in the interior of the Silo is determined mainly by the gas generation, since gas can not escape from the Silo. Water is expelled from the Silo according to the pressure in its interior and the hydraulic conductivity of the barriers. Since the gas generation initially is very high, it is expected that the pressure in the interior of the Silo will reach very high values. Since, the Silo is not designed to handle high pressure, it is expected that fractures will be created in the Silo walls. However, in the calculations it is assumed that all the free water is expelled from the Silo through the walls before the Silo is damaged and that fractures are created to allow the gas to escape from the Silo.

The relative releases for the Case E1 are shown in Figure 7-6. These values are compared with the Case B1a and the case without gas generation. The relative release for the Case E1a, where good construction concrete is used, is much larger than the relative release for the Case B1 due to the large volume of water expelled from the Silo. The release for the Case E1b (poor construction concrete) is less than for the Case B1a, since the sorption capacity of the concrete lid is used in this case

7.6 Summary of the results for the Silo

The Silo is the repository part that contains most of the activity deposited in SFR. For the Case B1, where the gas escapes through the evacuation pipes, the release is most increased for ^{3}H. For concrete with a hydraulic conductivity of $8 \cdot 10^{-10}$ m/s in the Silo construction the increase is about five orders of magnitude. The increase is less when concrete with lower hydraulic conductivity ($8 \cdot 10^{-12}$ m/s) is used. For the long-lived radionuclides the impact of the gas generation is negligible in this case.

For the case with an initial fracture at the bottom and when all the water is expelled from the Silo, the release is increased up to seven orders of magnitude for ^{3}H, ^{90}Sr and ^{137}Cs. The impact on the release of long-lived radionuclides is much smaller.

For the case with no evacuation pipes, where all the free water is expelled through the walls, the radionuclide release is also quite large.

The radionuclide release, for some radionuclides, may be increased by several orders of magnitude when water is expelled from the Silo by effect of the gas generated in its interior. However, the impact on the total doses during the first thousands years after closure of the repository is limited. The total dose is dominated by the release of organic ^{14}C. Since the radionuclides are released to the coastal area during the first thousand years the dilution is considerable, which results in a very low dose.

8 Results for the BMA vault

8.1 Water expelled from BMA

When gas generation starts, water has to be expelled from BMA in order to open paths for the gas flow through the concrete and the cement conditioned wastes. Water is also expelled from BMA if an overpressure is created in the interior of the concrete structure, the water level is lowered to equilibrate the pressure in the interior. This overpressure is created if there are no gaps between the concrete lid and the walls on top of the structure.

The calculations for BMA are performed for the first 1000 years when the water flow is predominantly vertical. In order to simplify the calculations, only one room is modelled and it is assumed that the waste containers are evenly distributed between the different rooms.

8.1.1 To establish flow paths for gas

According to laboratory measurements carried out by Björkenstam /1996; 1997/ for the porous concrete the volume of water expelled is in the range 0.04 to 0.7% of the sample volume. Since the porosity of the porous concrete is about 0.30, this corresponds to 0.1 to 2.0% of the volume of the pore-water. In the calculations is assumed that 2% of the pore-water is expelled. For construction concrete this figure is expected to be less /Jacobsson and Forsberg, 1986/. However, the same value will be used due to lack of data. For the cement-conditioned waste, the value for the porous concrete is used.

Table 8-1 shows the volume of water to be expelled from the waste containers to allow the gas flow. The volume of water to be expelled from all BMA is about 20 m^3. The

Table 8-1. Volumes of water expelled from different parts in all BMA to allow the gas flow.

	No. of packages	Pore water m^3	Expelled water to allow gas flow m^3
Concrete mould	3818		
Concrete mould walls		334	6.7
Cement conditioned waste		437	2.5**
Steel mould	1062		
Cement conditioned waste		166	2.1
Steel drum	1875		
Cement conditioned waste		25	0.3
Odd waste	238	37	0.7
Concrete structures			
Side walls		139	1.4*
Bottom		82	0.8*
Lid		310	3.1*
Inner walls		86	1.7*
Total			**19.3**

* 50% assumed to flow into interior parts.

** Only from waste with gas producing metals.

major contribution is from the concrete moulds (walls) and the concrete structures. For the concrete structures, it is assumed that only a half of the water expelled from the lateral walls, bottom and lid flows into the interior parts, the other fraction flows into the gravel surrounding the encapsulation. Water is also expelled from cement conditioned waste containing metals (iron, aluminium). This volume is about 5 m^3.

8.1.2 Due to pressure induced lowering of the internal water level

The volume of free water possible to expel from BMA if the water level is lowered is shown in Table 8-2. The water contained in the free space surrounding the waste containers, over 2000 m^3, dominates the volume of free water. Another important volume of free water is found in the interior of the waste containers. This volume is about 1000 m^3. Finally a volume of about 100 m^3 of free water may be expelled from the cement-conditioned waste. This water volume is assumed to be 20% of the pore water volume.

Table 8-2. Volumes of free water in all BMA that may be expelled when the water level is lowered.

Parts	Pore water volume m^3	"Free water" m^3	Internal void m^3	Water possible to expel m^3
Concrete/cement			442	442
Concrete mould walls	334			
Cement conditioned waste	437	87		87
Steel mould			91	91
Cement conditioned waste	166	33		33
Steel drum			11	11
Cement conditioned waste	25	5		5
Steel package with bitumen conditioned waste			249	249
Odd waste			185	185
Space around the waste containers			2095	2095
Total		**125**	**3073**	**3198**

8.2 Radionuclide release by expelled water

The description of the calculation cases for BMA is given in Section 6.3 and the following cases are calculated:

- Case B1. Gas escapes through gaps between the concrete walls and the lid.
- Case ID. Initial fracture at the concrete bottom. Only the case with hydraulic conductivity of the construction concrete of $8 \cdot 10^{-12}$ m/s will be studied.
- Case E1. No existing gaps between the concrete walls and the lid. Only one case is calculated, that with a hydraulic conductivity of the construction concrete of $8 \cdot 10^{-10}$ m/s.
- Case E2. The space between the waste containers is filled with porous concrete.

The calculations are done for some generic radionuclides:

- Non-sorbing nuclide with rather long half-life (organic ^{14}C).
- Non-sorbing nuclide with short half-life (^{3}H).
- Slightly sorbing radionuclide with short half-life (^{90}Sr).
- Slightly sorbing radionuclide with very long half-life (^{36}Cl).

In the calculations, it is considered that the water penetrates the waste containers (concrete and steel moulds, and steel drums) after sealing of the repository and that the gas escapes from the waste containers through the top.

The calculations are divided into three steps. In the first step, with a duration of one year, 20 m^3 of water is expelled from the concrete and cement-conditioned waste to allow the gas flow. Due to the presence of waste containing aluminium, it is expected that the gas generation starts early and that during the first year, enough gas is generated to expel the 20 m^3 water. The gas production during the first year is estimated to be about 1500 m^3/year, considering a pressure of 500 kPa. The concentration in the water surrounding the waste containers increases with time. The activity in the waste is transported into the water surrounding the containers mainly by diffusion through the concrete walls of the concrete moulds and by water expelled from the container to allow the gas flow. Diffusion from the steel containers is not considered, since it is expected that the steel mould and drums are intact when the gas generation starts.

In the second step, water is expelled from BMA to lower the water level if overpressure is created in the interior of the encapsulation. The volume of water to be expelled and the hydraulic conductivity of the concrete walls determine the duration of this step. In the third step, which starts when the pressure has been equilibrated, no more water is expelled from BMA and the radionuclides escape by diffusion and by the water flowing through BMA. The calculations are done only for 1000 years.

8.3 Gas escapes through gaps between the concrete walls and lid (Case B1)

In this case, water is only expelled to allow the gas flow, since no overpressure is needed to expel the gas from the concrete structure, the gas escape through gaps existing between the concrete walls and the lid.

Figure 8-1 shows the release from BMA for a non-sorbing radionuclide with a long half-life (organic ^{14}C). The release is expressed as the fraction of the initial mass/activity in BMA released per year. The results show that the release is increased during the first year, compared with the case without gas generation. However, the maximum release in this period is much lower than the release reached after a thousand years for the case without gas generation.

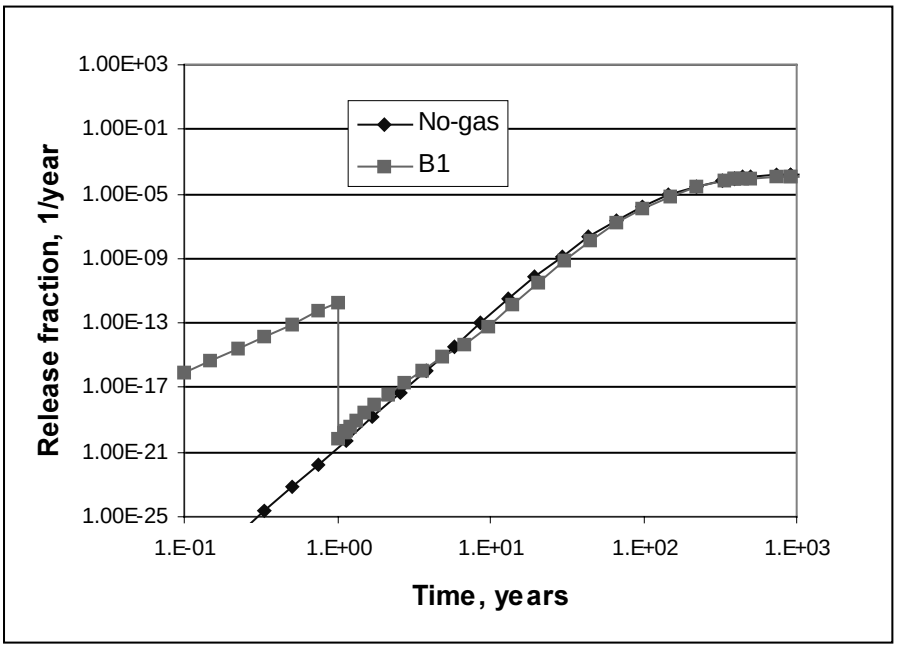

Figure 8-1. *Release of organic ^{14}C from BMA as a function of time, for the Case B1, gas escapes through gaps between the concrete walls and the lid. The release is expressed as the fraction of the initial activity per year.*

Figure 8-2 shows the relative release for the case with gas generation (Case B1). The relative release is calculated as the ratio between the maximum release with and without gas generation for the first thousand years. For the case B1, the increase in the release is negligible for all radionuclides. Only a slightly increase of ^{90}Sr is observed.

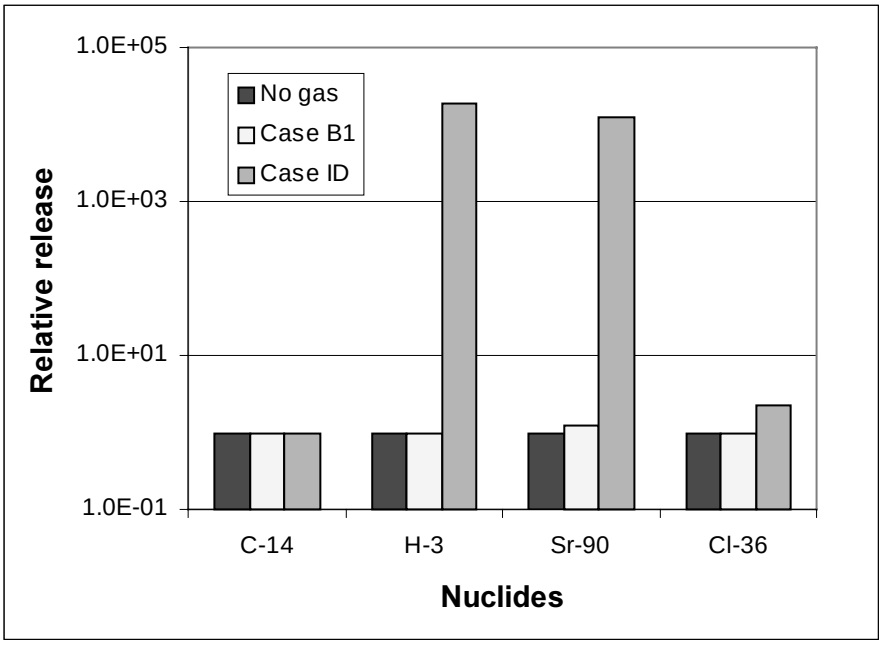

Figure 8-2. *Relative release for the Case B1, gas escapes through gaps between the walls and the lid, and Case ID, initial fracture at the bottom and no existing gaps. The values for the case without gas generation are also shown.*

8.4 Initial fracture at the bottom and no existing gaps between the walls and the lid (Case ID)

In this case, most of the water escapes through the fracture at the bottom. The water flow may be large and the time to expel the water from the encapsulation will be very short. In the calculations it is assumed that the water is expelled in one year, due to the expected large gas generation during the initial period.

The calculations are made for the case with good concrete in the encapsulation walls, since in this case the volume of water to be expelled is larger. Due to the fact that the overpressure to lift the lid is high, all free water will be expelled from the concrete structure. For the case with poor concrete the volume of water to be expelled is smaller and the radionuclide release will be smaller. The overpressure in the encapsulation will be about 15 kPa for a fracture aperture of 10 μm. This case is not calculated.

The relative release for the case with an initial fracture at the bottom is shown in Figure 8-2. The relative release is calculated as the ratio between the maximum release with and without gas generation for the first thousand years. The maximum release is increased by several orders of magnitude for the short-lived radionuclides compared to the case without gas generation. The impact of the gas generation on radionuclides with a long half-life is negligible.

8.5 No existing gaps between walls and lid (Case E1)

If there are no gaps between the walls and the lid a certain overpressure is required in the interior of the concrete construction in order to allow the gas to escape. Here, only one case is considered, the case where the concrete has a high hydraulic conductivity ($8 \cdot 10^{-10}$ m/s) and the gas may escape through the concrete lid if the overpressure is larger than 15 kPa. In this case, the water level is lowered by 1.5 metres and water is expelled through the lateral walls and the bottom during a period of about two years. This time is determined by the overpressure and the hydraulic conductivity of the concrete walls and bottom.

For the case, where it is assumed that the concrete in the encapsulation walls has a low hydraulic conductivity ($8 \cdot 10^{-12}$ m/s) gas can not escape from the construction since an excessively high overpressure is required to allow a gas flow through the concrete walls or lift the lid. Fractures will be created in the concrete construction, since BMA is not designed for high overpressures. If the fractures or micro-fractures are created in the upper part of the walls, no more water will be expelled and the situation will be similar to the case with poor concrete. If the fractures are created in the lower part of the walls the situation is similar to the Case ID. Therefore, this case is not calculated.

Figure 8-3 shows the relative release for the case, where concrete with high hydraulic conductivity ($8 \cdot 10^{-10}$ m/s) is used. The relative release is calculated as the ratio between the maximum release with, and without gas generation for the first thousand years. The release for the non-sorbing radionuclides with short half-lives (^{3}H) is increased. The maximum release takes place when the water level is lowered. Figure 8-4 shows the release for the short-lived non-sorbing radionuclide ^{3}H. The release is expressed as the fraction of the initial activity in BMA released per year. For this nuclide the maximum release is some orders of magnitude higher than the maximum value for the Case B1. For the long-lived radionuclides the increase in the maximum release is small.

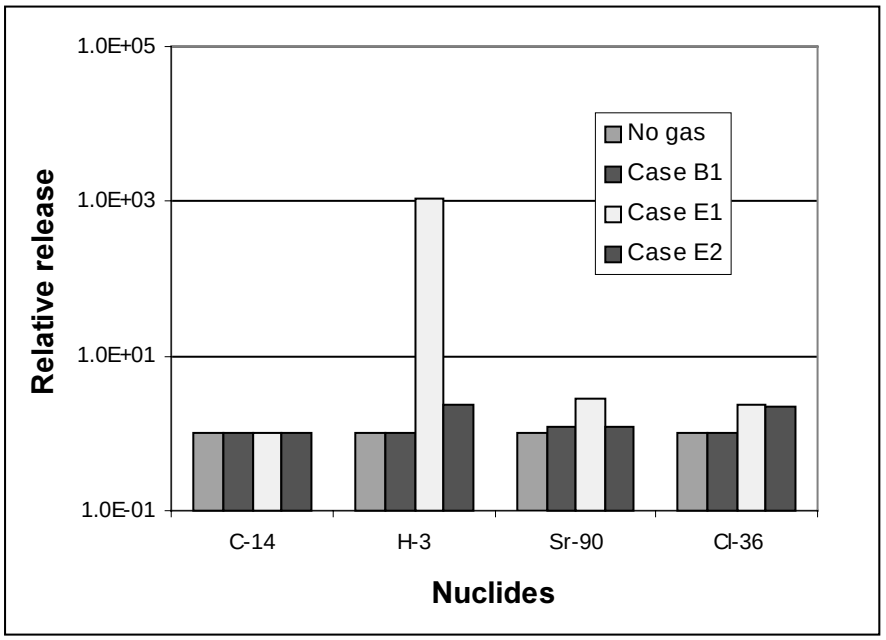

Figure 8-3. *Relative release for the Cases E1, no existing gaps between walls and lid, and Case E2, space between waste containers filled with porous concrete. The values for the case without gas generation and Case B1 are also shown.*

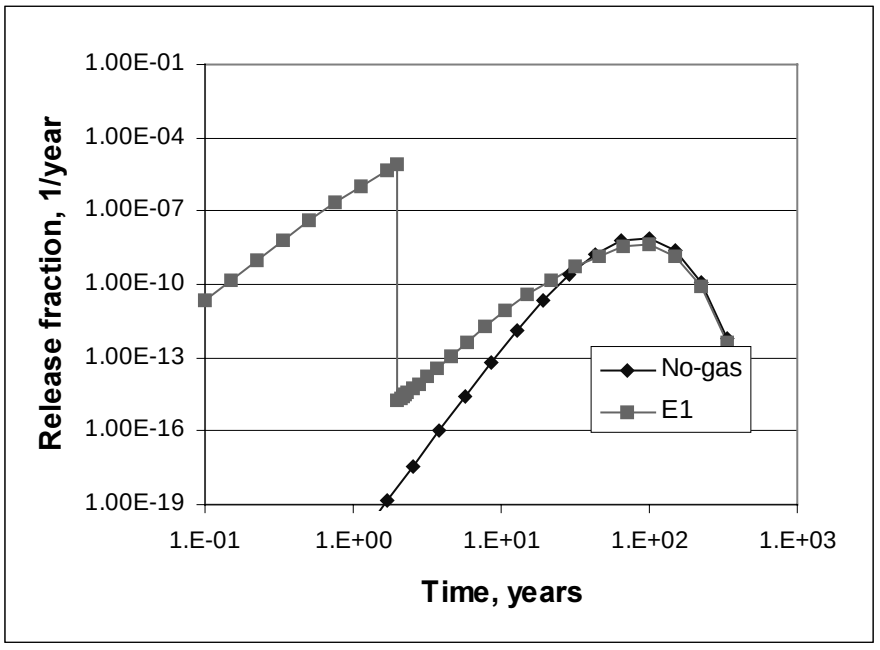

Figure 8-4. *Release of ^{3}H from BMA as a function of time, for the Case E1, no existing gaps between walls and lid. The release is expressed as the fraction of the initial activity per year.*

8.6 The space between the waste containers is filled with porous concrete (Case E2)

In the calculations shown above, the maximum releases take place when large volumes of water are expelled from the concrete encapsulation to equilibrate the overpressure needed to push out the gas generated in the interior of the encapsulation. If water is not expelled from the concrete construction, the release will take place mainly by diffusion and the maximum release will take place later.

The water to be expelled from the concrete construction is mainly the water in the space between the waste containers. This water volume represents about the 67% of the free water in BMA. A possible alternative to reduce the radionuclide release is to fill the space between the containers with some porous concrete similar to that used in the silo repository. In this case, most of the water will be bound to the concrete by capillary forces. However, a small part has to be expelled to allow the gas flow. Another advantage of filling the space between the packages with concrete is that the flow rate with which the water is expelled will be decreased. However, this is not considered in the modelling.

Figure 8-3 shows the relative release for the case when the space between the waste containers is filled with porous concrete and an initial fracture exists at the bottom. The relative release is calculated as the ratio between the maximum release with, and without gas generation for the first thousand years. The release is dramatically reduced when concrete is added as filling material between the waste tanks (Compare with the Case ID in Figure 8-2). The reason for this large decrease of the release is that in this case the volume of contaminated water expelled from BMA is much smaller. Another advantage of backfilling the space between the waste packages is the increase in the sorption capacity of BMA.

8.7 Summary of the results for BMA

BMA contains only about 6% of the activity deposited in SFR. For the Case B1, gas escaping through gaps between the walls and the lid, the releases are similar to the case without gas generation. For the case with an initial fracture at the bottom and no gaps between walls and lid, the release of the short-lived radionuclides (^{3}H and ^{90}Sr) is increased by about four orders of magnitude.

The release of the long-lived radionuclides (organic ^{14}C and ^{36}Cl) is kept almost constant for all the cases studied. This is due to that the transport by diffusion is large for these radionuclides. The release caused by the expelled water plays then only a small role.

The radionuclide release, for some radionuclides, may be increased several orders of magnitude when water is expelled from BMA by the effect of the gas generated in its interior. However, the impact on the total doses during the first thousands years after closure of the repository is limited. The total dose is dominated by the release of organic ^{14}C. Since the radionuclides are released to the coastal area during the first thousand years the dilution is considerable, which results in a very low dose.

For the case with an initial fracture at the bottom and no gaps for the gas flow on the top, the impact of the gas generation is strongly reduced if porous concrete is used to fill the space between the waste containers. This is because the volume of water to be expelled from BMA is decreased. For the case where gas escapes through gaps on the top, the backfill concrete has no function. It may have a negative effect on the release, since some water has to be expelled to open paths for the gas flow through the porous concrete.

9 Results for the 1BTF vault

9.1 Water expelled from the 1BTF vault

Similar to the Silo repository and BMA, water is expelled from the 1BTF vault to allow the gas flow through the concrete/cement. The BTF repository contains a large volume of backfill concrete, since the waste containers are surrounded by concrete. Moreover, concrete is poured in the space between the waste and the lateral walls of the vault. Only the section containing the steel drums has been modelled, due to the higher gas generation. The length of this section is about 41 m. In the sections containing the other type of containers, the gas generation is lower and it is expected that the impact on the radionuclide release is less.

9.1.1 Water expelled to establish flow paths for the gas

Water is expelled from the concrete grout surrounding the waste containers and from the cement used to condition the waste. The volume of water expelled from the different parts are shown in Table 9-1, the values correspond to the water expelled from the 41-m section containing the steel drums with ashes. The volume expelled from the backfill concrete is about 8 m^3, another fraction is expelled from the waste containers. Since there is no over pressure in the waste, it is expected that no more water will be expelled from the waste or backfill concrete.

Table 9-1. Volumes of water expelled from different parts in the 41-m section of 1BTF (containing the steel drums with ashes) to allow the gas flow.

Parts	No. of packages	Pore volume m^3	Expelled water to allow gas flow m^3
Steel drums with ashes	6479	62	1.2
Concrete mould/cement	216	49	1.0
Concrete tanks	56	38	0.8
Concrete grout		165	3.3
Ceiling		72	1.4
Bottom		77	1.5
side		61	1.2
Total			**10.4**

9.2 Radionuclide release by expelled water

The radionuclide release is calculated for two cases. In the first one, the Case B1, the backfill around the waste containers is intact and water is expelled through the backfill concrete. In the other, Case ID, a fracture crosses all the section, in the transverse direction. In this case only a part of the sorption capacity of the backfill concrete is used. The calculation cases are described in Section 6.4.

The calculations are done for some generic radionuclides:

- Non-sorbing nuclide with rather long half-life (organic ^{14}C).
- Non-sorbing nuclide with short half-life (^{3}H).
- Slightly sorbing radionuclide with short half-life (^{90}Sr).
- Slightly sorbing radionuclide with very long half-life (^{36}Cl).

In the calculations, it is considered that the water penetrates the waste containers (concrete and steel moulds, and steel drums) after sealing of the repository and that the gas escapes from the waste containers through the top.

9.2.1 Case B1. Gas escape through the backfill concrete

In this case, the water expelled from the waste and concrete is transported through the backfill concrete. The water expelled from the encapsulation escapes through the bottom, ceiling and lateral rock walls. Its flow rate is proportional to the cross section through which the flow takes place. The results of the radionuclide release are shown in Figure 9-1. The relative release is calculated as the ratio between the maximum release with and without gas generation for the first thousand years. For the Case B1, only the release of tritium is increased. This due to its short half-life and that it is a non-sorbing radionuclide.

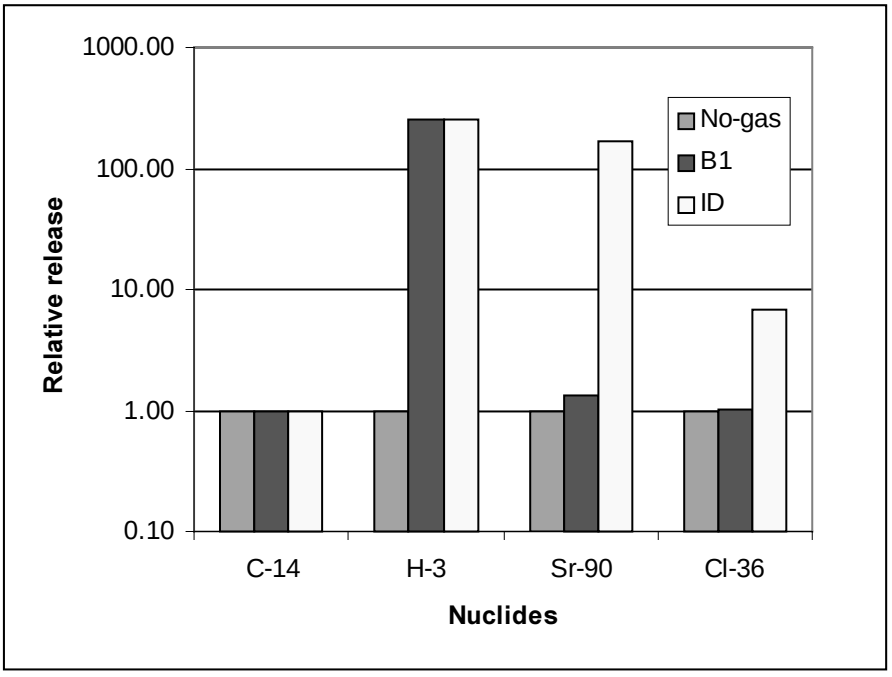

Figure 9-1. *Relative release from 1BTF for the Case B1, gas escapes through the backfill concrete, and Case ID, initial transversal fracture crosses all the section. The release for the case without gas generation is also shown.*

9.2.2 Case ID. Initial transversal fracture crosses all the section

For the case with a fracture crossing transversally the modelled section, the water flow rate is increased by a factor about 6 /Holmén and Stigsson, 2001b/. The water expelled from the waste and backfill will flow from the vault into the surrounding rock through the ceiling, bottom and lateral sides. The same proportion that in the case without fracture was used. The results are shown in Figure 9-1.

The relative release for organic ^{14}C is similar to the value obtained in the case B1, but the release is increased for the two sorbing nuclides (^{90}Sr and ^{36}Cl) since a part of the sorption capacity of the backfill concrete is not used.

9.3 Summary of the results for 1BTF

A very small fraction of the activity deposited in SFR is located in 1BTF. The release of organic ^{14}C is not influenced by the gas generation. The impact on the radionuclide release is larger for the short-lived radionuclides. The maximum relative release is increased by a factor of about 200 for both cases (B1 and ID).

The radionuclide release, for some radionuclides, may be increased in 2–3 orders of magnitude when water is expelled from 1BTF by effect of the gas generated in its interior. However, the impact on the total doses during the first thousands years after closure of the repository is limited. The total dose is dominated by the release of organic ^{14}C. Since the radionuclides are released to the coastal area during the first thousand years the dilution is considerable, which results in a very low dose.

10 Discussion and conclusions

10.1 Discussion

The radionuclide release from SFR repository caused by gas generation was calculated for different scenarios. For the three repositories (Silo, BMA and 1BTF) two basic cases were calculated, B1 and ID. The Case B1 corresponds to the situation that we expect to occur. The Case ID, for the Silo and BMA, is the situation where an initial fracture exists at the bottom of the respective encapsulation and there is no passage for the gas to escape. For 1BTF, the Case ID is represented by a fracture transversely crossing the section containing the steel drums with ashes. Other cases were also calculated (Case En) with the purpose of studying some special situations. For example, to determine the consequences of a silo repository without evacuation pipes.

In the models, it is assumed that all the structures and waste containers are totally water saturated directly after the repository is sealed. If air is present in the concrete structure when the gas generation starts, the volume of potentially contaminated water to be expelled in the initial period from the respective concrete structure will be smaller.

In the calculations, it is assumed that the gas generation starts early in the repository and that the gas generation rate is large enough to expel the water in one year. The first assumption implies that the oxygen entrapped in the repository is consumed quickly. It is expected that the volume of oxygen entrapped is small and a large part of the gas may escape through the ceiling before the vaults are filled with water. The remainder can be consumed by aerobic corrosion of the metals present in the repository.

The second assumption implies that the volume of gas generated in the first year, at the pressure of the repository, is larger than the volume of water to be expelled to open the gas paths. Since the corrosion rate of aluminium is very high, it is expected that the gas generation from aluminium start directly once that the oxygen is consumed and the waste is put in contact with water. Moreover, this implies that the gas production in the first year is enough to expel the water required to open paths for the gas flow. If the volume of gas generated is not enough to expel the water in one year, the water expulsion will take a longer time. This means that the radionuclides are transported from the repository with a smaller water flow rate, but the concentration will be somewhat higher.

It is also considered in the calculations that water is not a limiting factor for the gas generation, once that water has penetrated the waste containers. This is due to that the volume of water needed to generate gas is quite small. About one litre of water is used for generating one Nm^3 of gas. The maximum gas generation rate in a container is a few Nm^3/year. This means that a few litres of water are used by the reaction. The water content in these containers is several tens of litres. Moreover, water bound by capillary forces is not expelled from the concrete even if a moderate overpressure is applied.

Since the waste packages are not hermetic, it is considered that water may flow into the waste when the repository is sealed and that the gas generated in the interior may escape through openings in the top of the waste packages.

The activity around the waste packages will increase with time. Initially, the activity is located only in the interior of the waste packages. Before the start of the gas generation, the radionuclides are only transported by diffusion through the concrete walls of the concrete moulds. In the steel containers, radionuclides can not be transported by diffusion through the steel walls as long as the walls are intact. The activity of the non-sorbing radionuclides around concrete moulds increases rapidly. After 2–3 years the activity reaches 10% of its maximum value. For sorbing nuclides such as ^{36}Cl, the activity is about 0.1% of the maximum value after 10 years. In the calculations, intact steel walls are only assumed in the first step, when water is expelled to allow the gas flow. This step is considered to occur during the first year.

It is assumed that the steel walls are totally corroded when the amount of contaminated water expelled to equilibrate the overpressure is calculated. This is a very conservative assumption, since it is expected that the steel walls act as a diffusion barrier for a long time.

10.2 Conclusions

As indicated above, the radionuclide release was calculated for different scenarios, from realistic scenarios to very conservative scenarios where a large volume of contaminated water is expelled. From the calculations, it may be pointed out that:

- For the base scenario (the situation that is expected to occur) the impact of the gas generation on the radionuclide release is small. For the long-lived nuclides this is negligible. For the short-lived and non-sorbing ^{3}H, the release is increased to some extent.

- For the case where an initial fracture exist at the bottom of the encapsulation the impact of the gas generation on the radionuclide release may be important for certain radionuclides. The release is increased by 5–7 orders of magnitude for the short-lived radionuclides with little or no sorption properties.

- The impact of the gas generation on the release of the long-lived radionuclides is, in general, small. For these radionuclides the maximum release is determined mainly by diffusion.

- The radionuclide release, for some radionuclides, may be increased by several orders of magnitude when water is expelled from the silo by effect of the gas generated in its interior. However, the impact on the total doses during the first thousands years after closure of the repository is limited. The total dose is dominated by the release of organic ^{14}C. Since the radionuclides are released to the coastal area during the first thousand years the dilution is considerable, which results in a very low dose.

- For the silo, the evacuation pipes are essential for its adequate function. If evacuation pipes are not mounted in the lid the pressure in the silo may be increased and a large volume of potentially contaminated water may be expelled.

- For BMA, the existence of gaps between the concrete lid and the walls where the lid is supported is also essential for its function.

- The use of backfill concrete in the BMA construction is very important if a fracture originates in the lower part of the concrete construction and gas can not escape through gaps on the top. Backfill reduces the volume of water that is possible to expel from the encapsulation.

11 References

Berger D, Braester C, 2000. Gas-water displacement through fracture networks. Water Resour. Res., 36, 3205–3210.

Björkenstam E, 1996. Sammanställning av gjutningar i SFR och provningar i Bångbro under 1994 och 1995. Vattenfall report, UC 96:Ö1. (In Swedish)

Björkenstam E, 1997. Utveckling av SFR-bruket. Vattenfall Utveckling AB. Rapport UC 97:4Ö. (In Swedish)

Braester C, Thunvik R, 1988. Gas migration from low level radioactive repositories in hard rocks. Nuclear Technology, 82, 60–70.

Firestone R B, 1998. Table of Isotopes, 8th ed., 1998 Update, Ed. C M Baglin. John Wiley & Sons, Inc., New York.

Forsgren E, Lange F, Larsson H, 1996. SFL 3–5 Layoutstudie. SKB AR D-96-016, Svensk Kärnbränslehantering AB. (In Swedish)

Holmén J, Stigsson M, 2001a. Project SAFE – Modelling of future hydrogeological conditions at SFR, Forsmark. SKB R-01-02, Swedish Nuclear Fuel and Waste Management Co.

Holmén J, Stigsson M, 2001b. Details of predicted flow in deposition tunnels at SFR, Forsmark. SKB R-01-21, Swedish Nuclear Fuel and Waste Management Co.

Höglund L O, Bengtsson A, 1991. Some chemical and physical processes related to the long-term performance of the SFR repository. SKB SFR 01-06, Swedish Nuclear Fuel and Waste Management Co.

Jacobsson A, Forsberg T, 1986. Mätning av gaspermeabilitet i vattenmätt betong. SFR Tek PM 40, Svensk Kärnbränslehantering AB. (In Swedish)

Möckel H, Köster R, 1980. Untersuchung zur Strahlenbeständigkeit von zementierten LAW-, MAW-Produkten. Institut für Nukleare Entsorgungstechnik, KfK 3045. (In German)

Möller G, Petersons N, Samuelson P, 1981. "Betonghandboken", Material. Svensk Byggtjänst, Stockholm. (In Swedish)

Pedersen K, 2001. Microbial features, events and processes in the Swedish final repository for low- and intermediate-level radioactive waste. SKB R-01-05, Swedish Nuclear Fuel and Waste Management Co.

Pettersson M, Elert M, 2001. Characterisation of bituminised waste in SFR-1. SKB R-01-26, Swedish Nuclear Fuel and Waste Management Co.

Push R, Hökmark H, 1987. Megapermeameterstudie av gas transport genom SFR-buffertar. SKB PR SFR 87-06, Svensk Kärnbränslehantering AB. (In Swedish)

Riggare P, Johansson C, 2001. Project SAFE – Low and Intermediate Level Waste in SFR-1. Reference Waste Inventory. SKB R-01-03, Swedish Nuclear Fuel and Waste Management Co.

Rodwell W R, Harris A W, Horseman S T, Lalieux P, Müller W, Ortiz Amaya L, Preuss K, 1999. Gas migration and two-phase flow through engineered and geological barriers for a deep repository for radioactive waste. A joint EC/NEA status report, EUR 19122 EN.

Romero L, Moreno L, Neretnieks I, 1995. The fast multiple-path Nuctran model – Calculating the radionuclide release from a repository. Nuclear Technology, 112 (1) 99–107.

SKB, 1998. Editors J Andersson, P Riggare and K Skagius, ”Project SAFE. Update of the SFR-1 safety assessment phase 1”. SKB R-98-43, Swedish Nuclear Fuel and Waste Management Co.

SKB, 2001. “Project SAFE – Compilation of data for radionuclide transport analysis. SKB R-01-14, Swedish Nuclear Fuel and Waste Management Co.

Thunvik R, Braester C, 1990. Gas migration in discrete fracture networks. Water Resour. Res., 26, 2425–2434.

Warrant M M, Brown N, 1989. “Contribution to Internal Pressure and Flammable Gas Concentration in RAM Transport Packages”. SAND-89-09040C, Conf-8980631–33.

Wiborgh M, Höglund L O, Pers K, 1986. Gas Formation in a L/ILW Repository and Gas Transport in the Host Rock. Nagra Technical Report 85-17.

Appendix A:

Quantity of materials and geometrical data for barriers, waste packages and gas generating materials

Contents

A.1 Introduction

This appendix contains tables with estimated quantities of materials and geometrical data for the barriers of the different repository parts as well as for the waste packages and gas generating materials. The information given is used to estimate the build up of gas pressure and expulsion of water from the waste packages.

The data in this appendix constitute the basis for the calculations in this report and in some cases they are given with an unnecessary number of significant figures. Data given for cement and concrete are given as wet weight.

The information in this appendix is based on information given in the background material to the SAFE study (SKB, 2001 and Riggare and Johansson, 2001).

A.2 Silo

A.2.1 Quantity of materials and geometrical data for barriers and waste packages

The estimated volumes of the different barriers, their thickness and the amount of reinforcement bars in the concrete structures are given in Table A.2-1. The void in the barriers is also given in Table A.2-1, the porosity of the materials is presented in Chapter 5 in this report.

Table A.2-1. Estimated volumes, thickness, pore volumes and quantity of reinforcement bars in the barriers in the Silo.

Barrier	Volume (m^3)	Thickness (m)	Pore volume (m^3)	Reinforcement Diameter (mm)		Fe (tonnes)
Concrete structures	**9 134**		**1 370**			**452**
Cylindrical walls	3 662	0.8	549	outer	25	32.7
					16	26.8
				inner	20	19.7
					16	25.2
Bottom	616	1	92		16	27.6
Lid	556	1	83		16	27.6
Inner walls	4 301	0.2	645		10	292
Concrete grout	**6 254**		**1 876**			
Bentonite	**5 663**	**1.2**	**3 455**			
10/90 bentonite/sand	**2 109**		**527**			
Bottom	977	1.5	244			
Top	1 132	1.5	283			

The estimated quantity of concrete and cement conditioning in the waste packages and the pore volume in these materials as well as the internal void in the waste packages are summarised in Table A.2-2. The estimated pore volume in concrete and in the cement waste matrix is based on the assumptions that the porosity of the concrete in the moulds is 15% and that the cement in the waste matrix has a porosity of 20%. Concrete moulds generally have a wall thickness of 0.1 m, but moulds with thicker walls (0.25 m) are used in exceptional cases for waste with higher concentrations of radionuclides. The

moulds with thicker walls contain more concrete and less raw waste, but the activity content is the same. Here it is assumed that all concrete moulds have a wall thickness of 0.1 m. More detailed information on amounts and dimensions of waste packages and gas generating materials are found in Section A.2.2. The estimated quantity of gas generating metals and organic materials in the waste packages is summarised in Table A.2-3.

Table A.2-2. Estimated quantity of concrete and cement as well as pore volume and internal void in waste packages allocated to the Silo.

Waste category (No of packages)	Concrete/cement			Pore volume	Internal void
	Mould (tonnes)	Waste (tonnes)	Total (tonnes)	(m^3)	(m^3)
Concrete mould (100 mm wall) with cement conditioned waste (4 389)	5 881	6 589	12 471	1 042	638
Steel mould (5 mm wall) with cement conditioned waste (3 829)		8 014	8 014	802	325
Steel drum (1.5–1 mm wall) with cement conditioned waste (564)		73	73	7	4
Steel mould (5 mm wall) with bitumen conditioned waste (938)					160
Steel drum (1.2 mm wall) with bitumen conditioned waste (6 902)					207
All waste (16 622)	**5 881**	**14 676**	**20 558**	**1 851**	**1 334**

Table A.2-3. Estimated quantity of gas generating metals and organic materials in the waste packages allocated to the Silo.

Waste category (No of packages)	Metals		Organic materials			
	Fe	Al+Zn	Cellu-lose	Resins	Bitumen	Others
	(tonnes)	(tonnes)	(tonnes)	(tonnes)	(tonnes)	(tonnes)
Concrete mould (100 mm wall) with cement conditioned waste (4 389)	1 278		5.2	551		42
Steel mould (5 mm wall) with cement conditioned waste (3 829)	1 628		0.3	997		
Steel drum (1.5–1 mm wall) with cement conditioned waste (564)	90	2.2	3.4	9		2
Steel mould (5 mm wall) with bitumen conditioned waste (938)	375			563	900	
Steel drum (1.2 mm wall) with bitumen conditioned waste (6 902)	278			345	1 035	
All waste (16 622)	**3 649**	**2.2**	**8.9**	**2 465**	**1 935**	**44**

A.2.2 Detailed information on waste packages

Table A.2-4. Estimated quantity of concrete/cement and pore volumes in these materials as well as the internal void and quantity and dimensions of gas generating metals in concrete moulds with cement conditioned waste.

Waste category (No of packages)	Cement/ concrete (kg)	Pore volume (m^3)	Void (m^3)	Thickness Fe (mm)	Thickness Al+Zn (mm)	Quantity Fe (kg)	Quantity Al+Zn (kg)
O.02+C.02 (3532)	10 172 160	853	530			1 024 280	
Waste matrix	5 439 280	544					
Steel lid				2		45 916	
Steel stirrer				5		56 512	
Concrete mould	4 732 880	309	530	∅12		921 852	
R.02 (705)	1 931 700	160	106			204 450	
Waste matrix	987 000	99					
Steel lid				2		9 165	
Steel stirrer				5		11 280	
Concrete mould	944 700	62	106	∅12		184 005	
C.24 (15)	46 800	4	0.15			10 470	
Waste matrix	26 700	2.7		5		255	
Steel drum				50		6 300	
Concrete mould	20 100	1.3	0.15	∅12		3 915	
C.24 (135)	315 900	25.3	1.35			37 530	
Waste matrix	135 000	13.5		5		2 295	
Concrete mould	180 900	11.8	1.35	∅12		35 235	
S.24 (2)	3 810	0.29	0.1			774	7.6
Waste matrix	1 130	0.11		5	5	226	7.6
Steel lid				2		26	
Concrete mould	2 680	0.17	0.1	∅12		522	

Table A.2-5. Estimated quantities of organic materials in concrete moulds with cement conditioned waste.

Waste category (No of packages)	Cellulose (kg)	Resins (kg)	Other org (kg)	Cement additives Waste matrix (kg)	Cement additives Mould (kg)
O.02+C.02 (3532)		459 160	35 320		
R.02 (705)		91 650	7 050		
C.24 (15)	525				
C.24 (135)	4 725				
S.24 (2)					

Table A.2-6. Estimated quantity of conditioning cement and pore volumes in the cement as well as the internal void and quantity and dimensions of gas generating metals in steel moulds and drums with cement conditioned waste.

Waste category (No of packages)	Cement	Pore volume	Void	Thickness		Quantity	
				Fe	Al+Zn	Fe	Al+Zn
	(kg)	(m^3)	(m^3)	(mm)	(mm)	(kg)	(kg)
R.16 (3733)	7 839 300	784	317			1 586 525	
Waste matrix	7 839 300	784					
Steel stirrer				2		93 325	
Steel mould			317	5		1 493 200	
S.11 (96)	174 720	17.5	8.2			40 800	
Waste matrix	174 720	17.5					
Steel stirrer				2		2 400	
Steel mould			8.2	5		38 400	
S.04 (134)	31 892	3.2	1.3			10 268	
Waste matrix	31 892	3.2					
Steel drum + stirrer			1.3	1.5		8 040	
Steel plate for drums				4		2 228	
S.22[1] (430)	41 302	4.1	2.2			80 195	2 150
Waste matrix	41 302	4.1		5	5	31 820	2 150
Steel drum			2.2	1		12 900	
Steel box for drums				2.5		35 475	

[1] 100 l steel drum placed in a 200 l steel drum with cement in between the drums.

Table A.2-7. Estimated quantities of organic materials in steel moulds and drums with cement conditioned waste.

Waste category (No of packages)	Cellulose	Resins	Other org	Cement additives	
				Waste matrix	Mould
	(kg)	(kg)	(kg)	(kg)	(kg)
R.16 (3733)		933 250			
S.11 (96)	288	64 032			
S.04 (134)		8 710			
S.22 (430)	3 440		1 720		

Table A.2-8. Estimated internal void and quantity and dimensions of gas generating metals in steel moulds and drums with bitumen conditioned waste.

Waste category (No of packages)	Void	Thickness		Quantity	
		Fe	Al+Zn	Fe	Al+Zn
	(m^3)	(mm)	(mm)	(kg)	(kg)
F.18 (938)	160			375 200	
Waste matrix					
Steel mould	160	5		375 200	
B.06 (6902)	207			277 806	
Waste matrix					
Steel drum	207	1.2		158 746	
Steel plate for drums		4		84 550	
Steel expansion box		6		34 510	

Table A.2-9. Estimated quantities of organic materials in steel moulds and drums with bitumen conditioned waste.

Waste category (No of packages)	Bitumen (kg)	Resins (kg)
F.18 (938)	900 480	562 800
B.06 (6902)	1 035 300	345 100

A.3 BMA

A.3.1 Quantity of materials and geometrical data for barriers and waste packages

The estimated volumes of the different barriers, their thickness and pore volume as well as the amount of reinforcement bars in the concrete structures are summarised in Table A.3-1. The porosity of the materials is presented in Chapter 5.

Table A.3-1. Estimated volumes, thickness, pore volumes and quantity of reinforcement bars in the barriers in BMA.

Barrier	Volume (m^3)	Thickness (m)	Pore volume (m^3)	Reinforcement, Diameter (mm)	Reinforcement, Fe (tonnes)
Concrete structures	**4 118**		**617**		**401**
Side walls	928	0.4/0.6	139	16	92.8
Bottom	545	0.25	81.8	16	54.5
Lid	2 069	0.95	310	16	196
Inner walls	576	0.4	86.4	16	57.6
Void around packages, if no concrete grout	**2 095**				
Sand/gravel	**~24 000**		**~7 200**		
Long sides	~4 700	2	~1 410		
Bottom	~1 800	~0.5	~540		
Top	~17 500	~6.5	~5 250		
Concrete grout, if grout is used as filling	**2 095**		**628**		

The estimated quantity of concrete and cement conditioning in the waste packages and the pore volume in these materials as well as the internal void in the waste packages are summarised in Table A.3-2. More detailed information on amounts and dimensions of waste packages and gas generating materials are found in Section A.3.2.

Table A.3-2. Estimated quantity of concrete and cement as well as pore volume and internal void in waste packages allocated to BMA.

Waste category (No of packages)	Concrete/cement			Pore volume (m^3)	Internal void (m^3)
	Mould (tonnes)	Waste (tonnes)	Total (tonnes)		
Concrete mould (100 mm wall) with cement conditioned waste (3 818)	5 116	4 374	9 489	771	442
Steel mould (5 mm wall) with cement conditioned waste (1 062)		1 654	1 654	166	91
Steel drum (1.5–1 mm wall) with cement conditioned waste (1 875)		250	250	25	11
Steel mould (5 mm wall) with bitumen conditioned waste (879)					75
Steel drum (1.2–1.25 mm wall) with bitumen conditioned waste (5 948)					174
Odd waste		371	371	37	185
All waste (13 582)	**5 116**	**6 649**	**11 764**	**999**	**978**

The estimated quantity of gas generating metals and organic materials in the waste packages allocated to BMA is summarised in Table A.3-3.

Table A.3-3. Estimated quantity of gas generating metals and organic materials in the waste packages allocated to BMA.

Waste category (No of packages)	Metals		Organic materials			
	Fe (tonnes)	Al+Zn (tonnes)	Cellu-lose	Resins (tonnes)	Bitumen (tonnes)	Others (tonnes)
Concrete mould (100 mm wall) with cement conditioned waste (3 818)	1 193	3.3	31	317		96
Steel mould (5 mm wall) with cement conditioned waste (1 062)	677	3.3	62	78		170
Steel drum (1.5–1 mm wall) with cement conditioned waste (1 875)	308	7.5	12			6
Steel mould (5 mm wall) with bitumen conditioned waste (879)	352		1	571	721	
Steel drum (1.2–1.25 mm wall) with bitumen conditioned waste (5 948)	221			435	798	
Odd waste	288					
All waste (13 582)	**3 039**	**14.1**	**106**	**1 401**	**1 519**	**272**

A.3.2 Detailed information on waste packages

Table A.3-4. Estimated quantity of concrete/cement and pore volumes in these materials as well as the internal void and quantity and dimensions of gas generating metals in concrete moulds with cement conditioned waste.

Waste category (No of packages)	Cement/ concrete (kg)	Pore volume (m^3)	Void (m^3)	Thickness Fe (mm)	Thickness Al+Zn (mm)	Quantity Fe (kg)	Quantity Al+Zn (kg)
O.01+C.01 (738)	**2 125 440**	**178**	**111**			**214 020**	
Waste matrix	1 136 520	114					
Steel lid				2		9 594	
Steel stirrer				5		11 808	
Concrete mould	988 920	64.5	111	∅12		192 618	
R.01 (1702)	**4 663 480**	**387**	**255**			**493 580**	
Waste matrix	2 382 800	238					
Steel lid				2		22 126	
Steel stirrer				5		27 232	
Concrete mould	2 280 680	149	255	∅12		444 222	
R.10 (136)	**334 560**	**27.1**	**13.6**			**39 440**	
Waste matrix	152 320	15.2					
Steel lid				2		1 768	
Steel stirrer				5		2 176	
Concrete mould	182 240	11.9	13.6	∅12		35 496	
O.23+C.23 (784)	**1 493 520**	**113**	**39.2**			**302 624**	**2 744**
Waste matrix	442 960	44.3		5	5	87 808	2 744
Steel lid				2		10 192	
Concrete mould	1 050 560	68.5	39.2	∅12		204 624	
R.23 (343)	**653 415**	**49.4**	**17.2**			**102 557**	**343**
Waste matrix	193 795	19.4		5	5	8 575	343
Steel lid				2		4 459	
Concrete mould	459 620	30	17.2	∅12		89 523	
F.23 (54)	**102 870**	**7.8**	**2.7**			**16 416**	
Waste matrix	30 510	3		5		1 620	
Steel lid				2		702	
Concrete mould	72 360	4.8	2.7	∅12		14 094	
S.23 (61)	**116 205**	**8.8**	**3**			**23 607**	**232**
Waste matrix	34 465	3.4		5	5	6 893	232
Steel lid				2		793	
Concrete mould	81 740	5.3	3	∅12		15 921	

Table A.3-5. Estimated quantities of organic materials in concrete moulds with cement conditioned waste.

Waste category (No of packages)	Cellulose (kg)	Resins (kg)	Other org (kg)	Cement additives Waste matrix (kg)	Cement additives Mould (kg)
O.01+C.01 (738)		95 940	7 380		
R.01 (1702)		221 260	17 020		
R.10 (136)			1 360		
O.23+C.23 (784)	23 520		52 136		
R.23 (343)	3 773		8 575		
F.23 (54)	1 566		10 044		
S.23 (61)	1 769				

Table A.3-6. Estimated quantity of conditioning cement and pore volumes in the cement as well as the internal void and quantity and dimensions of gas generating metals in steel moulds and drums with cement conditioned waste.

Waste category (No of packages)	Cement (kg)	Pore volume (m^3)	Void (m^3)	Thickness Fe (mm)	Thickness Al+Zn (mm)	Quantity Fe (kg)	Quantity Al+Zn (kg)
R.15 (295)	**619 500**	**62**	**25.1**			**125 375**	
Waste matrix	619 500	62					
Steel stirrer				2		7 375	
Steel mould			25.1	5		118 000	
F.15 (11)	**8 855**	**0.9**	**1.9**			**4 675**	
Waste matrix	8 855	0.9					
Steel stirrer				2		275	
Steel mould			1.9	5		4 400	
R.23 (486)	**659 016**	**65.9**	**41.3**			**369 846**	**1 944**
Waste matrix	659 016	65.9		5	5	48 600	1 944
Steel lid				6		88 938	
Steel mould			41.3	5		232 308	
F.23 (270)	**366 120**	**36.6**	**23**			**177 390**	**1 350**
Waste matrix	366 120	36.6		5	5	40 500	1 350
Steel lid				3		12 960	
Reinforcement				∅14		3 780	
Steel mould			23	5		120 150	
S.09 (382)	**106 960**	**10.7**	**3.8**			**29 271**	
Waste matrix	106 960	10.7					
Steel drum			3.8	1.5		22 920	
Steel plate for drums				4		6 351	
S.21[1] (1493)	**143 403**	**14.3**	**7.5**			**278 445**	**7 465**
Waste matrix	143 403	14.3		5	5	110 482	7 465
Steel drum			7.5	1		44 790	
Steel box for drums				2.5		123 173	
"Odd waste"	**370 566**	**37.1**	**185**			**288 218**	
Waste matrix	370 566	37.1	185	10		288 218	

[1] 100 l steel drum placed in a 200 l steel drum with cement in between the drums

Table A.3-7. Estimated quantities of organic materials in steel moulds and drums with cement conditioned waste.

Waste category (No of packages)	Cellulose (kg)	Resins (kg)	Other org (kg)	Cement additives Waste matrix (kg)	Cement additives Mould (kg)
R.15 (295)		73 750			
F.15 (11)		4 125			
R.23 (486)	21 384		48 600		
F.23 (270)	40 500		121 500		
S.09 (382)					
S.21 (1493)	11 795		5 972		
"Odd waste"					

Table A.3-8. Estimated internal void and quantity and dimensions of gas generating metals in steel moulds and drums with bitumen conditioned waste.

Waste category (No of packages)	Void	Thickness		Quantity	
		Fe	Al+Zn	Fe	Al+Zn
	(m^3)	(mm)	(mm)	(kg)	(kg)
F.17 (879)	**74.7**			**351 600**	
Waste matrix					
Steel mould	74.7	5		351 600	
B.05 (4230)	**137**			**149 108**	
Waste matrix					
Steel drum	137	1.2		97 290	
Steel plate for drums		4		51 818	
F.05 (1718)	**37.1**			**71 512**	
Waste matrix					
Steel drum	37.1		1.25	42 950	
Steel plate for drums			4	28 562	

Table A.3-9. Estimated quantities of organic materials in steel moulds and drums with bitumen conditioned waste.

Waste category (No of packages)	Cellulose (kg)	Bitumen (kg)	Resins (kg)
F.17 (879)	700[1)]	720 780	571 350
B.05 (4230)		634 500	211 500
F.05 (1718)		163 210	223 340

[1)]Cellulose only in 195 packages

A.4 1BTF and 2BTF

A.4.1 Quantity of materials and geometrical data for barriers and waste packages

The estimated volumes of the different barriers, their thickness and pore volume are summarised in Tables A.4-1 (1BTF) and A.4-2 (2BTF). The porosity of the materials is presented in Chapter 5.

Table A.4-1. Estimated volumes, thickness, pore volumes and quantity of reinforcement bars in the barriers in 1BTF.

Barrier	Volume	Thickness	Pore volume	Reinforcement	
				Diameter	Fe
	(m^3)	(m)	(m^3)	(mm)	(tonnes)
Concrete structures	**1 924**		**290**		**192**
Bottom	941	0.4	141	16	94
Prefabricated lid	160	0.4	24	16	16
Slate lid	823	0.4	125	16	82
Concrete grout	**2 397**		**479**		
Sand/gravel					
Bottom	705.6	0.3	212		
Top	~6 100	~2.5	~1 830		

Table A.4-2. Estimated volumes, thickness, pore volumes and quantity of reinforcement bars in the barriers in 2BTF.

Barrier	Volume	Thickness	Pore volume	Reinforcement	
	(m^3)	(m)	(m^3)	Diameter (mm)	Fe (tonnes)
Concrete structures	**2 548**		**384**		**254**
Bottom	941	0.4	141	16	94
Prefabricated lid	784	0.4	118	16	78
Slate lid	823	0.4	125	16	82
Concrete grout	**2 329**		**466**		
Sand/gravel					
Bottom	705.6	0.3	212		
Top	~6 100	~2.5	~1 830		

The estimated quantity of concrete and cement conditioning in the waste packages and the pore volume in these materials as well as the internal void in the waste packages are summarised in Tables A.4-3 (1BTF) and A.4-4 (2BTF). The walls of the concrete tanks are assumed to have the same porosity as the walls of concrete moulds. More detailed information on amounts and dimensions of waste packages and gas generating materials are found in Section A.4.2.

Table A.4-3. Estimated quantity of concrete and cement as well as pore volume and internal void in waste packages allocated to 1BTF.

Waste category (No of packages)	Concrete/cement			Pore volume	Internal void
	Mould (tonnes)	Waste (tonnes)	Total (tonnes)	(m^3)	(m^3)
Concrete mould (100 mm wall) with cement conditioned waste (216)	289	299	589	49	31
Steel drum in steel drum with ashes (6 479)		622	622	62	32
Concrete tank (150 mm wall) with unsolidified resins (186)	1 926		1 926	126	93
Steel box (3 mm wall) with unconditioned graphite (96)					3
Odd waste (415)					3 777
All waste (7 392)	**2 215**	**921**	**3 137**	**237**	**3 936**

Table A.4-4. Estimated quantity of concrete and cement as well as pore volume and internal void in waste packages allocated to 2BTF.

Waste category (No of packages)	Concrete/cement			Pore volume	Internal void
	Mould (tonnes)	Waste (tonnes)	Total (tonnes)	(m^3)	(m^3)
Concrete tank (150 mm wall) with unsolidified resins (800)	8 282		8 282	540	401

The estimated pore volume in unconditioned resins in 1BTF and 2BTF are given in Tables A.4-4–A.4-5.

Table A.4-5. Estimated pore volume in unconditioned resins in 1BTF and 2BTF.

Vault	Pore volume in unconditioned resins (m^3)
1BTF	614
2BTF	2 640

The estimated quantity of gas generating metals and organic materials in the waste packages allocated to 1BTF and 2BTF is summarised in Tables A.4-6 and A.4-7.

Table A.4-6. Estimated quantity of gas generating metals and organic materials in the waste packages allocated to 1BTF.

Waste category (No of packages)	Metals		Organic materials			
	Fe	Al+Zn	Cellu-lose	Resins	Bitumen	Others
	(tonnes)	(tonnes)	(tonnes)	(tonnes)	(tonnes)	(tonnes)
Concrete mould (100 mm wall) with cement conditioned waste (216)	63	0.01	0.1	24		2.2
Steel drum in steel drum with ashes (6 479)	194	42.0				
Concrete tank (150 mm wall) with unsolidified resins (186)	121			227		21.5
Steel box (3 mm wall) with unconditioned graphite (96)	14	0.5				
Odd waste (415)	2 905					
All waste (7 392)	**3 297**	**42.5**	**0.1**	**251**		**23.7**

Table A.4-7. Estimated quantity of gas generating metals and organic materials in the waste packages allocated to 2BTF.

Waste category (No of packages)	Metals		Organic materials			
	Fe	Al+Zn	Cellu-lose	Resins	Bitumen	Others
	(tonnes)	(tonnes)	(tonnes)	(tonnes)	(tonnes)	(tonnes)
Concrete tank (150 mm wall) with unsolidified resins (800)	518			902		93

A.4.2 Detailed information on waste packages

Table A.4-8. 1BTF, estimated quantity of concrete/cement and pore volumes in these materials as well as the internal void and quantity and dimensions of gas generating metals in concrete moulds with cement conditioned waste.

Waste category (No of packages)	Cement/ concrete (kg)	Pore volume (m^3)	Void (m^3)	Thickness Fe (mm)	Thickness Al+Zn (mm)	Quantity Fe (kg)	Quantity Al+Zn (kg)
O.01+C.01 (66)	**190 080**	**16.0**	**9.9**			**19 140**	
Waste matrix	101 640	10.2					
Steel lid				2		858	
Steel stirrer				5		1 056	
Concrete mould	88 440	5.8	9.9	∅ 12		17 226	
R.01 (119)	**326 060**	**27.1**	**17.9**			**34 510**	
Waste matrix	166 600	16.7					
Steel lid				2		1 547	
Steel stirrer				5		1 904	
Concrete mould	159 460	10.4	17.9	∅ 12		31 059	
R.10 (24)	**59 040**	**4.8**	**2.4**			**6 960**	
Waste matrix	26 880	2.7					
Steel lid				2		312	
Steel stirrer				5		384	
Concrete mould	32 160	2.1	2.4	∅ 12		6 264	
R.23 (7)	**13 335**	**1.0**	**0.4**			**2 093**	**7**
Waste matrix	3 955	0.4		5	5	175	7
Steel lid				2		91	
Concrete mould	9 380	0.6	0.4	∅ 12		1 827	

Table A.4-9. 1BTF, estimated quantities of organic materials in concrete moulds with cement conditioned waste.

Waste category (No of packages)	Cellulose (kg)	Resins (kg)	Other org (kg)	Cement additives Waste matrix (kg)	Cement additives Mould (kg)
O.01+C.01 (66)		8 580	660		
R.01 (119)		15 470	1 190		
R.10 (24)			240		
R.23 (7)	77		175		

Table A.4-10. 1BTF, estimated quantity of concrete/cement and pore volumes in these materials as well as the internal void and quantity and dimensions of gas generating metals in concrete tanks with unsolidified resins and odd waste.

Waste category (No of packages)	Cement/ concrete (kg)	Pore volume (m^3)	Void (m^3)	Thickness Fe (mm)	Thickness Al+Zn (mm)	Quantity Fe (kg)	Quantity Al+Zn (kg)
O.07 (83)	**859 299**	**56.0**	**41.5**			**53 701**	
Waste matrix							
Concrete tank	859 299	56.0	41.5	∅8		53 701	
B.07 (103)	**1 066 359**	**69.5**	**51.5**			**66 641**	
Waste matrix							
Concrete tank	1 066 359	69.5	51.5	∅8		66 641	
Odd waste (415)			**3 777**			**2 905 000**	
Waste matrix				10		2 905 000	
Concrete tank							

Table A.4-11. 1BTF, estimated quantities of organic materials in concrete tanks with unsolidified resins and odd waste.

Waste category (No of packages)	Cellulose (kg)	Resins (kg)	Other org (kg)	Cement additives Waste matrix (kg)	Cement additives Mould (kg)
O.07 (83)		83 000	9 628		
B.07 (103)		144 200	11 948		
Odd waste (415)					

Table A.4-12. 1BTF, estimated quantity of concrete/cement and pore volumes in these materials as well as the internal void and quantity and dimensions of gas generating metals in steel drums with ashes.

Waste category (No of packages)	Cement/ concrete (kg)	Pore volume (m^3)	Void (m^3)	Thickness Fe (mm)	Thickness Al+Zn (mm)	Quantity Fe (kg)	Quantity Al+Zn (kg)
S.13 (6 479)	**622 308**	**62.2**	**32.4**			**194 370**	**42 114**
Waste matrix	622 308	62.2			∅4 [1)]		42 114
Outer steel packaging				1		129 580	
Inner steel packaging			32.4	1		64 790	

[1)]Spherical

Table A.4-13. 1BTF, estimated internal void and quantity and dimensions of gas generating metals in steel boxes with unconditioned graphite.

Waste category (No of packages)	Void (m^3)	Thickness Fe (mm)	Thickness Al+Zn (mm)	Quantity Fe (kg)	Quantity Al+Zn (kg)
S.19 (96)	**2.8**			**13 920**	**480**
Waste matrix			5		480
Steel packaging	2.8	3		13 920	

Table A.4-14. 2BTF, estimated quantity of concrete/cement and pore volumes in these materials as well as the internal void and quantity and dimensions of gas generating metals in concrete tanks with unsolidified resins.

Waste category (No of packages)	Cement/ concrete (kg)	Pore volume (m^3)	Void (m^3)	Thickness Fe (mm)	Thickness Al+Zn (mm)	Quantity Fe (kg)	Quantity Al+Z (kg)
O.07 (545)	**5 642 385**	**368**	**273**			**352 615**	
Waste matrix							
Concrete tank	5 642 385	368	273	∅8		352 615	
B.07 (255)	**2 640 015**	**172**	**128**			**164 985**	
Waste matrix							
Concrete tank	2 640 015	172	128	∅8		164 985	

Table A.4-15. 2BTF, estimated quantities of organic materials in concrete tanks with unsolidified resins.

Waste category (No of packages)	Cellulose (kg)	Resins (kg)	Other org (kg)	Cement additives Waste matrix (kg)	Cement additives Mould (kg)
O.07 (545)		545 000	63 220		
B.07 (255)		357 000	29 580		

A.5 BLA

A.5.1 Quantity of materials and geometrical data for barriers and waste packages

The estimated volumes of the different barriers, their thickness and pore volume are summarised in Table A.5-1. The porosity of the materials is presented in Chapter 5.

Table A.5-1. Estimated volumes, thickness, pore volumes and quantity of reinforcement bars in the barriers in BLA.

Barrier	Volume (m^3)	Thickness (m)	Pore volume (m^3)	Reinforcement Diameter (mm)	Reinforcement Fe (tonnes)
Concrete structures	**941**		**141**		
Bottom	941	0.4	141	16	94
Void around packages	**~12 000**				
Sand/gravel	**706**		**212**		
Bottom	706	0.3	212		

The estimated quantity of cement conditioning in the waste packages and the pore volume in these materials as well as the internal void in the waste packages are summarised in Table A.5-2. More detailed information on amounts and dimensions of waste packages and gas generating materials are found in Section A.5.2.

Table A.5-2. Estimated quantity of concrete and cement as well as pore volume and internal void in waste packages allocated to BLA.

Waste category (No of packages)	Concrete/cement			Pore volume (m^3)	Internal void (m^3)
	Mould (tonnes)	Waste (tonnes)	Total (tonnes)		
ISO-container (1.5 mm wall) with unsolidified trash (514)					3 856
Steel drums in ISO-container (1.5 mm wall) with bitumenised resins (27)					193
Steel drum with unsolidified trash in steel drum in a container (73)		252	252	25	464
Odd waste (64)					1 107
All waste (678)		**252**	**252**	**25**	**5 620**

The estimated quantity of gas generating metals and organic materials in the waste packages allocated to BLA is summarised in Table A.5-3. More detailed information on dimensions and amounts of gas generating materials is found in Section A.5.2.

Table A.5-3. Estimated quantity of gas generating metals and organic materials in the waste packages allocated to BLA.

Waste category (No of packages)	Metals		Organic materials			
	Fe (tonnes)	Al+Zn (tonnes)	Cellulose (tonnes)	Resins (tonnes)	Bitumen (tonnes)	Others (tonnes)
ISO-container (1.5 mm wall) with unsolidified trash (514)	3 290	51	373			1 542
Steel drums in ISO-container (1.5 mm wall) with bitumenised resins (27)	75		8	92	116	
Steel drum with unsolidified trash in steel drum in a container (73)	412	13	43			11
Odd waste (64)	851					
All waste (678)	**4 628**	**65**	**424**	**92**	**116**	**1 553**

A.5.2 Detailed information on waste packages

Table A.5-4. Estimated internal void and quantity and dimensions of gas generating metals in ISO-containers with unsolidified trash.

Waste category (No of packages)	Void	Thickness		Quantity	
		Fe	Al+Zn	Fe	Al+Zn
	(m^3)	(mm)	(mm)	(kg)	(kg)
O.12 (80)	**600**			**512 000**	**8 000**
Waste matrix		5	5	360 000	8 000
Steel packaging	600	1.5		152 000	
R.12 (103)	**773**			**659 200**	**10 300**
Waste matrix		5	5	463 500	10 300
Steel packaging	773	1.5		195 700	
B.12 (272)	**2 040**			**1 740 800**	**27 200**
Waste matrix		5	5	1 224 000	27 200
Steel packaging	2 040	1.5		516 800	
F.12 (28)	**210**			**179 200**	**2 800**
Waste matrix		5	5	126 000	2 800
Steel packaging	210	1.5		53 200	
S.12 (31)	**233**			**198 400**	**3 100**
Waste matrix		5	5	139 500	3 100
Steel packaging	233	1.5		58 900	

Table A.5-5. Estimated quantities of organic materials in ISO-containers with unsolidified trash.

Waste category (No of packages)	Cellulose (kg)	Resins (kg)	Other org (kg)
O.12 (80)	40 000		240 000
R.12 (103)	83 430		309 000
B.12 (272)	220 320		816 000
F.12 (28)	14 000		84 000
S.12 (31)	15 500		93 000

Table A.5-6. Estimated internal void and quantity and dimensions of gas generating metals in steel drums with bitumenised ion-exchange resin in ISO-containers.

Waste category (No of packages)	Void	Thickness		Quantity	
		Fe	Al+Zn	Fe	Al+Zn
	(m^3)	(mm)	(mm)	(kg)	(kg)
B.20 (12)	**88**			**32 736**	
Waste matrix					
Outer steel packaging		1.5		22 800	
Inner steel packaging		1.2		9 936	
F.20 (15)	**105**			**42 000**	
Wwaste matrix					
Outer steel packaging		1.5		28 500	
Inner steel packaging		1.25		13 500	

Table A.5-7. Estimated quantities of organic materials in steel drums with bitumenised ion-exchange resin in ISO-containers.

Waste category (No of packages)	Cellulose (kg)	Bitumen (kg)	Resins (kg)
B.20 (12)	3 720	64 800	21 600
F.20 (15)	4 650	51 300	70 200

Table A.5-8. Estimated quantity of concrete/cement and pore volumes in these materials as well as the internal void and quantity and dimensions of gas generating metals in steel drums with unsolidified trash in steel drums placed in a container.

Waste category (No of packages)	Cement/ concrete (kg)	Pore volume (m^3)	Void (m^3)	Thickness Fe (mm)	Thickness Al+Zn (mm)	Quantity Fe (kg)	Quantity Al+Zn (kg)
S.14 (73)	**252 434**	**25.2**	**464**			**412 012**	**13 140**
Waste matrix	252 434	25.2		5	5	194 472	13 140
Outer steel packaging				1.5		138 700	
Inner steel packaging			464	1		78 840	

Table A.5-9. Estimated quantities of organic materials in steel drums with unsolidified trash in steel drums placed in a container.

Waste category (No of packages)	Cellulose (kg)	Resins (kg)	Other org (kg)	Cement additives Waste matrix (kg)	Cement additives Mould (kg)
S.14 (73)	43 391		10 512		

Table A.5-10. Estimated internal void and quantity and dimensions of gas generating metals in odd waste.

Waste category (No of packages)	Void (m^3)	Thickness Fe (mm)	Thickness Al+Zn (mm)	Quantity Fe (kg)	Quantity Al+ (kg)
Odd waste (64)	**1 107**			**851 200**	
Waste matrix		10		851 200	

A.6 References

Riggare P, Johansson C, 2001. Project SAFE – Low and Intermediate Level Waste in SFR-1. Reference Waste Inventory, R-01-03.

SKB, 2001. Project SAFE – Compilation of data for radionuclide transport analysis. SKB R-01-14, Swedish Nuclear Fuel and Waste Management Co.

Appendix B:

Gas generation in radioactive waste repositories

Current advances

Jinying Yan, Luis Moreno
Department of Chemical Engineering and Technology
Royal Institute of Technology

January 2000

Abstract

Current advances on gas generation and its migration from radioactive waste repositories are reviewed with respect to sources of gas generation and mechanisms of gas migration. With regard to gas generation, attention is given to the hydrogen generation from anaerobic corrosion of iron/steel in a cementitious environment. The near-field effects of gas release are focused on pressure build-up and related parameters that affect the pressure in a repository. Gas migration through the far-field geological formations is discussed in terms of mechanisms, multiphase flow, modelling or simulation and model validation with experiments. The emphasis is on the interaction and relationship between different processes and between the near- and far-field effects.

Sammanfattning

Nya rön angående gasbildning och dess transport från djupförvar för radioaktivt avfall sammanfattas angående gasbildningens ursprung och transportsättet för den bildade gasen. Vad gasbildningen beträffar, belyses särskilt bildningen av vätgas i samband med anaerobisk korrosion av järn/stål i en omgivning av cement. Gasbildningens effekter i närområdet studeras också. Detta gäller främst avseende uppbyggnad av tryck, och andra parametrar som kan ha sin betydelse för tryckstegringen i förvaret. Transport av gas i storskaliga geologiska formationer behandlas angående transportsätt, flöde genom flera faser, modellering eller simulering och modellvalidering genom experiment. Tyngdpunkten ligger på samspelet mellan olika processer samt effekter i den omedelbara omgivningen kontra yttre omgivningen.

Contents

B.1 Introduction and background

It is recognised that gas generation may potentially affect the safe disposal of radioactive waste in a repository. Gases may accelerate the movement of radioactive, contaminated water from the repository and may increase the pressure inside the repository causing the gas to escape through the surrounding barriers and geological formations. Gas generation may also create an unsaturated environment in a repository or surrounding engineered or geological barrier materials and thus decrease the migration of radionuclides. There are several processes acting simultaneously in gas generation and gas migration. Therefore, an understanding of the individual processes and their interactions is essential in an assessment of gas generation and migration.

Moreno and Neretnieks /1991/ studied the gas generation in the silo in the Swedish Final Repository for Radioactive Waste (SFR). They also studied the radionuclide release caused by this gas generation. A value of 3 μm/year for the rate of corrosion of the iron/steel was used in these calculations. In order to update the knowledge on gas generation and its migration in nuclear waste disposal repositories for use in a new safety assessment of the SFR, a review of the literature was carried out. The present review covers the literature from 1986 to 1998. The number of references relating to the anaerobic corrosion of iron/steel in a concrete environment is scarce. Research into the corrosion and gas generation under anoxic conditions is restricted to the assessment of nuclear waste disposal. Moreover, most of the studies concerning gas migration are related to the assessment of nuclear waste deposits.

Several sources and processes account for the gas generation and migration. The contribution of a given source to the gas generation depends on waste type and specific disposal conditions (system characteristics). There is an obvious difference between the mechanisms of gas generation between high level waste (HLW) and low and intermediate level wastes (LLW and ILW) /Brewitz and Mönig, 1992; Rees, 1992/. Radiolysis may increase the gas generation in a repository for HLW. In this report, attention is focused mainly on the low and intermediate level wastes.

Gas generation leads to gas migration and this in turn leads to near-field effects in the repository and far-field effects through the surrounding engineering or geological barriers. Contaminated water may be pushed out from the repository by the generated gas. Gas from the repository may also modify the hydrology around the repository. Current research is directed towards an understanding of these relationships.

B.2 Gas generation in anaerobic conditions

Gas generation will pass through different phases from an aerobic to an anaerobic phase in a nuclear waste repository. The aerobic phase may be important only at the initial stage when oxygen is present. After this, the processes of gas generation in an anaerobic environment are dominant. There are many potential sources of gas generation in a repository, including corrosion of metals, degradation of organic materials and radiolysis. Some of these processes may be dominant under specific environmental or site-specific conditions.

B.2.1 Corrosion mechanisms of iron and steel

The corrosion of iron/steel is generally considered to be the most important mechanism for gas generation in a nuclear waste repository. Under anaerobic conditions, iron or steel corrodes by reaction with water /Simpson and Schenk, 1989; Naish et al., 1990; Reardon 1995/

$$Fe(s) + 2H_2O \rightarrow Fe(OH)_2(s) + H_2(g) \quad (1)$$

$Fe(OH)_2$ is stable at low temperature, but it may be converted to magnetite from a thermodynamic point of view.

$$3Fe(OH)_2(s) \rightarrow Fe_3O_4(s) + H_2(g) + 2H_2O \quad (2)$$

If the corrosion reaction is continued from reaction (1) to reaction (2), the hydrogen production increases by 33%.

The choice between reaction (1) and (2) is uncertain in some corrosion environments /Voinis et al., 1992/. In most of the samples in cement/concrete environments, the corrosion products were not found /Naish et al., 1990/. They suggested that a relatively soluble ferrous hydroxide is formed, which moves into the concrete. In only a few samples was the formation of magnetite observed. In anoxic groundwater, however, Fe_3O_4 (magnetite) is expected to be the corrosion product /Simpson and Schenk, 1989; Reardon 1995/.

Corrosion experiments /Simpson and Schenk, 1989/ indicate that there are three basic types of corrosion:

- General corrosion with oxide layer formation
- Unstable corrosion with pitting formation (local corrosion)
- Stable passive layer formation.

The rates of corrosion of iron and steel depend on the type of corrosion, which is strongly affected by the pH and concentration of chloride under anoxic conditions. No obvious differences in corrosion rate were found between iron and technical steels /Grauer et al., 1991/.

In alkaline solutions such as cement pore water, iron and steel are in a passive state and covered by a non-porous oxide film that may be only a few nanometres in thickness. The corrosion rate is thus governed by the dissolution of the passive layer in the alkaline medium. The stable passivity under anoxic conditions in the pH range from 12.5 to 13 is supported by many observations /Grauer et al., 1991; Kreis, 1991/. The passivation and localised corrosion behaviour have been studied for mild steel in alkaline solution /Nakayama and Akashi, 1991/. The critical pH for transition from general corrosion to localised corrosion is 9.4. The mild steel can acquire immunity to pitting corrosion and corrosion will be inhibited as the pH is higher than 11.5.

In anoxic sulphide-free groundwater, general corrosion is expected for cast steel containers /Simpson and Schenk, 1989/. The corrosion rate will decrease by one order of magnitude when the pH is increased from 7 to 10. It has also been found that the hydrogen generated begins to inhibit the corrosion of the iron as the pressure rises.

However the corrosion rate is reduced by a factor of only 4 when the pressure of hydrogen is increased from 1 to 100 atmospheres under anaerobic conditions /Naish et al., 1990; Kreis, 1991/.

The corrosion behaviour at a given pH depends very much on the chemical composition of the corrosion medium /Kreis, 1991/. Chloride has a large influence on the corrosion rate. The difference in corrosion rates can reach one order of magnitude between a chloride free medium and a medium with a high concentration of chloride /Schwarzkopf et al., 1989; Naish et al., 1990/.

The anaerobic corrosion of iron and steel is also influenced by the microbial activity. Cultures of sulphate-reducing bacteria utilise cathodic hydrogen and form H_2S, which accelerate both anodic and cathodic reactions and thus the corrosion rate of iron and steel /Deckena and Blotevogel, 1992; Pent et al., 1994; Jones, 1996/. These bacteria may increase the abiotic corrosion rate by a factor of 2 to 5 /Jones et al., 1997/. These results were however obtained at a pH much lower than the values expected in cementitious environments. High pH may restrict the microbial activity.

B.2.2 The rates of corrosion of iron and steel and of hydrogen generation

B.2.2.1 Corrosion rates

In general, the anaerobic corrosion rates of iron and steel are low in concrete environments (high pH). The corrosion rates are higher in neutral or weak alkaline environments or in environments with a high chloride concentration. There are some uncertainties in the corrosion rates determined for different corrosion media and different environments. It is also pointed out that initial corrosion rates are usually much larger than those measured in long-term corrosion /Schon and Heidendael, 1998/.

Three methods, electrochemical measurement, weight loss and evaluation of hydrogen generation, have been used for the determination of the corrosion rates of iron and steel under anaerobic conditions. For low corrosion rates, the corrosion rates measured by hydrogen generation may be more accurate than those determined by electrochemical and weight loss measurements. In cement/concrete environments, the long-term corrosion rates were found to be 0.1–1.5 μm/year /Naish et al., 1990; Kreis, 1993/. In an anoxic sulphide-free groundwater environment, the long-term average corrosion rates are expected to be 1 to 10 μm/year /Simpson and Schenk, 1989; Brush et al., 1992/. The maximum rate of corrosion of cast steel was found to be 120 μm/year for a HLW packaging in contact with brine and at a relatively high temperature (90 °C) /Schwarzkopf et al., 1989/.

The rates of corrosion of iron and steel used for the assessments of gas generation cover a range from 0.1–100 μm/year. A corrosion rate of 0.1 μm/year was used under alkaline conditions (e.g., in contact with concrete) and 10 μm/year was considered for other conditions (e.g., non-alkaline or non-concrete environments) in the calculations of gas generation in a LLW repository /Müller et al., 1992/. Corrosion rates of 0.3–0.5 μm/year were used to estimate the yield of hydrogen gas from the LLW and ILW silos /Haijtink and Maravic, 1992/. A range of corrosion rates from 1 to 10 μm/year was used in a safety analysis of gas formation in borehole disposal of ILW packages /Kroth et al., 1992/. In an analytical modelling of gas generation associated with HLW, steel corro-

sion rates of 0.1–100 μm/year were considered for their variations under several disposal conditions /Voinis et al., 1992/.

B.2.2.2 Hydrogen generation

Two basic methods are used for estimating the hydrogen generation due to the anaerobic corrosion of iron and steel under different disposal conditions. One is calculation from corrosion rates according to corrosion mechanisms and the stoichiometry of the reactions, and the other is direct measurement. Only the results from direct measurements are presented in this section. The conversion factors between hydrogen generation and iron corrosion can be estimated according to the corrosion reactions (1) and (2), assuming that hydrogen is an ideal gas and at standard conditions. If the iron corrosion takes place according to reaction (1), a hydrogen generation of 1 mmol/m^2 (22.4 ml/m^2) corresponds to an iron corrosion of 7.1 nm. However if the corrosion reaction occurs according reaction (2), a hydrogen generation of 1 mmol/m^2 corresponds to an iron corrosion of 5.3 nm.

A review of the literature on the corrosion of iron and steel at high pH in cementitious environments by Kreis /1991/ shows values between 22 and 220 mmol/m^2,year (or 0.15 to 1.5 μm/year if both reactions are considered). However, in corrosion experiments carried out during a period of two years in alkaline and anaerobic environments, he found that the rate of corrosion of iron is lower. The long-term hydrogen evolution from iron corrosion (low- and intermediate-level waste) was determined to be about 1.0–2.0 mmol/m^2,year (or 0.007 to 0.014 μm/year) /Kreis, 1991, 1993/.

It has been observed that corrosion media and site-specific conditions affect the rate of hydrogen generation. For iron or steel deposited in brine, Noack et al. /1997/ found that the average rate of hydrogen generation ranged from 0.4 to 400 mmol/m^2.year (or 0.003 to 2.8 μm/year). In two repositories for radioactive waste in deep geological formations in Germany, the average rate ranged from 0.04 to 2200 mmol/m^2.year (or 0.0002 to 11.4 μm/year) /Noack et al., 1997/. In neutral media (pH 8.5; Cl: 800 ppm), the rate of generation of hydrogen was 10–100 mmol/m^2.year (or 0.05 to 0.5 μm/year) /Kreis, 1991/. Simpson and Schenk /1989/ found that hydrogen evolution was 8–1000 mmol/m^2.year (or 0.04 to 5.2 μm/year) in two buffer systems (pH: 8.5–10, Cl: 0–8000 ppm).

B.2.3 Other potential sources of gas generation

Gases may be generated from other processes in a radioactive waste repository besides the corrosion of iron and steel. Other potential sources of gas generation may include corrosion of other metals and the microbiological degradation of organic materials.

At a high pH and under anaerobic conditions, aluminium and zinc may corrode with high corrosion rates (1 mm/year) because the protective layers on the metals are dissolved under such conditions /Grogan et al., 1992/.

$$2Al(s) + 3H_2O \rightarrow Al_2O_3(s) + 3H_2(g) \quad (3)$$

$$Al_2O_3(s) + 2OH^- + 3H_2O \rightarrow 2Al(OH)_4^- \quad (4)$$

$$Zn(s) + H_2O \rightarrow ZnO(S) + H_2(g) \quad (5)$$

$$ZnO(s) + OH^- + H_2O \rightarrow Zn(OH)_3^- \quad (6)$$

Because of the high rates of corrosion of aluminium and zinc, these processes are only important at the initial stage of disposal of waste containing aluminium and zinc.

Microbial activity in a waste repository is lesser well known than the metal corrosion. Biological degradation produces gases in both an initial aerobic phase and a later anaerobic phase. The typical microbial reactions /Agg and Sumner, 1992/ are:

In the aerobic phase,

$$C_6H_{12}O_6 + 6O_2 \rightarrow 6CO_2 + 6H_2O \quad (7)$$

$$5C_6H_{12}O_6 + 24HNO_3 \rightarrow 30CO_2 + 12N_2 + 42H_2O \quad (8)$$

In the anaerobic phase,

$$C_6H_{12}O_6 + H_2O \rightarrow 2CO_2 + 2H_2 + C_2H_5OH + CH_3COOH \quad (9)$$

$$C_2H_5OH + H_2O \rightarrow CH_3COOH + 2H_2 \quad (10)$$

$$CH_3COOH \rightarrow CO_2 + CH_4 \quad (11)$$

$$CO_2 + 4H_2 \rightarrow CH_4 + 2H_2O \quad (12)$$

$$CH_3COOH + H_2SO_4 \rightarrow H_2S + 2CO_2 + 2H_2O \quad (13)$$

$$4H_2 + H_2SO_4 \rightarrow H_2S + 4H_2O \quad (14)$$

In the anaerobic phase, gas generation due to microbial activity is affected by several factors such as pH, moisture content, nutrients and temperature. Although the cementitious environment suppresses the level of microbial activity, some microorganisms may be able to survive in the hostile environment. Microorganisms could be active within micro-environments in which the chemistry differs from that of the repository /Grogan et al., 1992/. Microbial degradation of organic materials in brine may be an important process of gas generation if sufficient water and nutrients are present at the disposal site /Brush et al., 1992/.

B.2.4 Modelling gas generation

Gas generation involves several processes that interact with each other and several efforts have been made to take these interactions into account when studying the impact of gas generation in a waste repository. In the modelling exercises, it was found that the coupling between the chemical and hydrological processes and the geometric properties of the repository determine the impact of the gas generation /Davies et al., 1992/. It was noted that a detailed waste characterisation and knowledge of pore water chemistry are important for an understanding of the gas generation processes /Brush et al., 1992/.

A specific gas generation model, GAMMON code, was used for modelling microbial degradation and metal corrosion /Holmes and Rosevear, 1992/. Agg and Sumner /1992/ use this model to relate metal corrosion to cellulose degradation

B.3 Gas migration

Gas migration from a repository into a surrounding geological formation is affected mainly by the rate of gas generation, the permeability of the surrounding formations and the difference in capillary pressure between the repository and the surrounding formation. The major concerns regarding the effects of gas migration are the build-up of gas pressure in a repository, and the induced water flow that could accelerate the transport of radioactivity from the repository into the geosphere. Therefore, many studies on gas migration focus on the pressure effect in a repository (near-field effects) and on the mechanisms of gas migration in surrounding engineering or geological formations (far-field effects).

B.3.1 Pressure effects in a repository

The build-up of gas pressure in a repository starts when the pore water in the repository is saturated with dissolved gases and free gases then start to form in the pore water. Even at low rates of gas generation, a gaseous phase will be formed. The gas pressure inside the repository will rise until it is sufficient to overcome the capillary pressure of the surrounding engineering and geological formations. It is obvious that the build-up of gas pressure depends not only on the rates of gas generation but also on the properties of the near- and far-field of the repository. The gas pressure build-up in a repository is determined mainly by gas generation rate, the permeability of the surrounding geological formation and the capillary pressure in the surrounding formation. The gas generation rate has a dominant influence on the pressure build-up /Resele and Illi, 1992/. However, the pressure in the repository is almost independent of the generation rate. It is dependent on the capillary pressure /Volckaert et al., 1992/.

The permeability to gas of surrounding formations was found to be strongly dependent on the degree of water saturation. For example the permeability of concrete varies from 10^{-17} m^2 in the dry condition to 10^{-21} m^2 at 100% relative humidity /Haijtink and Maravic, 1992/. The permeability of rock salt is determined by the size of the intercrystalline pores, the pore size distribution and the degree of interconnection of the pore volume /Brewitz and Mönig, 1992/. An in-situ permeability test based on a vacuum method was carried out to determine the gas permeability and gas diffusivity of the rock in the

Konrad mine /Liedtke et al., 1992/. The measured permeabilities ranged from 10^{-18} to $3.5 \cdot 10^{-15}$ m^2.

Some chemical processes in near-field environments may also affect the permeability of the rock. It was found that CO_2 may react with calcium hydroxide in a cement back-fill to precipitate calcium carbonate and decrease the permeability of the cement materials, and that this may in turn elevate the pressure build-up in a repository /Rees, 1992/. Moreover, chemical reactions could influence the radionuclide migration by changing the pH or redox potential in the near-field. The effects of these chemical reactions strongly depend on the waste type and on the specific disposal conditions /Nakayama and Akashi, 1991/.

In summary, in addition to the intrinsic permeability of the rock formation, the relative permeability combined with the capillary pressure are essential to describe the two-phase flow. However, reliable data for the relative permeability as a function of the saturation degree in rock fracture systems are not available in the literature. There is therefore a strong need for experimental work and for the development of models for the two-phase flow existing in the rock.

Capillary threshold pressure of the back-fill and host rocks is considered to be a key parameter in the evaluation of gas release or migration. The threshold pressure is required to overcome capillary resistance and drive gas into water-filled pores of back-fill material and host rocks. Different models are used to describe the capillary phenomena. Davies et al. /1992/ used a capillary tube model and an empirical correlation for the intrinsic permeability to estimate the threshold pressure. Several models using empirical or semi-analytical correlations to represent the relationship between capillary pressure and saturation are found in the literature /Resele and Illi, 1992; Rodwell and Nash, 1992/. A comprehensive review of capillary effects and multiphase flow in porous media is presented by Dullien /1998/.

Some researchers pointed out that all the near-field processes are coupled with each other, even for a low range of gas generation rates. A modelling approach including all these processes is therefore a useful tool for the assessment of the near-field effects. Davies et al. /1992/ found that chemical, mechanical and hydrologic processes are coupled through the pressure in the repository. The oil reservoir simulation programme PORES /Ponting et al., 1986/ was applied to gas movement through the near-field /Rodwell, 1989/.

B.3.2 Mechanisms of gas migration in the far field

There are three kinds of surrounding geological formations, crystalline (hard) rock, rock salt and clay or clay sediment, where gas migration through the far field has been studied. The far-field effects are discussed in a general way, although some of the comments may be related to a specific geological formation.

There are two principal mechanisms: a) the generated gas migrates through the far field either as bubbles or as a continuous gas stream and b) the dissolved gas diffuses away from the repository. The former mechanism is considered to be more important in most cases, transport by diffusion is important only for very low gas generation rates. Gas movement through the far field can in principle take place as bubbles, as a connected gas stream, or as a mixture of both /Rodwell and Nash, 1992/.

The far-field effects cannot actually be separated from the near-field effects. They always interact with each other. In order to assess the coupling between near-field and far-field effects, several models and codes have been used to simulate the multi-phase flow in geological formations. Davies et al. /1992/ carried out two-phase (brine and gas) flow simulations in a salt repository. Resele and Illi /1992/ studied the pressure build-up within and around a repository and the influence on groundwater flow. Rodwell and Nash /1992/, using the oil reservoir simulation programme PORES /Ponting et al., 1986/, calculated the gas flux from a repository including several mechanisms, e.g. the coupled repository pressure rise and gas flux, and gas compressibility and gas solubility in water.

A general-purpose numerical simulation program for multiphase, multi-component fluid and heat flows in porous and fractured media, TOUGH /Pruess, 1987/ and TOUGH2 /Pruess, 1991/ has been also used to study the gas impact in waste repositories. Mishra and Zuidema /1992/ simulated the maximum pressure within a repository and the rate of water outflow from engineered barriers to host rock. Finsterle et al. /1992/ used TOUGH2 to simulate the pressure response during a water injection test. Webb /1991/ used the code to study the gas migration distance at 1000 years.

Some advances have been made in two-phase flow by connecting field or laboratory experiments with modelling. However, there is still a significant lack of information in characterising the two-phase flow properties /Rodwell and Nash, 1992; Gascoyne and Wuschke, 1992/. Finsterle et al. /1992/ found that a water injection-falloff test sequence is appropriate to determine formation characteristics in a two-phase flow system.

B.4 Discussion and conclusions

Two aspects are important when the impact of gas generation is studied:

- The pressure build up in the repository is determined by the rate of gas generation
- The capillary forces in the barriers surrounding the repository determine the pressure in the repository.

The development of the pressure in the silo repository at the initial stage will therefore be determined by the rate of gas generation. The hydraulic conductivity and the relative permeability to the gas of the barriers will determine the value for this pressure development. After the initial stage, the capillary forces in the sand-bentonite layer determine the pressure in the silo.

The anaerobic corrosion may be described by two reactions. In the first, the iron is transformed to $Fe(OH)_2$ and, in the second, the reaction continues to magnetite (Fe_3O_4). According to the thermodynamics, the final product should be magnetite, but its formation is not commonly observed. However, the occurrence of the second reaction cannot be ruled out.

Since the reactions produce hydrogen gas, an increase in the pressure could theoretically stop the reaction, but a very high pressure is required (10 MPa) to do this.

Regarding the corrosion rate, there is a considerable degree of uncertainty. The measured values of corrosion rate are between 0.1 and 1 μm/year for the conditions existing in the silo repository, viz. high pH and anaerobic conditions.

According to new experimental data, values between 0.1 and 1.0 μm/year could be used for anaerobic corrosion in a concrete environment in future safety assessment.

Under anaerobic conditions and at a high pH, the rate of corrosion of aluminium and zinc is high, about 1 mm/year. The gas generation from anaerobic corrosion of aluminium and zinc is therefore important only in the initial stage.

Gas generation due to the degradation of organic material by microbial activity is expected to be negligible in the silo since a cementitious environment suppresses the level of microbial activity. However, some microorganisms may be able to survive in this hostile environment.

With regards to gas transport in the silo and other parts of the repository, there are several tools that may be used in these calculations, e.g. TOUGH2. They can be used to calculate the re-saturation of the repository after sealing, the mobility of the pore water in the porous materials in the repository and gas transport through, for example, the sand-bentonite layer.

B.5 References

Agg P J, Sumner P J, 1992. Modelling of gas generation in radioactive waste repositories. Gas generation and release, pp. 189–199, OECD and OCDE, Paris.

Brush L H, Molecke M A, Lappin A R, Westerman R E, Tong X, Black J N P, Grbic-Galic D, Vreeland R E, Reed D T, 1992. Laboratory and bin-scale tests of gas generation for the waste isolation pilot plant. Gas generation and release, pp. 143–154, OECD and OCDE, Paris.

Brewitz W, Möning J, 1992. Sources and migration pathways of gases in rock salt with respect to high level waste disposal. Gas generation and release, pp. 42–53, OECD and OCDE, Paris.

Davies P B, Brush L H, Mendenhall F T, 1992. Assessing the impact of waste-generated gas from the degradation of transuranic waste at the waste isolation pilot plant (WIPP): An overview of strongly coupled chemical, hydrologic, and structural processes. Gas generation and release, pp. 55–74, OECD and OCDE, Paris.

Deckena S, Blotevogel K H, 1992. Iron(0) oxidation in the presence of methanogenic and sulfate-reducing bateria and its possible role in anaerobic corrosion. Biofouling 5, 287–293.

Dullien F A L, 1998. Capillary effects and multiphase flow in porous media. J. Porous Media, 1 (1), 1–29.

Finsterle S, Mishra S, Lavanchy J M, 1992. Hydrogeologic site characterization under two-phase flow conditions. Gas generation and release, pp. 367–377, OECD and OCDE, Paris.

Gascoyne M, Wuschke D, 1992. Gas flow in saturated fractured rock: results of a field test and comparison with model predictions. Gas generation and release, pp. 353–365, OECD and OCDE, Paris.

Grauer R, Knecht B, Kreis P, Simpson J P, 1991. Hydrogen evolution from corrosion of iron and steel in intermediate level waste repositories. Mat. Res. Soc. Symp. Proc. 212, 279–286.

Grauer R, Knecht B, Kreis P, Simpson J P, 1991. Die langzeit-korrosionsgeschwindigkeit des passiven eisens in anaeroben alkalischen lösungen. VCH Verlagsgesellschaft mbH, D-6940 Weinheim, (In german)

Grogan H A, Worgan K J, Smith G M, Hodkinson D P, 1992. Post-disposal implications of gas generated from a repository for low and intermediate level wastes. NAGRA, NTB 92-07, Wettingen (Switzerland).

Haijtink B, von Maravic H, 1992. PEGASUS, a community project on the effects of gas in underground storage facilities for radioactive waste. Gas generation and release, pp. 89–110, OECD and OCDE, Paris.

Holmes R G G, Rosevear A, 1992. The generation and evolution of gas from a low-level radioactive waste repository. Gas generation and release, pp. 155–166, OECD and OCDE, Paris.

Jones D A, 1996. Principles and prevention of corrosion. 2ed. Macmillan Publishing Company, New York.

Jones D A, Pitonzo B, Castro P, Amy P S, 1997. Electrochemical characteristics of anticipated MIC in deep geologic nuclear waste storage environments at Yucca mountain, Nevada, USA. NATO ASI Ser. 1, 11, 23–32.

Kreis P, 1991. Hydrogen evolution from corrosion of iron and steel in low/intermediate level waste repositories. NAGRA, NTB 91-21, Wettingen (Switzerland).

Kreis P, 1993. Wasserstoffentwicklung durch korrosion von eisen und stahl in anaeroben, alkalischen medien im hinblick auf ein SMA-Endlager. NAGRA, NTB 93-27, Wettingen (Switzerland).

Kroth K, Barnert E, Morlock G, Müller W, 1992. Consequences of gas formation on borehole disposal of ILW packages. Gas generation and release, pp. 297–308, OECD and OCDE, Paris.

Liedtke L, Naujoks A, Pauhl A, Jockwer N, 1992. Gas migration in sedimentary rock. Gas generation and release, pp. 329–341, OECD and OCDE, Paris.

Moreno L, Neretnieks I, 1991. Some calculations of radionuclide release from the silo repository. SKB PR SFR 91-07, Swedish Nuclear Fuel and Waste Management Co.

Mishra S, Zuidema P, 1992. Modelling gas migration from a low/intermediate-level nuclear waste repository. Gas generation and release, pp. 253–264, OECD and OCDE, Paris.

Müller M, Morlock G, Jockwer N, Mönig J, 1992. Gas formation in low-level waste. Gas generation and release, pp. 167–174, OECD and OCDE, Paris.

Nakayama G, Akashi M, 1991. The critical condition for the initiation of localized corrosion of mild steel used for nuclear waste package. Mat. Res. Soc. Symp. Proc. 212, 279–286.

Naish C C, Balkwill P H, O'Brien T M, Taylor K J, Marsh G P, 1990. The anaerobic corrosion of carbon steel in concrete. NSS/R273, AEA Technology, Harwell Laboratory, Didoct, Oxfordshire.

Noack W, Brennecke P, Schenk R, 1997. Hydrogen generation in repositories for radioactive waste in deep geological formations. Proc. Int. Conf. Radioact. Waste Manage. Environ. Rem., 6th, 607–610. American Society of Mechanical Engineers, New York.

Pent C G, Suen S Y, Park J K, 1994. Modelling of anaerobic corrosion influenced by sulfate-reducing bacteria. Water Environ. Res., 66(5), 707–715.

Ponting D K, Foster B A, Naccache P F, Nicholas M O, Pollard R K, Rae J, Banks D, Walsh S K, 1986. An efficient fully implicit simulator. Society of Petroleum Engineers Journal, 23, 544–552.

Pruess K, 1987. TOUGH User's guide, Nuclear Regulatory Commission Report NUREG/CR-4645; also Lawrence Berkeley National Laboratory, Report LBL-29400, Berkeley, CA.

Pruess K, 1991. TOUGH2 – A general purpose numerical simulator for multiphase fluid and heat flow. Lawrence Berkeley National Laboratory, Report LBL-29400, Berkeley, CA.

Reardon E J, 1995. Anaerobic corrosion of granular iron: measurement and interpretation of hydrogen evolution rates. Environ. Sci. Technol. 29, 2936–2945.

Rees J H, 1992. An overview of research on gas evolution and migration relevant to the disposal of low and intermediate level radioactive wastes in clays and fractured hard rock. Gas generation and release, pp. 31–40, OECD and OCDE, Paris.

Resele G, Illi H, 1992. Modelling of gas release from a nuclear waste repository. Gas generation and release, pp. 378–389, OECD and OCDE, Paris.

Rodwell WR, 1989. Near-field gas migration — A preliminary review. UK Nirex Ltd. Report NSS/R200.

Rodwell W R, Nash P J, 1992. Modelling of far-field gas migration from a deep radioactive waste repository. Gas generation and release, pp. 391–403, OECD and OCDE, Paris.

Schon T, Heidendael M, 1998. Hydrogen evolution by metal corrosion. Ber. Forschungszent. Juelich, Juel-3495, 1–68.

Schwarzkopf W, Smailos E, Köster R, 1989. In situ corrosion studies on cast steel for a high-level waste packaging in a rock salt repository. Mat, Res. Soc. Symp. Proc. 127, 411–418.

Simpson J P, Schenk R, 1989. Corrosion induced hydrogen evolution on high level waste overpack materials in synthetic groundwaters and chloride solution. Mat. Res. Symp. Proc., 127, 389–396.

Voinis S, Gago J, Müller W, 1992. The analytical modelling of gas generation. Gas generation and release, pp. 111–119, OECD and OCDE, Paris.

Volckaert G, Grindrod P, Impey M, Fioravante V, Horseman S, 1992. MEGAS: modelling and experiments on gas migration in argillaceous host rocks. Gas generation and release, pp. 405–416, OECD and OCDE, Paris.

Webb S W, 1991. Sensitivity studies for gas release from the waste isolation pilot plant. In: Waste-generated gas at the waste isolation pilot plant. Papers presented at the Nuclear Energy Agency Workshop on gas generating and release from radioactive waste repositories. SAND-91-2378.

Appendix C:

Review of experiments with porous concrete

Contents

C.1 Introduction

Porous concrete will be deposited around the containers containing the intermediate radioactive waste. The containers may be concrete moulds, steel moulds or steel drums. It is expected that the porous concrete occupy all the space between the containers and the interior silo walls. Important properties of the porous concrete are: permeability, strength, and the capability to fill all the free spaces. Here, the water and gas permeability, and the volume of water expelled from the porous concrete by the gas flow will be discussed in detail.

Several experimental determinations of hydraulic properties of porous concrete have been performed. Here, the reports "Sammanställning av gjutningar i SFR och provningar i Bångbro under 1994 och 1995 /Björkenstam, 1996/" and "Utveckling av SFR-bruket /Björkenstam, 1997/" are discussed.

The basic composition of the porous concrete is shown in Table 1. The values shown correspond to a concrete with a water cement number (vct) of 1.34.

Table C.1-1. Formula of the porous concrete.

Material	
Cement	170 kg/dry concrete
Sand	830 Kg/dry concrete
Cellulose	2.0 Kg/dry concrete
Foam inhibitor	2.0 Kg/dry concrete
Water	228.5 Kg/dry concrete

The silo is composed of 57 cells with capacity for 4 concrete/steel moulds or 16 drums. There are also 12 half-cells and 20 cells with varying dimensions (equivalent to 10 normal cells). In total 73 normal cells.

The maximum gas production rate is estimated to be 1900 Nm^3/year (Volume at normal conditions).At the pressure at the top (0.5 MPa) the total gas flow will be 380 m^3/year distributed in the 73 cells. This is equivalent to gas flow of 5.2 m^3/cell,year. Since the total cross section occupied by the porous concrete in each cell is 0.74 m^2, the maximum gas flux in the porous concrete will be 7.0 m^3/ m^2,year or 0.80 litre/ m^2,hour.

The water flow in the porous concrete would be less than the gas flow. At the gas generation starts, somewhat water is expelled to allow the gas flow. When the gas generation increases, new paths need to be opened and more water is expelled from the concrete. 68 m^3 will be expelled from the silo to allow gas flow. So the time that takes to expel 68 m3 of water is at least the time that takes to generate 68 m^3 of gas, at the pressure within the silo. To avoid large pressure in the silo, a hydraulic conductivity of $3 \cdot 10^{-8}$ m/s is required.

C.2 Results from experimental measurements on porous concrete

The discussion will be limited to the water and gas permeability and the volume of water expelled from the concrete to allow a certain gas flow.

C.2.1 Hydraulic conductivity.

The results reported by Björkenstam /1997/ show that the hydraulic conductivity of the porous concrete is higher than $3 \cdot 10^{-8}$ m/s in the most of the cases. However, in some cases the hydraulic conductivity is less than $3 \cdot 10^{-8}$ m/s. This occurs when ballast with a small particle size is used. A long mixing time may also cause a less hydraulic conductivity.

Table C.2-1. Some examples of samples with low hydraulic conductivity

Recipe	Hydraulic Conductivity	Comments
R19	$0.2 \cdot 10^{-8}$ m/s	High cement content, fine ballast
R18 F5	$1.7 \cdot 10^{-8}$ m/s	Large scale mixing
R24 F6	$0.8 \cdot 10^{-8}$ m/s	Large scale mixing

C.2.2 Air relative permeability

Before discussing the results, some basic aspects are presented to differentiate between permeability and hydraulic conductivity. According the Darcy Law

$$q = \frac{k}{\mu}\frac{\Delta P}{L}$$

where

q	Darcy velocity, m/s
k	Permeability, m^2
P	Pressure, Pa
L	Length, m

The permeability is a property of the porous medium, independent of the fluid used. If the pressure is expressed in function of metres of column of water,

$$q = \frac{k}{\mu}\frac{\Delta P}{L} = \frac{k\rho g}{\mu}\frac{\Delta H}{\Delta L} = K\,i$$

$$\text{where} \quad K = \frac{k\rho g}{\mu}$$

$$i = \frac{\Delta H}{\Delta L}$$

K	Hydraulic conductivity, m/s
i	Hydraulic gradient, m/m

When we are working only with a water-saturated porous medium the use of hydraulic conductivity is recommendable. When we are working with two phases, the use of permeability and relative permeabilities are more convenient. In this case, the Darcy's equation is written for each of the fluid as

$$q_i = \frac{k \cdot k_{ri}}{\mu_i} \frac{\Delta P}{L}$$

The relative permeability, k_{ri}, depend on the fluid and the saturation degree. For a porous medium saturated in the respective fluid the relative permeability is equal to one. Otherwise is less than one.

In the reports /Björkenstam, 1996, 1997/, the results of the experiments are present as "Water permeability and air permeability" in m/s. According the experimental description, the first one would be hydraulic conductivity. From the hydraulic conductivity, the permeability may be determined, since in these experiments the porous medium was water saturated and the water relative permeability is equal to one.

According the relationships above, the air relative permeability will be calculated by,

$$k_{r-air} = \frac{"air\,permeability"}{"water\,permeability} \frac{\mu_{air}}{\mu_{water}}$$

The value of the air relative permeability would be less than 1.0 since in the concrete there are two phases, water and air. The ratio between water and air viscosity is about 55 at 0°C and 85 at 20°C.

From the results of large scale experiments carried out at SFR /Björkenstam, 1997/, the average value for the air relative permeability (8 measurements) is about 0.7. This is a rather high value, considering that the porous concrete is almost water saturated. Moreover, the values for individual experiments show an extreme spreading. One value is low, 0.06, but three samples show values significantly larger than 1.0 (3.9, 2.3 and 7.5). These values correspond to those samples with low hydraulic conductivity.

Experiments described in a earlier report /Björkenstam, 1996/, the value of gas relative permeability was in many cases larger than 1.0, even in some cases values as large as 50 were found. No clear explanation is found for the fact that gas relative permeability is larger than 1.0. This anomaly is found in also found in other experiments /Mähonen, 1984, Moreno and Cederström, 1985/.

C.2.3 Water expelled from the porous concrete

Regarding the volume of water expelled from the porous concrete to allow the gas flow, the results show that a small volume of water is expelled. In the large-scale experiments carried out at SFR /Björkenstam, 1997/, the volume of water expelled from the porous concrete used in the silo is about 0.2–0.4% of the volume of the sample. Earlier experiments /Björkenstam, 1996/ shows volumes of expelled water between 0.04 and 0.71% of the sample volume. For a porosity of about 0.30, this means that between 0.13 to 2.4% of the water content is expelled by the flow of air.

The hydraulic gradient in the experiments was 1.8 m/m. So, the hydraulic gradient was much larger than the value expected for the gas flow through the porous concrete in the silo. In general the gas flux was about 100 m^3/ m^2year, the value for the silo is 7.0 m^3/m^2,year. This means that the volumes of water expelled in the experiments may be considered as maximum values. The actual value in the silo is expected to be smaller.

C.3 References

Björkenstam E, 1996. Sammanställning av gjutningar i SFR och provningar i Bångbro under 1994 och 1995, Vattenfall rapport, UC 96:Ö1, Vattenfall Utveckling AB, Betongteknik, Älvkarleby. (In Swedish).

Björkenstam E, 1997. Utveckling av SFR-bruket. Vattenfall rapport UC 97:4Ö, Vattenfall Utveckling AB, Betongteknik, Älvkarleby. (In Swedish).

Moreno L, Cederström M, 1985. Permeability of porous concrete. SKB, Teknisk PM, Swedish Nuclear Fuel and Waste Management Co.

Mähönen P, 1984. Laboratory tests to determine the air and water permeability of concrete specimens at different pressures. SKB, Teknisk PM 24, Swedish Nuclear Fuel and Waste Management Co.